nks

Nordisk kernesikkerhedsforskning
Norrænar kjarnöryggisrannsóknir
Pohjoismainen ydinturvallisuustutkimus
Nordisk kjernesikkerhetsforskning
Nordisk kärnsäkerhetsforskning
Nordic nuclear safety research

NKS-191
ISBN 978-87-7893-258-7

Urban Gamma Spectrometry: Report 2

[1]Helle Karina Aage, [2]Satu Kuukankorpi, [2]Mikael Moring,
[2]Petri Smolander and [2]Harri Toivonen

1) Technical University of Denmark, Kgs. Lyngby, Denmark
2) Radiation and Nuclear Safety Authority, Helsinki, Finland

June 2009

Abstract

Urban gamma spectrometry has been given only minor attention with the focus being on rural gamma spectrometry. However, in recent years the Nordic emergency management authorities have turned focus towards border control and lost or stolen sources. Gamma spectra measured in urban areas are characterized by a wide variety of spectrum shapes and very fast changes in environmental background.
In 2004 a Danish CGS survey took place in Copenhagen. It was found that gamma spectrometry in urban areas is far more complicated to interpret than had previously been thought and a new method "Fitting with Spectral Components", FSC, based on NASVD, was tested with some success. In Finland, a database “LINSSI” has been developed for spectral data management. In CGS search mode a "peak hypothesis test" is applied to the measured spectra. This system was tested during the Helsinki 2005 Athletics World Championship and it provides fast and reliable automated alarms for intermediate and high level signals. In Sweden mobile detector systems are used for border controls and problems are encountered when making measurement in harbour, container areas.
The methods for handling data and for interpretation of urban gamma spectrometry measurements were compared and tested on the same data sets from Copenhagen and Helsinki. Software tools were developed for converting data between the Finnish LINSSI database and the binary file formats used in Denmark and Sweden.
The Processing methods used at DTU and STUK have different goals. The ASSS and FSC methods are designed to optimize the overall detection capability of the system, while sacrificing speed, usability and to a certain level robustness. These methods cannot always be used for real time analysis. The Peak Significance method is designed to give robust alarms in real time, while sacrificing some of the detection capability. Thus these methods are not interchangeable, but rather complementary. An ideal system based on these methods would use the Peak Significance method simultaneously with the data collection and the ASSS and FSC methods in post processing to achieve both an optimal detection capability and a fast response. Ideally, the three systems would run simultaneously in a user-friendly environment, such as the LINSSI database.

Key words

Urban Carborne Gamma Spectrometry, Spectrum Stripping, Peak hypothesis, LINSSI, FSC, ASSS, NASVD, Harbour, source search

NKS-191
ISBN 978-87-7893-258-7

Electronic report, June 2009

NKS Secretariat
NKS-776
P.O. Box 49
DK - 4000 Roskilde, Denmark

Phone +45 4677 4045
Fax +45 4677 4046
www.nks.org
e-mail nks@nks.org

URBAN GAMMA SPECTROMETRY

NKS
Nordic Nuclear Safety Research

Report 2 from the AFT/B(06)3 project group
03 November 2006

Helle Karina Aage[1)]
Satu Kuukankorpi[2)]
Mikael Moring[2)]
Petri Smolander[2)]
Harri Toivonen[2)]

1) Technical University of Denmark, Lyngby, Denmark
2) Radiation and Nuclear Safety Authority, Helsinki, Finland

1 SUMMARY

This is the final report for the NKS UGS-project per 03 November 2006. The previously issued report (Report 1) was intended to be incorporated into this main report. However, for file size reasons, this has not been done.
The two volumes, the Report 1 and Report 2, can be studied separately.

The Status report contains thorough descriptions of the CGS systems used by the Finnish and Danish Emergency Managements and a general description of the measurement file formats. The Status report also includes detailed mathematic descriptions of data processing methods. The main report can be read as a document comparing different data processing tool without the knowledge of the mathematics behind. This report includes some references to the Status report – mathematics and tables – but it can be read easily without looking up the references.

In general the Status report contains the results of the DTU data processing using Danish processing methods and the STUK data processing using Finnish processing methods.
The final report includes the results of the data processing using one organisations data processing methods on the other organisations measurements. The Status report therefore can be seen as an introduction to three different methods and the final report as a comparison of three different methods used on the very same measurement data.
In addition the final report includes a section about SSI custom controls measurements made in Frihamnen and a section of data conversions. The Swedish measurements were processed using two basically different Danish processing methods.

For readers who have not studied the Status report, a short introduction to the three different processing methods is presented here. It is also suggested that the reader studies the introduction to the project. This introduction presented in the status report is repeated in this report as Section 2.

STUK uses a peak hypothesis test method to get robust real time alarms (within 10 seconds) when significant peaks from a previously defined set of nuclides are detected. An alarm for a significantly elevated total pulse rate is sent if none of the predefined nuclides is identified. The UGS project uses measurements made by STUK in Helsinki during the Athletics World Championship in 2005.

DEMA/DTU bases their calculations on full spectrum fitting using NASVD and the Danish software NucSpec where source signals are found from spectrum fitting residuals. This is called the FSC method, Fitting with Spectral Components.
Alternatively sources are searched for by stripping energy windows of low energy using stripping factors derived from the measurements themselves. This is referred to as the ASSS method, Area Specific Spectrum Stripping.
The UGS project uses measurements made by DEMA in Copenhagen and suburbs in 2004 and 2006. To the Danish measurements some source signals originating from other measurement tasks were added to a set of spectra of different shapes to investigate if any of the three methods were superior in finding the signals.

During the project, software tools were developed for converting data between the Finnish LINSSI database and the binary Exploranium file formats largely used in Denmark and

Sweden. The conversion has been tested and successfully used between Danish and Finnish systems, and it is believed that also Swedish Exploranium data could be converted with no or small adjustments to the software. These data conversion routines can be seen as a major result of this project and they are now freely available for anyone who might need them. The problems with using Swedish Exploranium data in a Danish Exploranium system (chapter 6.2) gives a good example of the danger of relying on commercial binary data formats. They might change, without any prior notice or warning and the data structure is not always known.

The Peak Significance method is robust and well suited for use in any environment, urban or rural. Its main goal and advantage is its ability to work in real time. The system used in the survey vehicle SONNI has repeatedly demonstrated its ability to generate automatic alarms of moderate and strong sources within 10 seconds of the beginning of measurement, while generating a minimum of false alarms (theoretically one per a million measurements).
The Peak Significance method is based on simple and sound statistics and gives predictable results. However the method is not as sensitive as the two other methods tested here, and additionally it has two major weaknesses. It cannot generally detect sources of nuclides not on the predefined list of nuclides to be tested or heavily shielded sources where only scattered radiation reaches the detector. Additional analysis methods need to be adopted when searching for unknown or potentially shielded sources. Currently STUK relies on skilled personnel performing visual inspection of rainbow plots and raw count rate levels in certain regions of the spectrum for detecting such cases.

ASSS and FSC both proved available for the detection of source signals added to the original Danish measurements. In general, the ASSS method detected more sources than FSC. Depending on the measurement geometry sometimes ASSS was the preferred method and sometimes FSC was superior. The FSC method used on the Finnish measurements showed that problems exist for the method if a radionuclide pollutant is present in the environment. However, if this is a known problem it can be overcome easily.
In Denmark a method of spectrum fitting based on NASVD is used on-line the Danish Early Warning Stations and it is believed that this method can be improved by implementing FSC to operate on-line with spectral shapes based on annual averages. FSC has been tested on the EWS in the post processing phase with good results. For urban data where the spectrum shapes vary fast spectrum drift could lead to problems due to the possibility of fitting source signals with natural radionuclide shapes. When a set of spectral components containing spectrum drift and poor resolution data was used for fitting of a good data set, the fitting errors from the fitting of ^{137}Cs signals were in fact too low, i.e. too good a fit due to fitting with 609keV bismuth.
ASSS with ASSS factors calculated from previous data sets is used on-line with the Danish Exploranium systems. A possible baseline offset resulting from e.g. driving from the country side to urban environments could lead to missing alarms for systems with alarm level settings if the ASSS counts follow a negative baseline (however, peaks will be detected by an attentive operator). ASSS therefore requires the presence of a skilled operator if used as a stand alone method.

The Swedish data sets were delivered without information on file layout and without maps, which caused some additional unexpected work, however the problems were solved. The SSI data contain interesting measurements from the Frihamnen container area where surveys were made with and without sources. The ASSS factors and FSC components were calculated from the file without source signals. The no-source measurements were analysed for spectrum shapes not previously found in urban measurements. One spectrum shape in particular

concerning potassium was quite unusual signifying a very different composition of the materials used in the harbours areas, i.e. independent potassium variations. The occurrence of spectral shapes (coordinates) was compared to the Harbour layout and the geometry variations of the harbour area were found to be of high importance.
A set of measurements containing source signals (10,000 spectra approx.) were stripped using ASSS and fitted using FSC and the results were analysed. Unfortunately the sources measured were too strong to discus the detection levels for the methods.

The Processing methods used at DTU and STUK have different goals. The ASSS and FSC methods used by DTU are designed to optimize the overall detection capability of the system, while sacrificing speed, usability and to a certain level robustness (e.g. negative ASSS baselines).
These systems are normally used in post processing, and they cannot always be used for real time analysis. The Peak Significance method used at STUK is designed to give robust alarms in real time, while sacrificing some of the systems detection capability. Thus these methods are complementary. An ideal system based on these methods would use the Peak Significance method during data collection for real-time processing, and then use the ASSS and FSC methods in post processing mode to achieve an optimum detection capability. Ideally, the three systems would run simultaneously in a user-friendly environment, such as the LINSSI database.

CONTENTS PAGE

2 INTRODUCTION

Earlier urban gamma spectrometry has been given only minor attention with the focus being on rural gamma spectrometry. However, in recent years the Nordic emergency management agencies have turned focus towards border controls and the topic of lost sources. Gamma spectra measured in urban areas are characterized by a wide variety of spectrum shapes and very fast changes in environmental background values.

In 2004 a Danish CGS survey in the capital Copenhagen took place. It was found that gamma spectrometry in urban areas is far more complicated to interpret than had previously been thought. Known and available methods of data processing were not enough to interpret the results and a new method "Fitting with Spectral Components", FSC, based on NASVD, was tested with some success. Yet, the method still needs a lot of improvement.

In Finland a database “LINSSI” has been developed for spectrum data. In CGS search mode a "peak hypothesis test" is applied to the measured spectra. This system was tested during the Helsinki 2005 Athletics World Championship and it provides fast and accurate automated alarms for intermediate and high level signals, but optimisation of detecting weak signals is needed.

In Sweden mobile detector systems are used for border controls and problems are encountered when making measurement in harbour container areas.

The aim of this project is to improve the methods for handling data and for interpretation of urban gamma spectrometry measurements. The Finnish and Danish methods will be compared and tested on the same data sets from Copenhagen and Helsinki and, if available, SSI customs measurements with a possible combination of the two methods in mind. Data sets with and without source signals will be examined, with special emphasis on difficult background signals.

3 FINNISH DATA TREATMENT BY DANISH METHODS

3.1 The Finnish Measurements

All data delivered by STUK have been NASVD processed and treated by the methods of ASSS and FSC. However, it has not been within the time frame to comment on all results. A selection of files has been made on the grounds that the data should be urban data, some files including source signals (intended and unintended) and some highway driving results. The latter because the definition of urban is somewhat relative referring to the fact that Helsinki in suburbs and industrial areas has actual highways of widths not found in Copenhagen (or elsewhere in Denmark).

The Finnish data also contains a set of calibration measurements made in Vesivehmaa Airfield. Those measurements contain signals from ^{99m}Tc, ^{241}Am, ^{137}Cs and ^{60}Co. The measurements were made with different distances from source to vehicle and with different driving speeds.
The results from the data processing of the calibration measurements using Danish methods have been described in some detail focusing on the comparison of source detection capability for the three methods. In addition the results were used for checking the energy calibration for the system.
No attempt has been made to calibrate the Finnish measurement system as this is considered out of scope for the UGS projects.

Plots of results for the Finnish data were made in the coordinate system WGS84 UTM zone 34, because of problems creating XY plots on the Finnish coordinates using EXCEL. However, in the result files the original coordinates from the LINSSI xml-files are assigned to the results.
The use of this coordinate system means that the plots are slightly distorted compared to the plots made by STUK showing the daily routes and the marathon route in Helsinki during the Championships.

Because the Finnish data includes the same route measured numerous times on a day to day basis a part of this route focused on the Olympic Stadium area was selected for a check of the consistency of the methods. In urban areas fluctuations occur rapidly due to changes in city geometry, high buildings, low building, open squares, wide roads, narrow streets, new and old houses etc. but also the results may very well be influenced by the time of day the measurements were performed with respect to traffic and road works and the like. The data selected originate from the period from 5 August 2005 to 14 August 2005. Thus, one element not included to blur the findings is the seasonal variations that in particular has been found to affect potassium signals (examination of data from Danish Early Warning Stations using data from 12 months; snow covering the ground was found to have a large effect).

3.2 STUK: Energy Calibration for 512-Channels Spectra

The energy calibration for the Finnish system was supplied by STUK and checked by DTU, Figure 3.2.1. The DTU energy calibration differed only very little from the STUK energy calibration. The energy calibration used in this report is the one calculated by STUK.

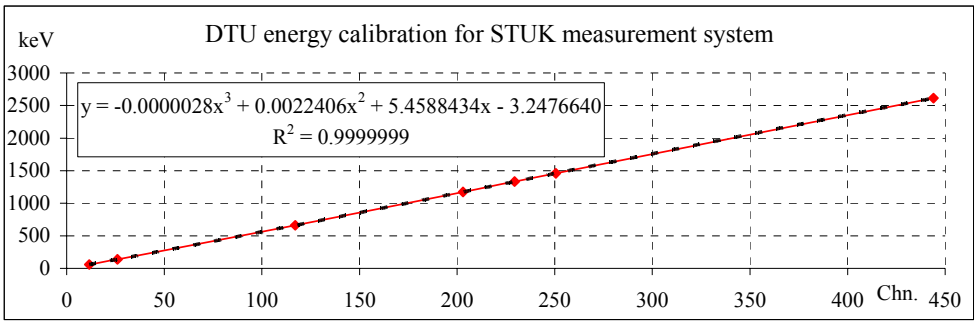

Figure 3.2.1. DTU check of STUK energy calibration.

The original Finnish energy calibration for 1024 channel spectra starting from channel 1 is:

$En=-3.2082437E-7*chn^3+0.00050618197*chn^2+2.7652338*chn-9.2141762$

To use the Danish data processing methods on the Finnish data sets STUK had to compress the data from 1024 channel spectra to 512 channel spectra. Also, it was taking into consideration that the Danish methods in general starts counting from channel 0. After compressing the spectra to 512 channel spectra starting from channel 0, the energy calibration is:

$En=-2.5665950E-6*chn^3+0.0020189530*chn^2+5.5335008*chn-10.1311340$ keV

The following windows were used for the ASSS and FSC calculations on the STUK data sets:

Table 3.2.1. Standard radionuclide window.

Window	LL (chn.)	UL (chn:)	LL (keV)	UL (keV)	E_γ (keV)
Am	11	14	51.0	67.7	59.5
Tc	23	28	118.2	146.3	140.5
Ra	32	37	168.9	197.2	186.2
Ir	48	68	259.8	374.7	316.5
I	59	76	322.8	420.9	364.5
Pb	59	69	322.8	380.4	351.9
Ir	73	95	403.6	531.6	468.1
Bi	98	115	549.1	649.0	609.3
Cs	110	130	619.6	737.7	661.7
Bi	187	199	1078.5	1150.8	1120.2
Co	190	216	1096.5	1253.4	1173.2
Co	217	243	1259.5	1416.9	1332.5
K	235	268	1368.4	1568.4	1460.8
U	283	316	1659.4	1859.1	1764.5
Th	408	477	2409.3	2810.2	2614.5

3.3 STUK: Data Processing by Danish Methods

3.3.1 NASVD Processing

The standard NASVD processing channel interval is from channel 20 to channel 470 unless low energy emitters are searched for meaning lowering of the LL to channel 10.

The STUK measurement set-up however makes use of very high-numbered channels also, please confer Figure 3.3.1.1. From calibration measurements it was known that the full energy peak from ^{241}Am began in channel 8 approx. To ensure that americium signals would not be lost the value of LL was set to 6 during NASVD processing and the placement of the 2614 keV peak from ^{208}Tl determined the placement of the UL to channel 480.

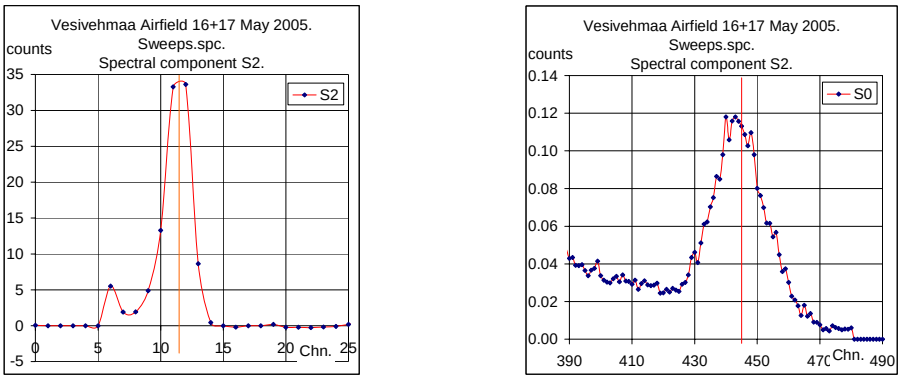

Figure 3.3.1.1. STUK data file Sweeps.spc: Windows for ^{241}Am and ^{208}Tl. NASVD cut offs in channel 6 and channel 480 (zeroes).

A few of the data files contain intentional or non-intentional source signals from ^{137}Cs and ^{99m}Tc. Despite the source signals it is evaluated that the information contained in the first five spectral components are quite sufficient for the FSC reproduction of the data. Therefore all the FSC calculations on the Finnish data sets were made using five spectral components in addition to the mean spectrum except for the files 20050811.spc (7 spectral components) and 20050812.spc (six spectral components) due to the occurrence of spectrum drift determined by NASVD to be of higher importance than changes in caesium levels and natural radionuclide levels, confer Figure 3.3.1.2.

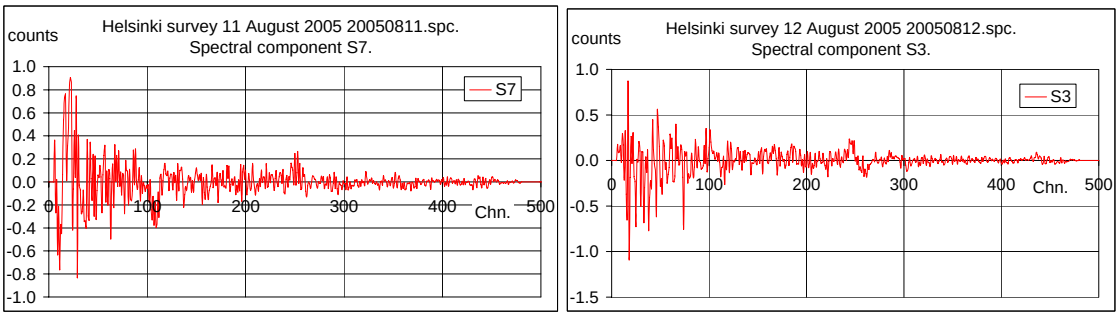

Figure 3.3.1.2. Spectrum drift of importance.

Examples of average spectra are shown in Figure 3.3.1.3. On the highway survey plot the signal from ^{137}Cs is visible.

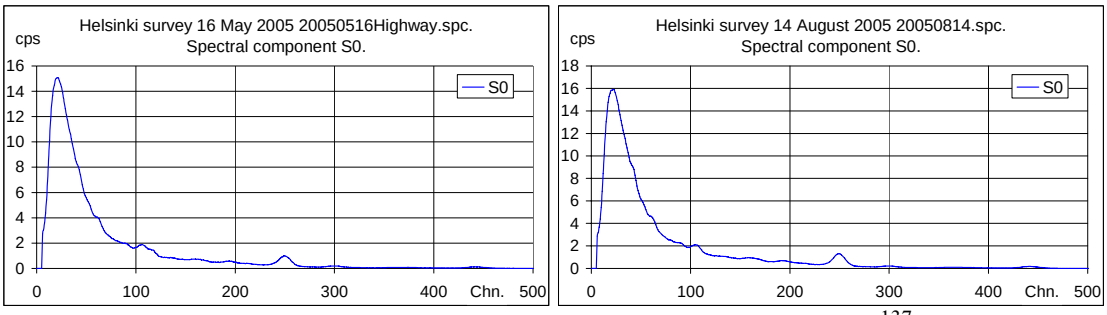

Figure 3.3.1.3. STUK mean spectra with and without environmental ^{137}Cs background.

3.3.2 Area Specific Spectrum Stripping.

ASSS factors were calculated for all Finnish data files for the twelve windows described in Table 3.2.1. Results for May, July and August have been plotted on separate plots. The numbers on the x-axis is the month followed by the date.
The potassium stripping factors in Figures 3.3.2.1 to 3.3.2.3 apparently decrease with increasing time which may very well be an indication of weather related detection efficiencies. But, it should be remembered that not all surveyed distances are the same. The measurements in May relate to highway driving and the May thorium stripping factors are significantly different from the August thorium stripping factors leading to the most probable conclusion that it is the road types that are the most responsible for the differences observed.

During the Championships in August, the ASSS factors fluctuate for all three radionuclides, but only very little. The dive in the americium stripping factor for uranium for 10 August (810) does look a little strange but might be explained by the weather conditions during the Games. On Tuesday 9th of August there was a mighty downpour in the evening, resulting in 1-3 centimetres of water on the stadium (television broadcasting was halted). SONNI had already driven all the routes by then and was in the garage at that time, but the downpour resulted in very humid conditions (and continued light rain) on Wednesday morning, when the routes were surveyed the next time.

Apart from that it can be said, that for source search purposes during the Championships it would have been sufficient to calculate the ASSS factors once and use the same stripping factors on the rest of the files and still obtain detection of sources not supposed to be present in the data sets.

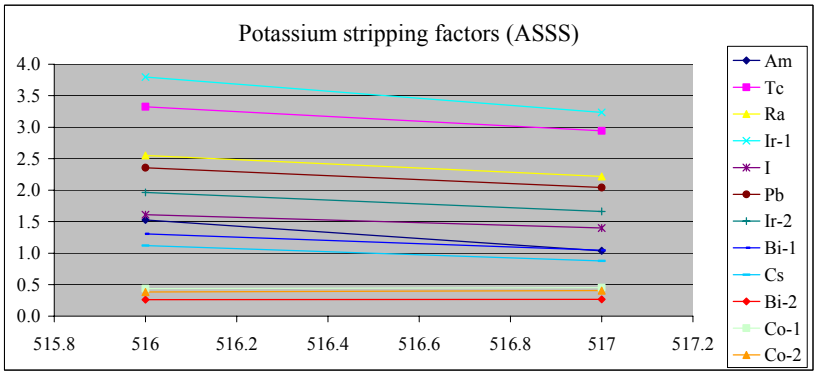

Figure 3.3.2.1. Potassium ASSS factors May 2005.

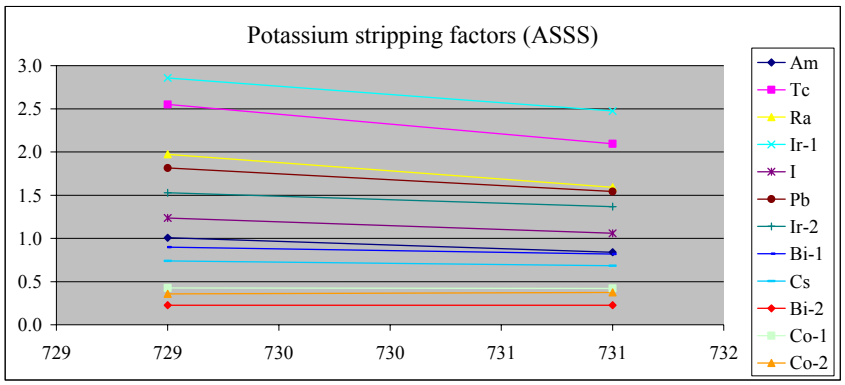

Figure 3.3.2.2. Potassium ASSS factors July 2005.

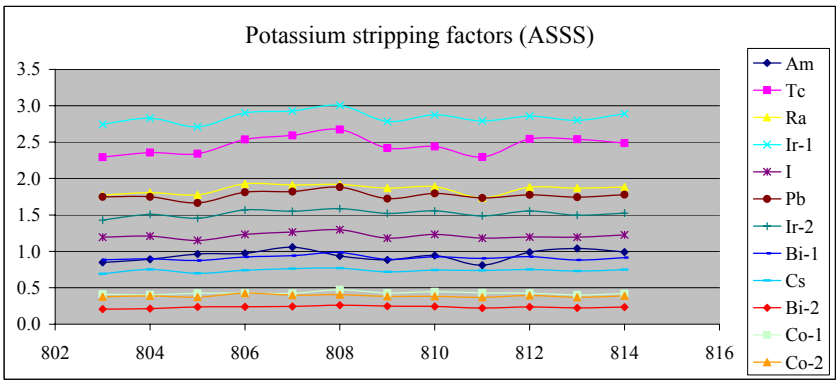

Figure 3.3.2.3. Potassium ASSS factors August 2005.

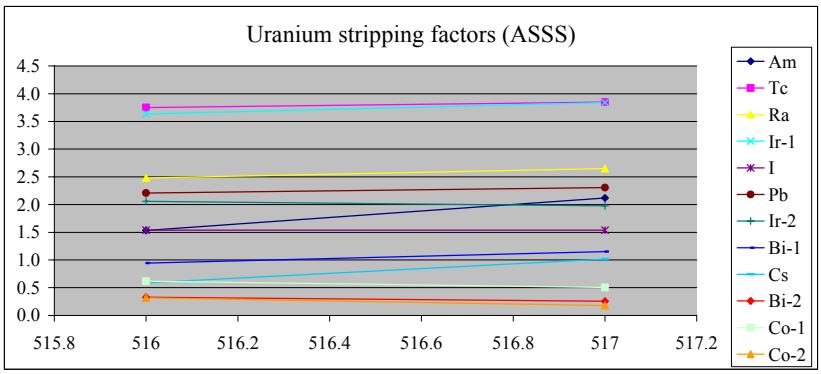

Figure 3.3.2.4. Uranium ASSS factors May 2005.

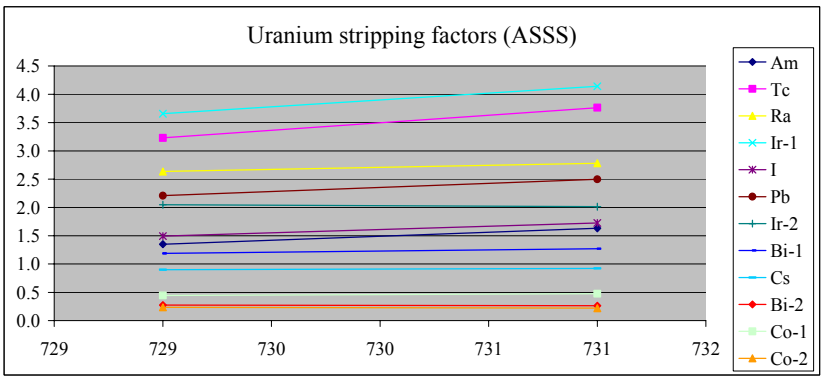

Figure 3.3.2.5. Uranium ASSS factors July 2005.

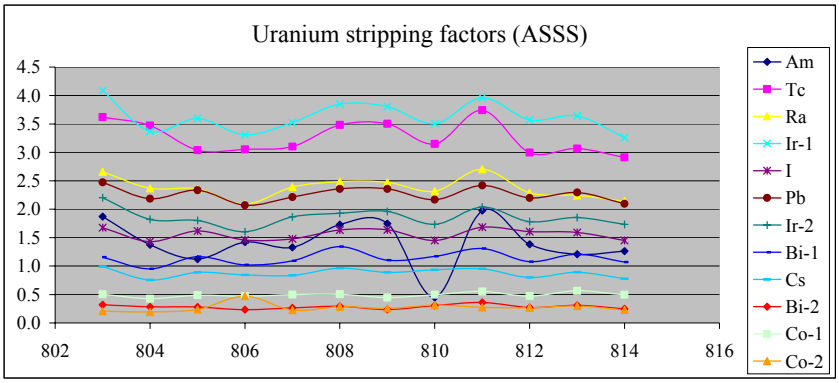

Figure 3.3.2.6. Uranium ASSS factors August 2005.

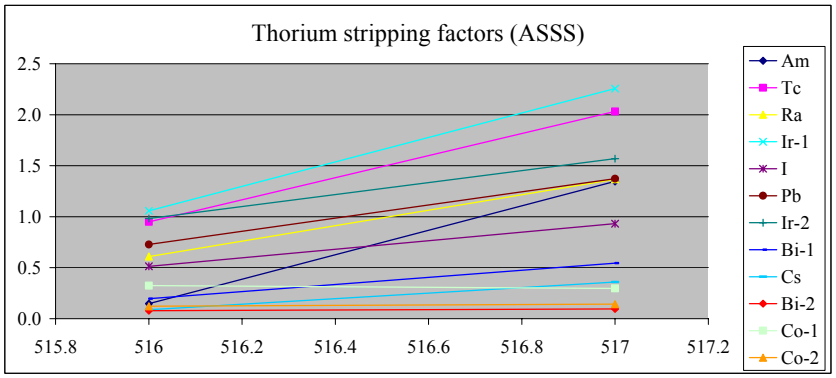

Figure 3.3.2.7. Thorium ASSS factors May 2005.

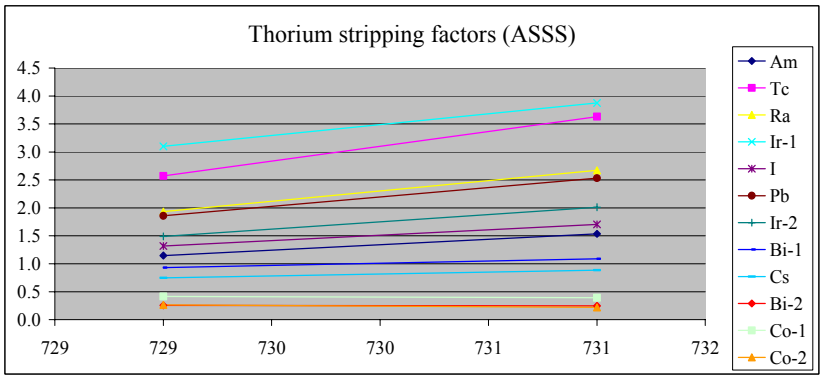

Figure 3.3.2.8. Thorium ASSS factors July 2005.

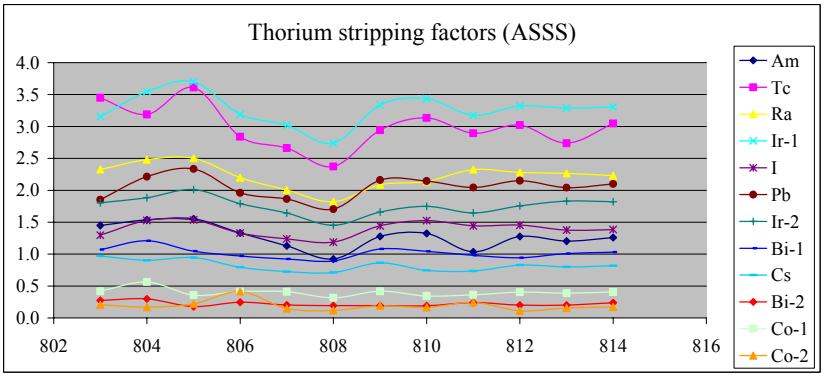

Figure 3.3.2.9. Thorium ASSS factors August 2005.

3.4 Selected Spectra

Here some general and special spectra will be commented on. Some are identified by all or some of the data processing methods, some only by NASVD as being special.

Figure 3.4.1 shows an example of a high caesium count rate spectrum for the file 20050516Highway (Id. 55577). This spectrum has a high content of ^{137}Cs and a higher than usual ^{214}Bi (609 keV) signal compared to the mean spectrum, Figure 3.4.2.
NASVD points to this spectrum with huge signals in S1 (not shown), but none of the data processing methods finds anything special.
FSC which fits the spectra aiming at minimising errors and ASSS that strips the windows does not signal anything due to caesium and uranium both giving strong signals in energy regions that partly overlap each other. The peak hypothesis method does not find anything special here either, possibly related to the width of the peak search area with either peak more or less ”camouflaged by the other”.

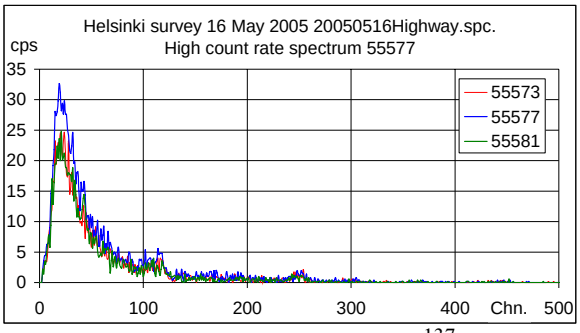

Figure 3.4.1. High count rate for ^{137}Cs.

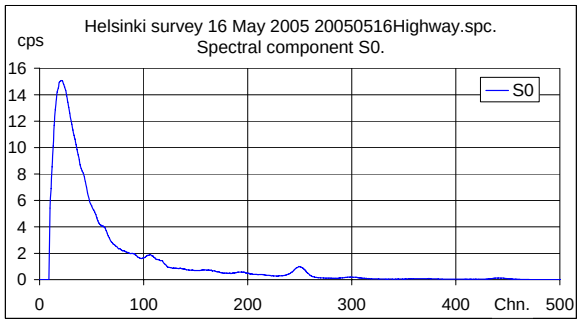

Figure 3.4.2. Mean spectrum.

The following colour plot, Figure 3.4.3, shows the NucSpec representation of spectrum Id 6516 and Id 7058 from the file 20050729. Those measurements show a high degree of symmetry, and one may consider whether this could be an the entrance and exit to a specified area. The same type of signals are found in measurement Id. 7774 and are caused by some natural or manmade (buildings) anomaly which is seen from a comparison of the gross counts for thorium, uranium and potassium that are all very high at those Ids to the ASSS count rates in the low (americium) window. The contribution from the gross count rate to this low energy window is stripped away, i.e. the contribution is "natural" and is not caused by a source.
This natural anomaly is in a reasonably narrow road bordered by a cliff on one side and uplifted railroad on the other side. The cliff ends approximately at the same point were the railroad comes to a bridge hence phasing out all rock and stone from both sides. In addition, when driving southwards, the road comes immediately in vicinity of a bay, lowering the radiation levels even further. A plot of track lines for file 20050729 shows that indeed it is exactly the same spot that has been passed three times, Figure 3.4.4.

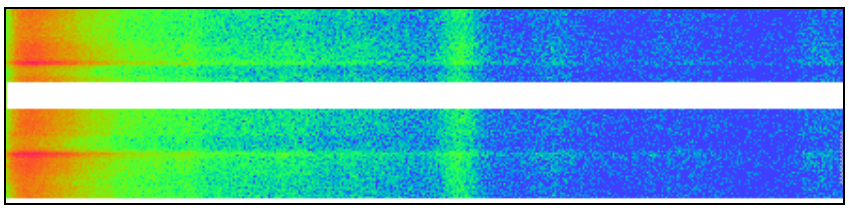

Figure 3.4.3. NucSpec rainbow plot for repeated road feature.

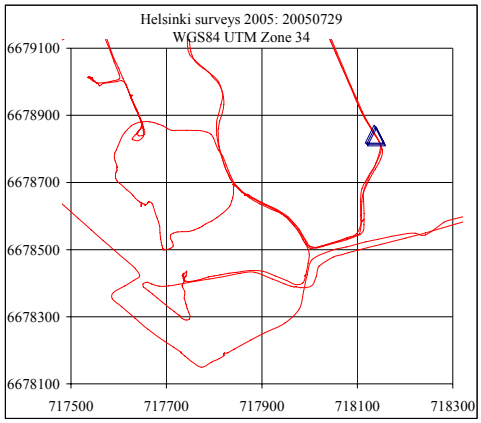

Figure 3.4.4. Track lines showing repeated passage of similiar measurement geometry.

The peak hypothesis method for which the results for the potassium and uranium window (same uranium window as for the ASSS method) are shown in Figures 3.4.5 and 3.4.6 does not come up with anything special here.
The peak hypothesis method therefore must be said not to be the best for looking for anomalies not caused by point sources. FSC based on NASVD also fits away the natural radionuclides.

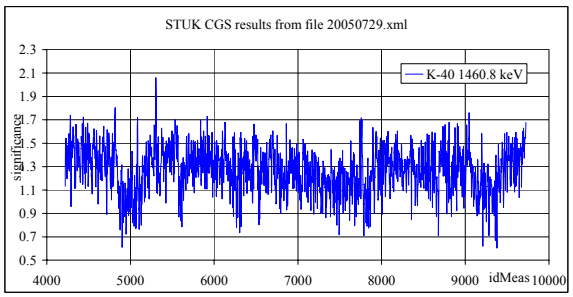

Figure 3.4.5. Potassium significance.

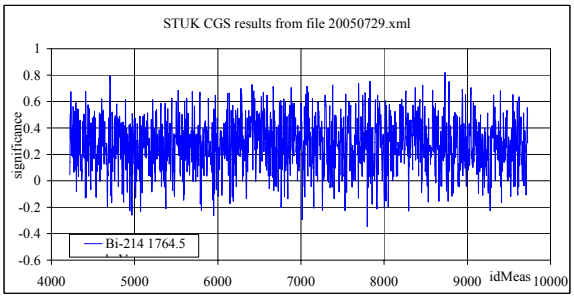

Figure 3.4.6. Uranium (Bismuth) significance.

The same type of signals "not related to a source" is found in an Athletetic's village survey in file 20050731 around measurement Id 11719 and 11786. This time, too, it is same feature driven past twice, Figure 3.4.7. This place is actually a hotel, with a wing pointing east. One can drive below the wing and this was the case during the survey. Under the wing one has concrete beneath, on top of and on the left and right sides of the vehicle. As with the previous case, this spot is located near a bay with reasonable low radiation levels.

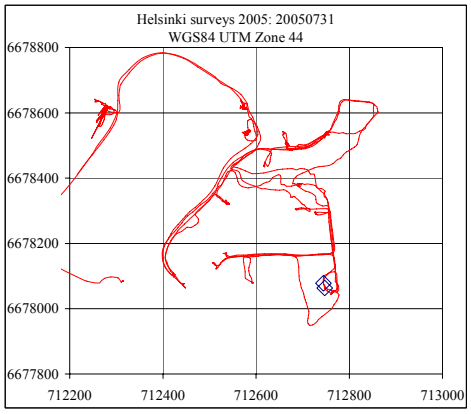

Figure 3.4.7. Athletic Village "peak" signals.

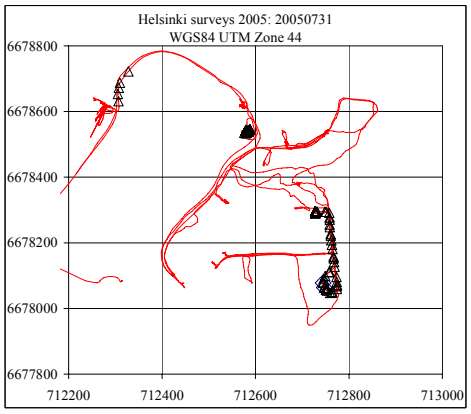

Figure 3.4.8. Athletic Village LT-variations.

During this drive the database input in the measurement system was choked, resulting in fluctuation of standard measurement time between 2 s and 8 s. This "choking" lasted through several sequential spectra as can be seen as horizontal stripes of varying intensity in the NucSpec rainbow plot, Figure 3.4.7.

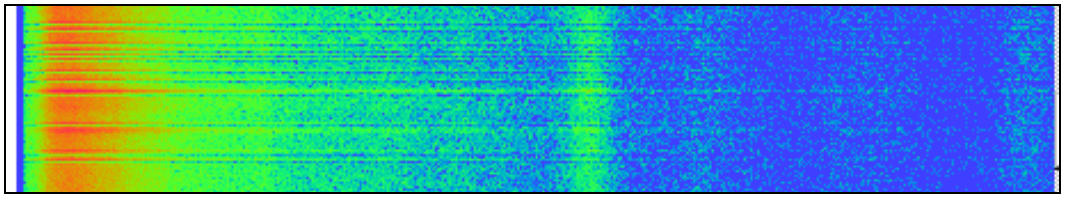

Figure 3.4.7. NucSpec rainbow plot showing live time fluctuations.

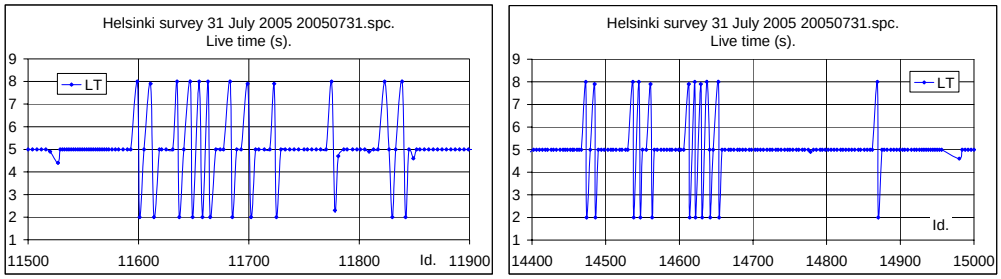

Figure 3.4.8. Measurement groups with live time fluctuations.

Another survey from 5 August 2005 covering the same area shows no signs of live time variation. In this file measurement Id. 21662 in the Otaniemi area is identified as a hot spot, especially with respect to uranium. This is indeed another place of high radiation levels of natural sources. It is a courtyard-like place with 270 degrees of concrete, brick and stone in a circular pattern around the vehicle.

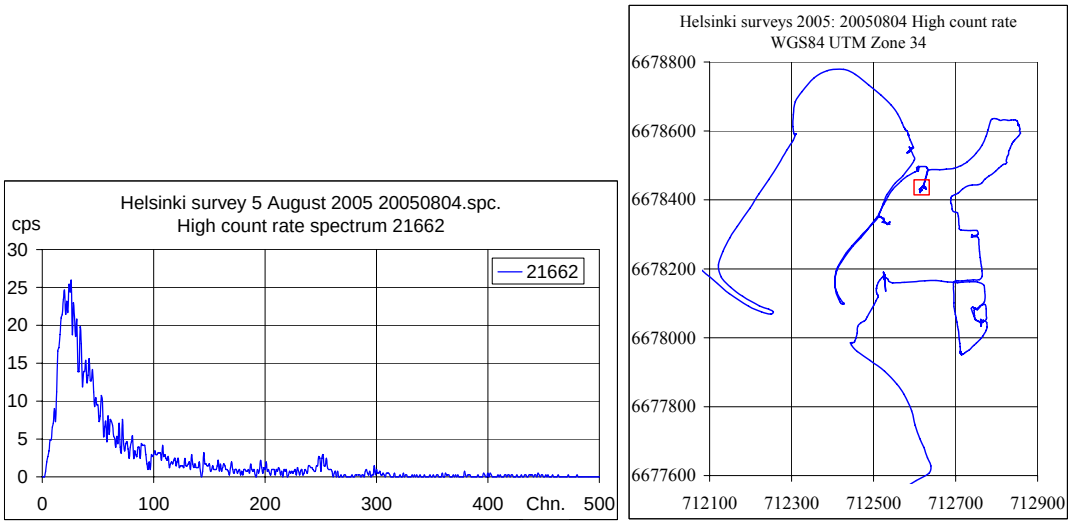

Figure 3.4.9. Hot spot in the Otaniemi area: Spectrum and position (WGS84 UTM zone34).

3.5 STUK: Highway Driving

The files 20050516Highway and 20050517Highway consist of measurements made to and from Helsinki to Vesivehmaa for field tests. The measurements are characteristic in representing a distribution of fall-out of ^{137}Cs increasing in the direction away from Helsinki.

NASVD processing of the data clearly shows the gradual increase (20050516Highway) and decrease (20050517Highway) and is mirrored in the ASSS calculations made on the data sets.

For an area of this character the FSC method, as it is at present, reaches its limit. The contents of ^{137}Cs pollutant are large enough to incorporate ^{137}Cs as a background isotope along with the natural radionuclides. The signal becomes part of the mean spectrum (S0), Figure 3.5.1, and changes in the content of this radionuclide are more ranked as of higher importance than changes to the natural radionuclide compositions which can be seen by the huge caesium signal in spectral component S1. (Note: Often caesium and potassium signals are found to be in anti-phase in rural environments possibly indicating plant substitution of caesium with potassium in areas with low contents of potassium in the ground).

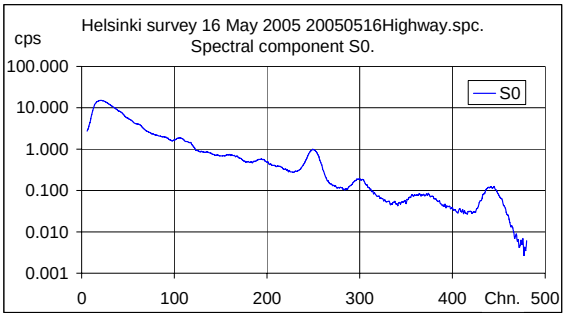

Figure 3.5.1. Mean spectrum.

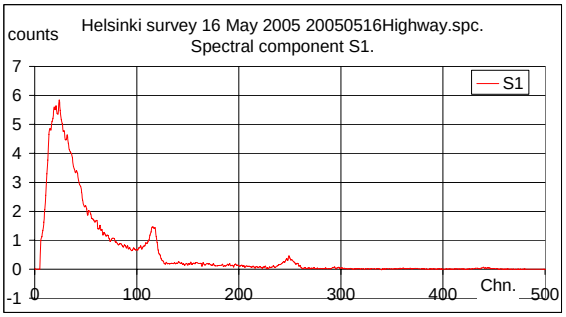

Figure 3.5.2 Spectral componenene S1.

This means that in a contaminated area the FSC method, as it is at present will not be the best method for search for point sources of the same radionuclide as the pollutant. (A possibility would be to change the fitting interval to exclude the channels of interest from the fitting.) Figure 3.5.3 shows the FSC results for file 20050516Highway. No significant spikes are seen. Figure 3.5.4 shows the results from the other Danish method, ASSS. Here a tall spike occurs in the gross counts for measurement No. 54558 that ASSS cannot strip away. This is a point source and consistent with the results found by STUK using a peak hypothesis method. The LINSSI database plot follows the ASSS plot in the same fashion, Figure 3.5.5.

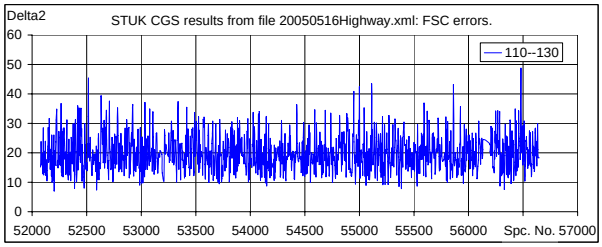

Figure 3.5.3. FSC caesium errors.

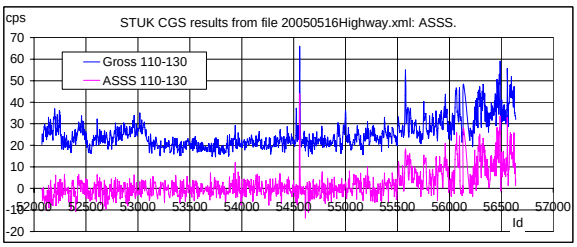

Figure 3.5.4. ASSS caesium count rates.

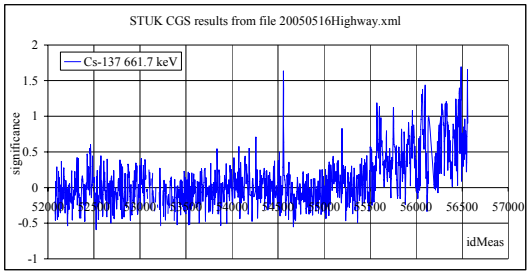

Figure 3.5.5. LINSSI caesium significance plot.

The point source signal is a real signal and originates from a transport vehicle carrying calibration sources to Vesivehmaa airfield. The transport vehicle was passed by SONNI twice, once to the detector side and once opposite the detector side. Neither of the methods is able to identify both passes by of the source vehicle due to the use of two collimated NaI detectors (right and left) for which only the left side NaI detector data has been treated here.

However, since it is known that for these files ^{137}Cs is present as a pollutant, one may cheat in the fitting and base the spectral shapes only on half of the file using measurements containing only weaker signals from the pollutant. Now the FSC shows quite different results. Neither the signal in the caesium window (channel 110-130) or in the partly overlapping bismuth window (609 keV) can be fitted away. Please confer Figure 3.5.6 and Figure 3.5.7. - And the increase in caesium content in and on the ground at the end of file 20050516Highway now shows. Therefore the FSC method is still applicable but should not be used blindly disregarding a spectrum shape analysis prior to the calculations.

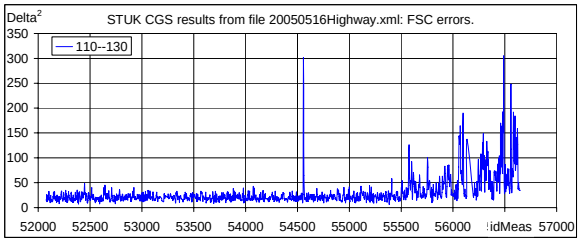

Figure 3.5.6. FSC errors for caesium.

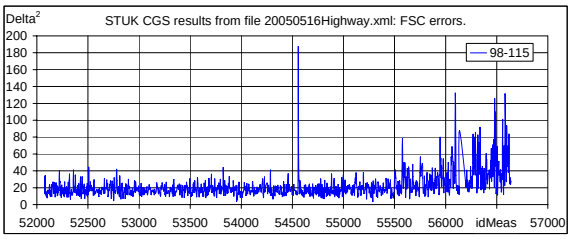

Figure 3.5.7. FSC errors for 609 keV bismuth.

In contaminated areas, the best methods for point source search are the peak hypothesis method or the ASSS method. (The ASSS method is now a standard feature in the software tool NucSpec.)

For mapping of fall-out the ASSS method is at present considered the most efficient tool of the three methods because the stripped count rates are extracted directly from the data sets without further calculations needed. The FSC method will still need optimisation, e.g. fitting spectra but excluding the energy interval of interest from the fitting could be an option. In general the FSC method gives a "cleaner" result not infected by the changes in natural radionuclide composition. But for mapping the error values need to be calibrated.

The file 20050516Highway mentioned above and the results shown tell how a calibration of the error could be done. Here, there are point source and ground contamination signals both. If the strength of the point source was known it would be possible to attribute a (e.g.) kBq/m^2-axis to the error axis. This has yet not been tried. Until the FSC method is included with a user friendly software tool it is for experts when used in contaminated areas.

3.6 Source Signals

Another source signal, this time not intended to be there, is found in the file linssiToXMLtest at measurement Id. 3065 with the LINSSI database coordinates 24.816085, 60.20985333, 22, 1.7. (WGS84 Zone 34-coordinates 711424 6680896). For this measurement also the uranium and potassium count rates peak indicating a very strong source with pile up, Figure 3.6.3 and Figure 3.6.4. In general the count rates are low before and after the source. The source was found with very high significance by all three methods. The ASSS, FSC and peak hypothesis results are shown in the Figures 3.6.5 to 3.6.7.

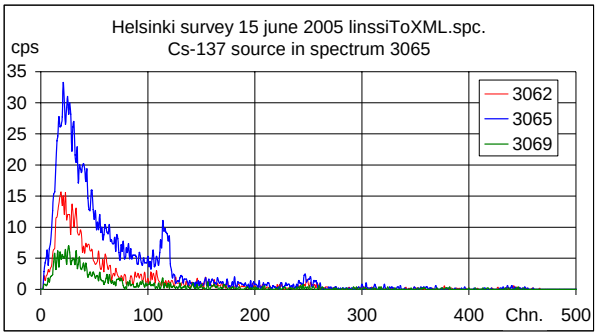

Figure 3.6.1. Caesium source measurement.

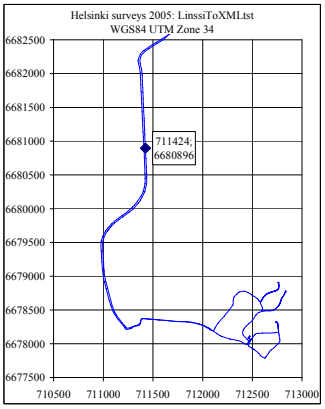

Figure 3.6.2. Map of source position.

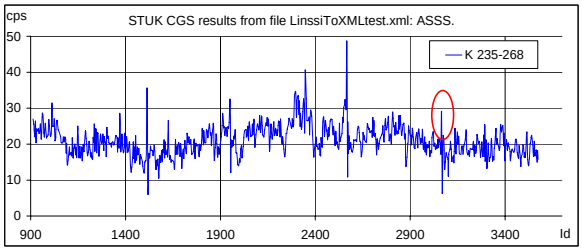

Figure 3.6.3. Potassium gross count rates.

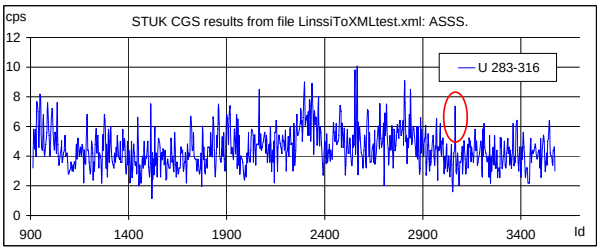

Figure 3.6.4. Uranium gross count rates.

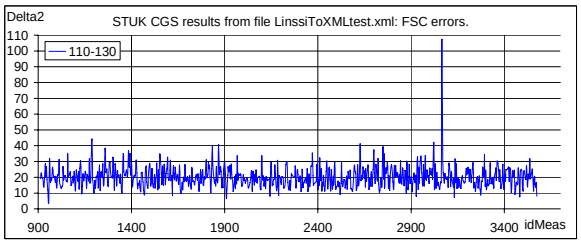

Figure 3.6.5. Source detected by FSC.

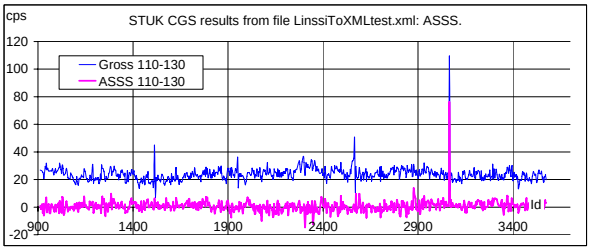

Figure 3.6.6. Source detected by ASSS.

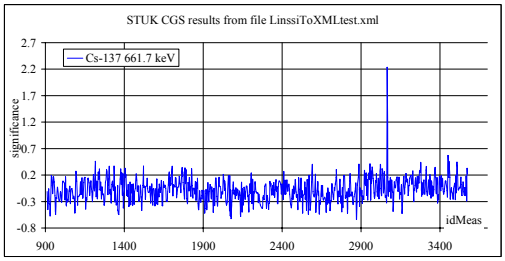

Figure 3.6.7. Source detected by the peak hypothesis method.

The file 20050805 includes the measurements of a medical radionuclide signal from ^{99m}Tc at measurement Id 29252 with the LINSSI database coordinates 24.88893833, 60.19561333, 18, 114.6 (WGS84 Zone 34-coordinates 711424 6680896). The measured spectrum and the source position are shown in Figures 3.6.8 and 3.6.9.

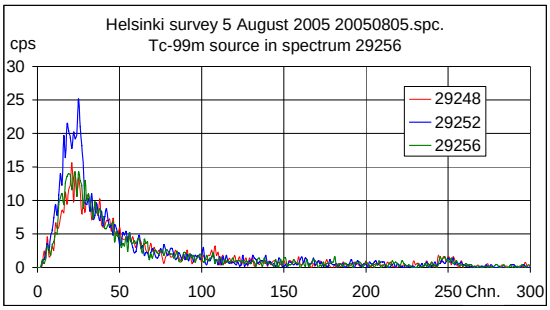

Figure 3.6.8. ^{99m}Tc source measurement.

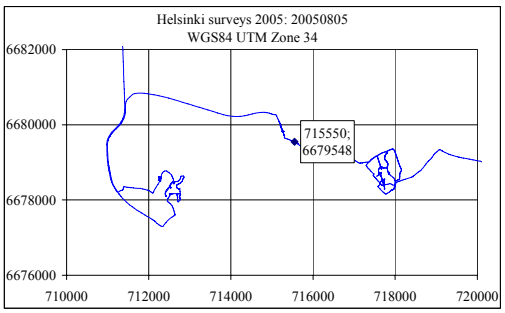

Figure 3.6.9. Map of source position.

This source was detected by all three methods. FSC also indicates other possible sources at measurement Id 30096, Id 30629 and Id 31276, Figures 3.6.10 and 3.6.12. Those measurements are all in the Olympic Stadium area and could be weaker signals from patients undergoing treatment or false alerts.
The peak hypothesis method, Figure 3.6.12, does not find anything of significance here whereas the ASSS method also identifies measurement Id 30629 as an outlayer, however with low source probability, Figure 3.6.11.

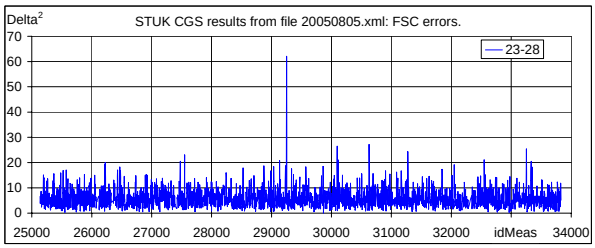

Figure 3.6.10. Source detected by FSC.

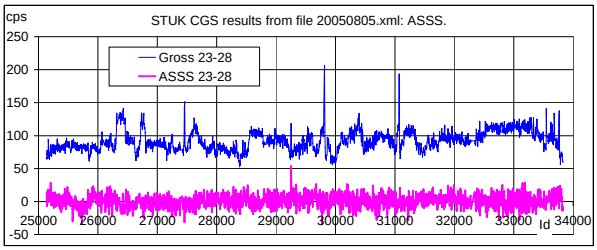

Figure 3.6.11. Source detected by ASSS.

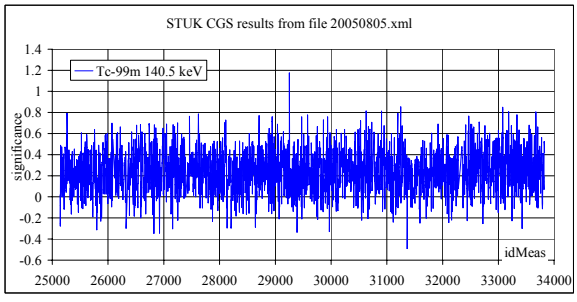

Figure 3.6.12. Source detected by the peak hypothesis method.

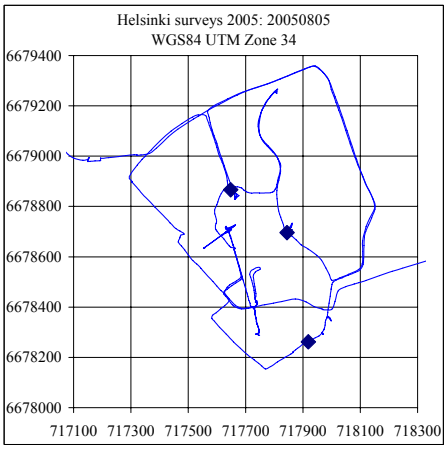

Figure 3.6.13. Additional weak source suggestions by FSC.

In the file 20050812 one more tecnetium source signal is found at mesurement Id 87364 with the LINSSI database coordinates 24.90787.667, 60.19127833, 38, 275.1. Confer the Figures 3.6.14 and 3.6.15. All three data processing tools were able to detect the source.
The technetium source signals in the files 20050805 and 20050812 are only 1.1 km apart, Figure 3.6.18. The reason for the occurrence of the sources is a nearby hospital.
From these surveys, it is clear that the systems used are capable of detecting signals from medical sources, such as technetium, and such signals are also found when sufficient amounts of data are collected in urban areas.

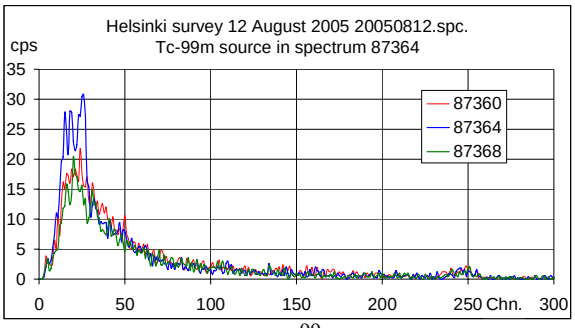

Figure 3.6.14. Another ^{99m}Tc source.

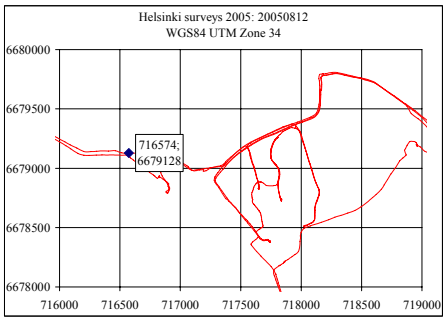

Figure 3.6.15. Map of source position.

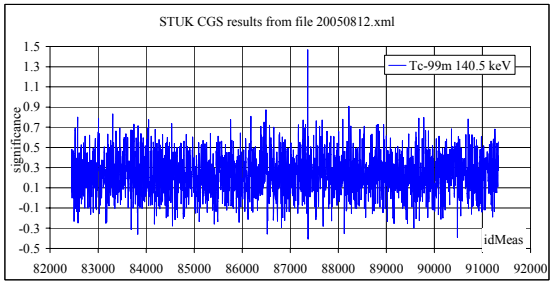

Figure 3.6.15. Source detected by the peak hypothesis method.

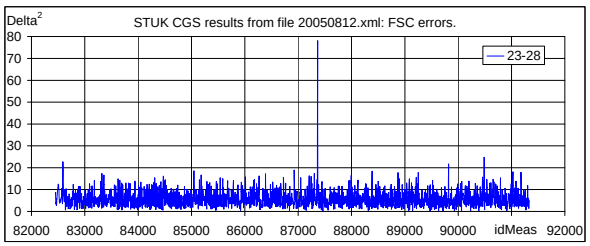

Figure 3.6.16. Source detected by FSC.

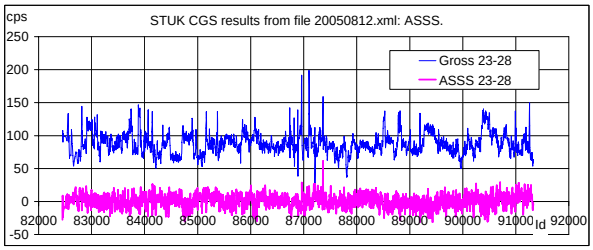

Figure 3.6.17. Source detected by ASSS.

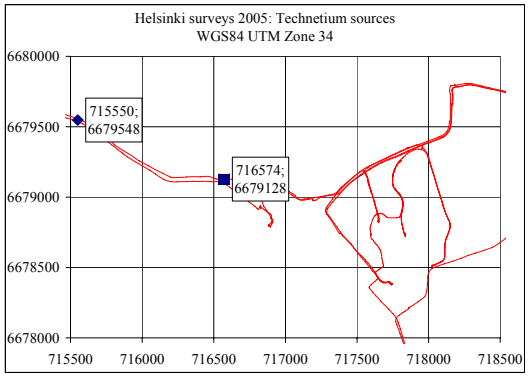

Figure 3.6.18. The two technetium sources found.

3.7 STUK: Calibration Using Point Sources

The file Sweeps cover calibration measurements made at Vesivehmaa airfield. Due to the nature of the file being a calibration measurement file it contains many different combinations of spectral shapes. And using the FSC method with shapes extracted from the file itself is not an option. Instead the spectral components from the file 20050516Highway processed without the stronger, ground level caesium signals can be used.
Since there are no source signals present in the spectral components used (besides a smaller caesium signal) one will obtain errors every time a spectrum containing non-natural radionuclides is attempted fitted. Consider the two figures: Figure 3.7.1 and Figure 3.7.2.

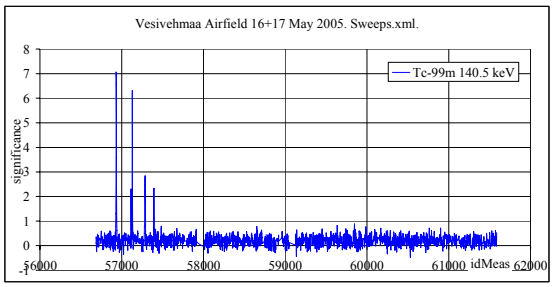

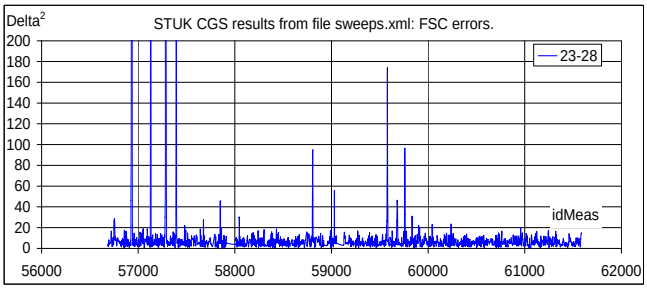

Figure 3.7.1. Peak hypothesis Tc-significance. Figure 3.7.2. FSC errors for technetium.

The figure to the left shows the peak hypothesis results for technetium and the figure to the right shows the FSC results for technetium. There are far more spikes in the figure to the right than in the figure to the left, where the four (double) passes of the sources are the only spikes of significance.
FSC attempts to fit the entire spectrum. In particular strong signals from cobalt and caesium sources will result in large error values also in the technetium window. (One could compare these extra peaks to a full scale of 226129 in technetium error value for measurement No. 58806. Full scale error axis is not shown.)
The peak hypothesis method obtains the following significances for caesium and cobalt:

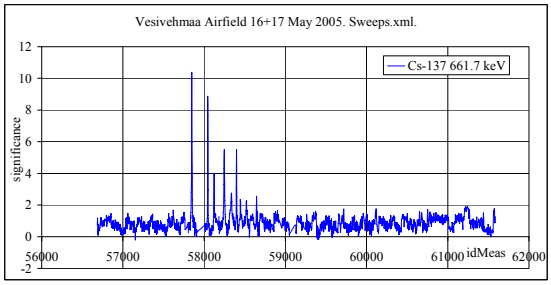

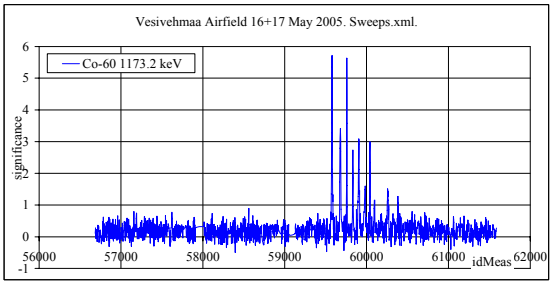

Figure 3.7.3. Peak hypothesis Cs-significance. Figure 3.7.4. Peak hypothesis Co-significance

The corresponding FSC results shown in Figures 3.7.5 and 3.7.6 also present errors in the cobalt window when the caesium sources are passed at the shorter distances.
The reason is that FSC attempts to fit the caesium peak the best way possible which means using the 609 keV peak for ^{214}Bi. ^{214}Bi, however, also has a strong gamma line at 1120.2 keV

that partly overlaps with the 1173 keV line from ^{60}Co. Huge caesium signals therefore also lead to errors in the cobalt window.
The caesium window results, Figures 3.7.5 and 3.7.6 on the contrary does not show significant traces of the cobalt passes although this is to be expected under normal circumstances. The reason is that the number of scattered photons from the cobalt source is few. The maximum caesium error value scale is 25090.

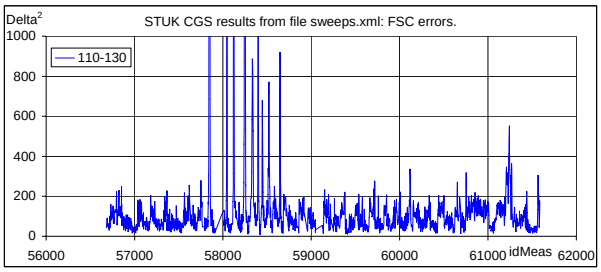

Figure 3.7.5. FSC Cs-errors.

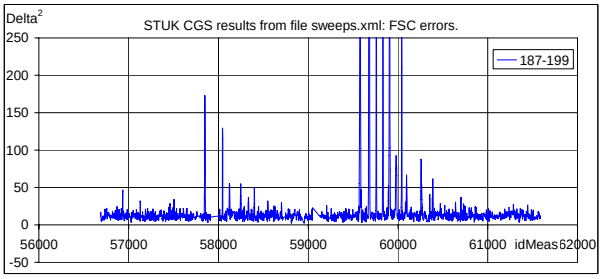

Figure 3.7.6. FSC Co-errors.

ASSS also carries errors from higher energy windows downwards to the lower energy windows but there is no upwards inheritance. The window from the channels 23-28 representing technetium therefore also shows the caesium and cobalt errors and the window from the channels 110-130 shows the cobalt errors along with the caesium errors.
To identify a source as technetium one therefore has to evaluate upper windows for remaining non-stripped counts.
Because ASSS does not fit the spectrum the resulting count rates in the technetium window results from scattered photons. This means that when searching for shielded sources ASSS is superior to the peak hypothesis method whereas for nuclide identification the peak hypothesis method will tell the user which radionuclide with no further evaluation necessary.

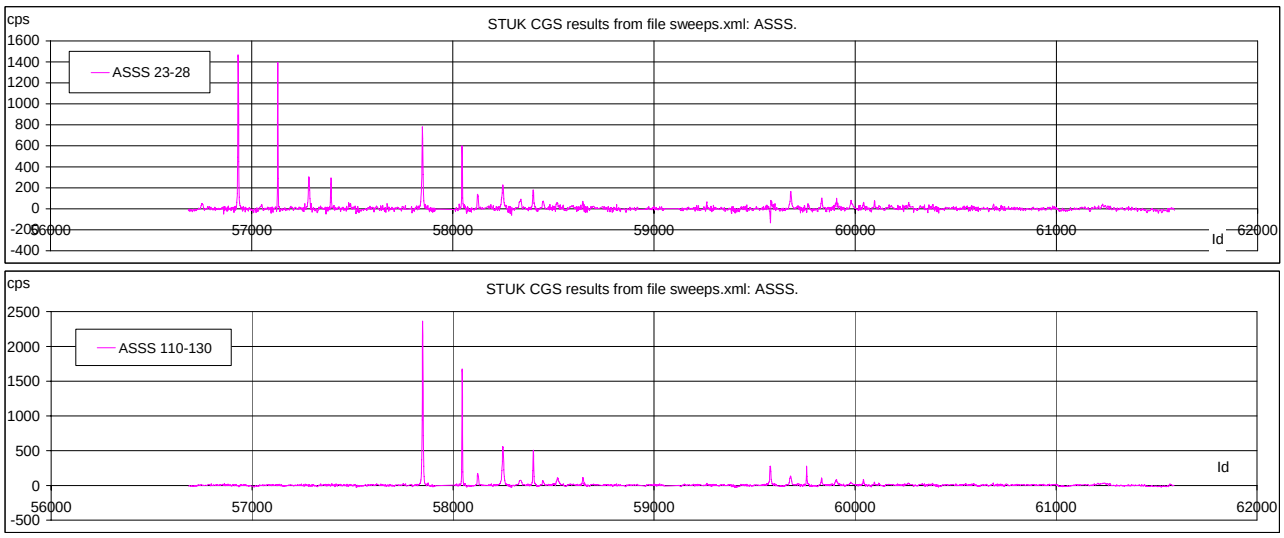

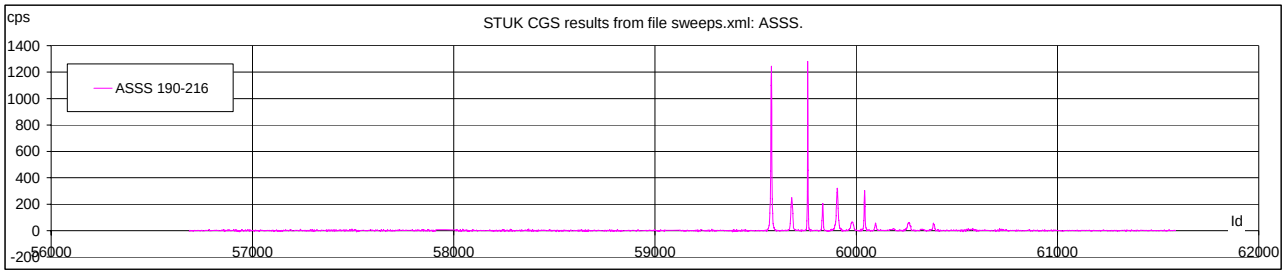

Figure 3.7.7. ASSS count rates for technetium (top), caesium (middle) and cobalt (bottom).

3.8 Repeated Surveys

From the daily routine measurements made at the Olympic Stadium area, Figure 3.8.1, three spots were selected for further data analysis, Figure 3.8.2. Point A is at the survey entrance to the stadium, point B is close to the Olympic Stadium itself (North, close to the black dot in Figure 7.6 in the status report) and point C is also close to the Stadium to the East.

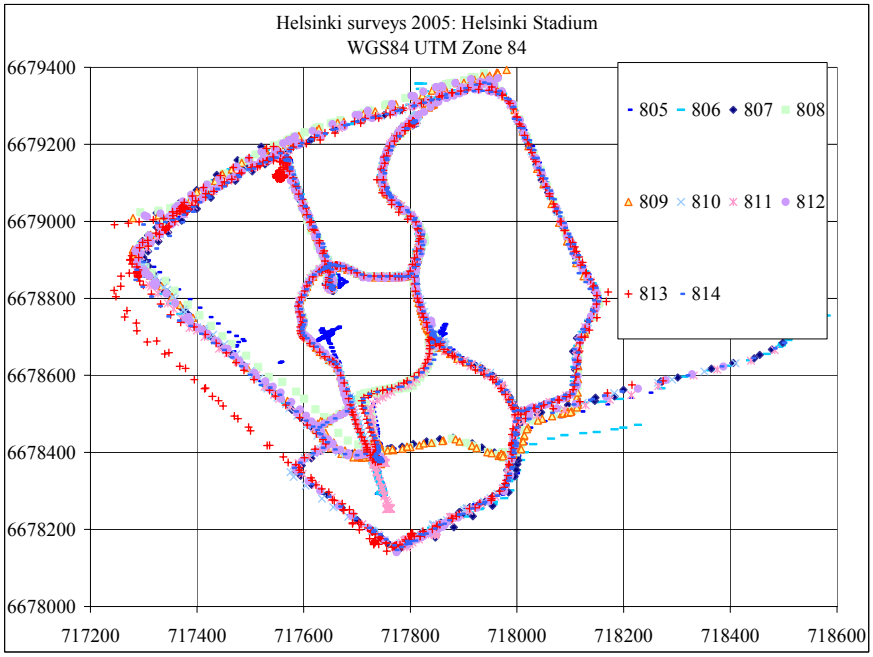

Figure 3.8.1. STUK Survey measurements at the Olympic Stadium area.

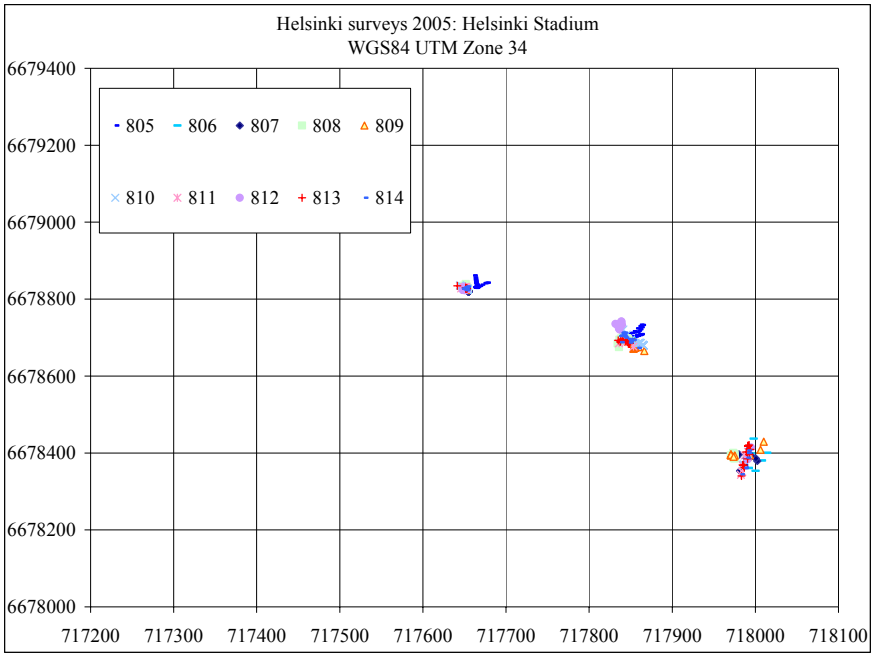

Figure 3.8.2. Selected measurements. Point A, B, and C.

Information about the selected data is shown in Tables 3.8.1 to 3.8.3.

The daily mean values for the FSC results, the ASSS results and the results from the LINSSI database using the peak hypothesis method were plotted as a function of date, see overleaf. It can be seen in the tables where the mean distance from the mean coordinates of each selected Id group to the mean coordinates for all selected measurements for the same point are shown, that there are some "outliers". The measurements were picked by visual inspection attempting to get as close as possible to a common reference point. From some of files more than one group of measurements were selected for the same point, i.e. the point was passed more than once.

Table 3.8.1. Point A: Mean coordinates in WGS84 UTM 34: 717983.6, 6678386, 5.

Date	Measurement Id	Mean coordinates from LINSSI xml files				Mean WGS84 UTM 34		Distance to mean
805	29917-29941	24.93	60.18	4.57	112.01	717986.5	6678370.4	16.4
805	33465-33501	24.93	60.19	14.60	145.92	717970.6	6678390.0	13.4
806	24165-34173	24.93	60.18	6.67	196.83	718007.5	6678378.0	25.3
806	41812-41820	24.93	60.18	4.67	189.90	717995.0	6678398.9	16.8
807	43056-43060	24.93	60.18	1.00	191.15	717985.3	6678370.1	16.5
807	43403-43415	24.93	60.18	4.00	237.08	717994.7	6678388.2	11.2
807	49684-49688	24.93	60.18	7.50	187.60	717989.7	6678389.7	6.9
808	54132-54189	24.93	60.18	8.60	16.64	717973.9	6678394.0	**12.3**
809	60711-60751	24.93	60.18	6.55	20.62	717979.9	6678399.1	13.1
809	61864-61868	24.93	60.18	9.00	98.25	717982.2	6678389.8	3.6
810	66977-67001	24.93	60.18	4.71	27.36	717985.7	6678368.8	17.8
811	74139-74143	24.93	60.18	3.00	190.30	717986.9	6678373.0	13.9
811	75907-75915	24.93	60.18	2.00	183.90	717985.3	6678370.6	16.0
812	83156-83160	24.93	60.18	7.00	193.95	717992.8	6678398.7	15.3

813	91580-91584	24.93	60.18	7.50	190.45	717989.1	6678394.1	9.4
813	93276-93288	24.93	60.18	11.50	94.68	717989.0	6678402.0	16.4
813	98464-98481	24.93	60.18	10.00	188.20	717989.5	6678378.4	10.1
814	102772-102776	24.93	60.18	4.00	191.55	717986.7	6678372.0	14.9
814	109025-109033	24.93	60.18	4.67	192.20	717989.5	6678385.0	6.1

Table 3.8.2. Point B: Mean coordinates in WGS84 UTM 34: 717653.9, 6678828, 3.

Date	Measurement Id	Mean coordinates from LINSSI xml files				Mean WGS84 UTM 34		Distance to mean
805	30706-30883	24.93	60.19	13.58	7.51	717664.0	6678836.0	12.7
806	34599-34668	24.93	60.19	12.56	9.87	717653.0	6678828.5	0.9
807	43722-43798	24.93	60.19	13.95	35.89	717654.7	6678820.9	7.4
808	52353-52421	24.93	60.19	19.28	0.00	717653.6	6678827.8	0.6
808	52515-52559	24.93	60.19	21.33	57.98	717650.7	6678832.3	5.1
809	59897-59957	24.93	60.19	15.15	59.74	717652.1	6678827.9	1.8
810	67538-67662	24.93	60.19	8.44	2.98	717652.7	6678826.9	1.8
811	74570-74618	24.93	60.19	16.33	32.93	717650.4	6678830.1	3.9
812	85526-85642	24.93	60.19	22.31	29.84	717649.9	6678824.6	5.4
813	91958-92001	24.93	60.19	8.42	92.19	717651.4	6678828.3	2.5
814	103076-103158	24.93	60.19	11.77	25.79	717650.5	6678826.1	4.1

Table 3.8.3. Point C: Mean coordinates in WGS84 UTM 34: 717850.5, 6678692, 5.

Date	Measurement Id	Mean coordinates from LINSSI xml files				Mean WGS84 UTM 34		Distance to mean
805	31164-31285	24.93	60.19	18.03	0.00	717851.5	6678707.9	15.4
806	38959-39055	24.93	60.19	14.84	26.59	717848.2	6678693.3	2.5
806	39858-39866	24.93	60.19	27.33	194.87	717839.3	6678696.5	11.9
807	50445-50548	24.93	60.19	8.76	43.46	717847.5	6678695.0	3.9
808	53203-53234	24.93	60.19	23.44	158.60	717841.5	6678692.9	9.0
808	53393-53409	24.93	60.19	16.80	129.96	717844.6	6678698.2	8.3
809	60847-61200	24.93	60.19	11.76	27.69	717855.5	6678680.2	13.3
810	68032-68097	24.93	60.19	17.18	75.01	717858.3	6678685.7	10.4
811	75827-75835	24.93	60.19	16.00	87.43	717844.4	6678683.2	11.1
812	86664-86737	24.93	60.19	34.05	110.36	717836.7	6678731.7	**41.6**
813	92352-92380	24.93	60.19	13.78	70.26	717847.7	6678685.9	7.1
813	93184-93200	24.93	60.19	19.00	60.00	717839.5	6678691.3	11.1
814	103506-103611	24.93	60.19	12.19	89.51	717845.5	6678699.4	8.6
814	104354-104361	24.93	60.19	11.33	208.47	717848.3	6678682.5	10.2

Because the measurements were not made at exactly the same coordinates the fluctuations of the results are very illustrative concerning reproducibility of data. It is believed that it would be very difficult to perform a survey with less uncertainty than shown here.

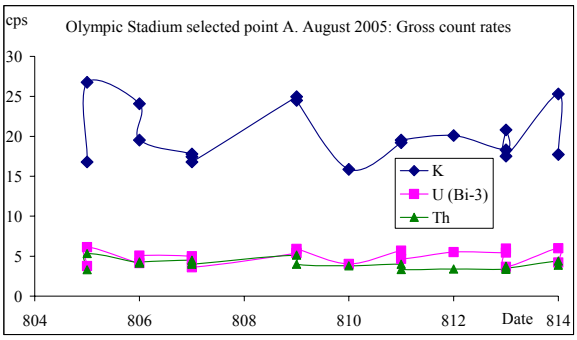

Figure 3.8.3. Gross count rate for the natural radionuclides at point A.

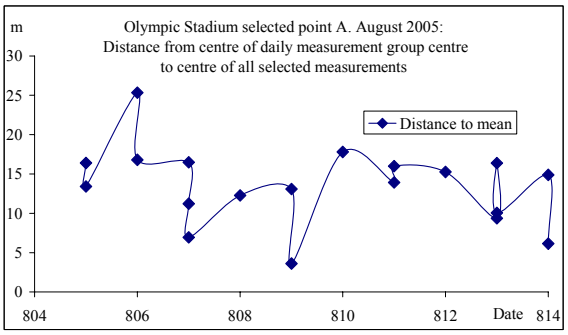

Figure 3.8.4. Distances to centre coordinates for point A.

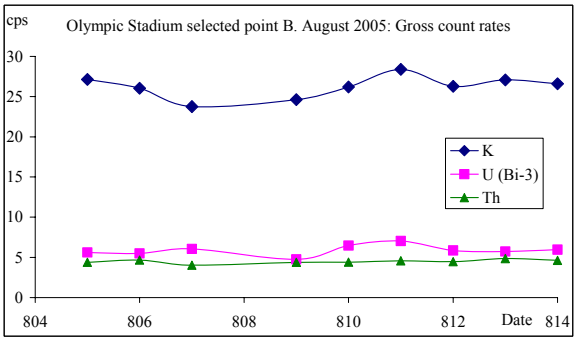

Figure 3.8.5. Gross count rate for the natural radionuclides at point B.

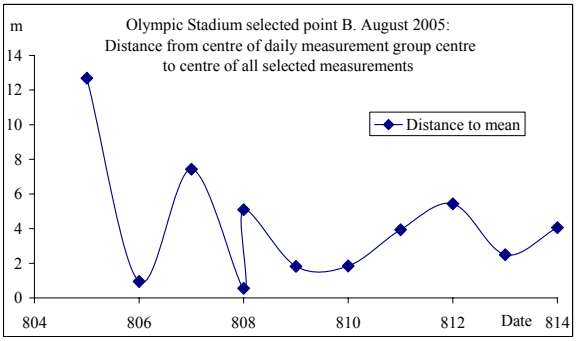

Figure 3.8.6. Distances to centre coordinates for point B.

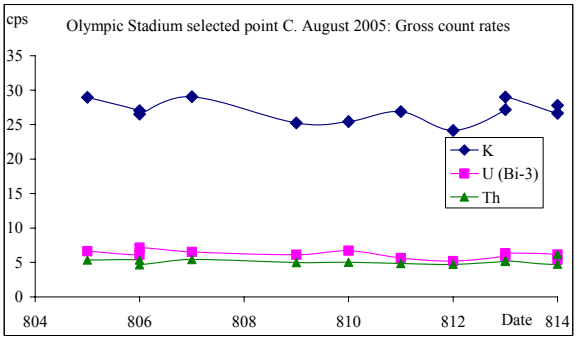

Figure 3.8.7. Gross count rate for the natural radionuclides at point C.

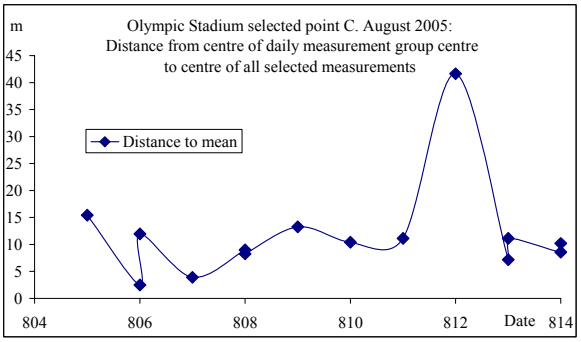

Figure 3.8.8. Distances to centre coordinates for point C.

When comparing the gross count rates (Figures 3.8.3, 3.8.5 and 3.8.7) it can be seen that the results for point B and C are more consistent than for point A. Point A is close to a wide road and sometimes the point was passed in one direction and some times in the other direction. The gross count rates for point A from 7 August (20050807) show the difference found for a road of medium width. In the same way the gross count rates for point C on 13 and 14 August (813 and 814) show the uncertainty for a smaller road.
The survey data quality related to keeping on the same track every day is considered good.

The gross count rates from 8 August (20050805) are not shown due a data processing error. This error, however, is not affecting the results for the FSC and ASSS calculations. The original extracted count rates for the file show normal levels and the error occurred during the sorting of the data using Excel.

To compare the results for the three different methods of data processing six radionuclide windows were selected: Ra, ^{241}Am, ^{99m}Tc, ^{137}Cs and the two windows for ^{60}Co (Co-1 lower energy, Co-2 higher energy). The results are shown as plots with three windows in each plot. For point A the ASSS results are shown in Figure 3.8.9, FSC results in Figure 3.8.10 and peak hypothesis results in Figure 3.8.11.

Point A shows no sources of interest. No significant results are found by the ASSS method. In general the overall result for the low energy windows is slightly positive. (Average ASSS factors for an entire file was used on a few data only.)
FSC and the peak hypothesis method neither shows any suspicious measurements.

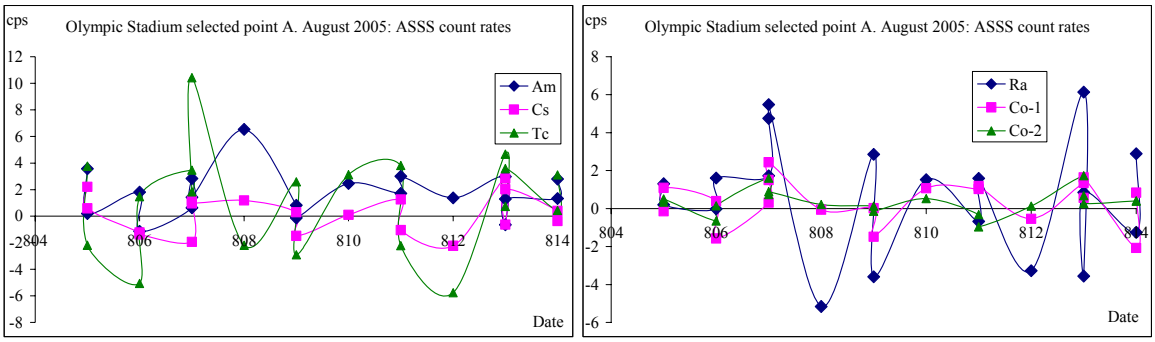

Figure 3.8.9. ASSS count rate for six radionuclide windows at point A.

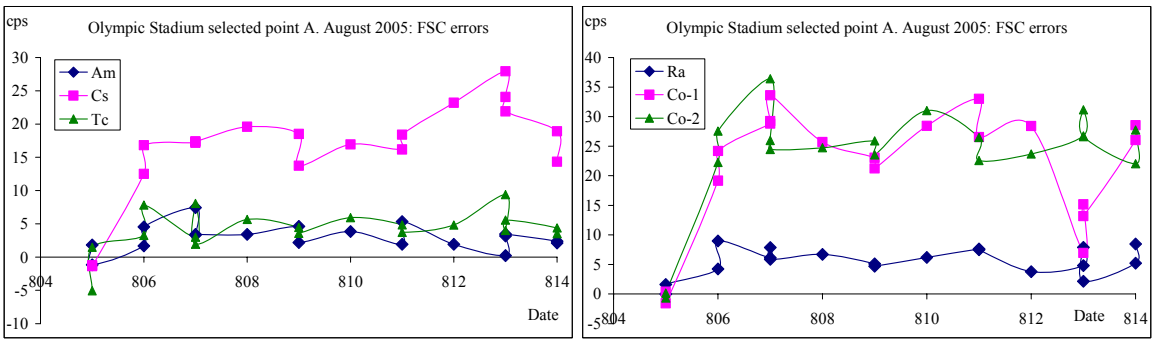

Figure 3.8.10. FSC errors for six radinuclide windows at point A.

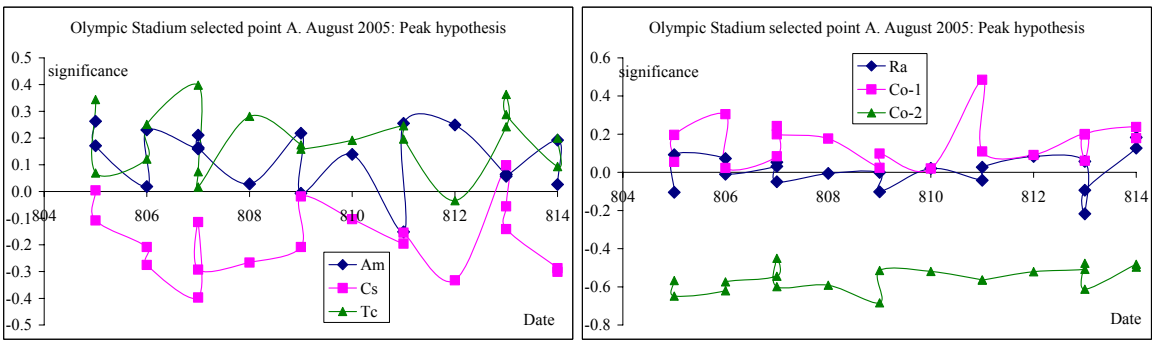

Figure 3.8.11. Peak hypothesis significances for six radinuclide windows at point A.

The FSC errors for point B fluctuates much less than for point A. The reason is thought to be the measurement geometry. Interestingly, the ASSS results show a tendency towards over-stripping in the Ra- and Tc-windows as the days go by. This could mean that at point B some special feature exists that are affected by the number of measurements in the survey file. The first surveys and the latest surveys cover slightly diffent routes. The latter surveys also includes a drive on the marathon route.
The peak hyphothesis method again shows the "negative significances" for the high energy cobalt peak that shares energy interval with ^{40}K. (The corresponding greater than 1 results for potassium is not shown here). The results for point B are shown in Figure 3.8.12 (ASSS), Figure 3.8.13 (FSC) and Figure 3.8.14 (peak hypothesis significance).

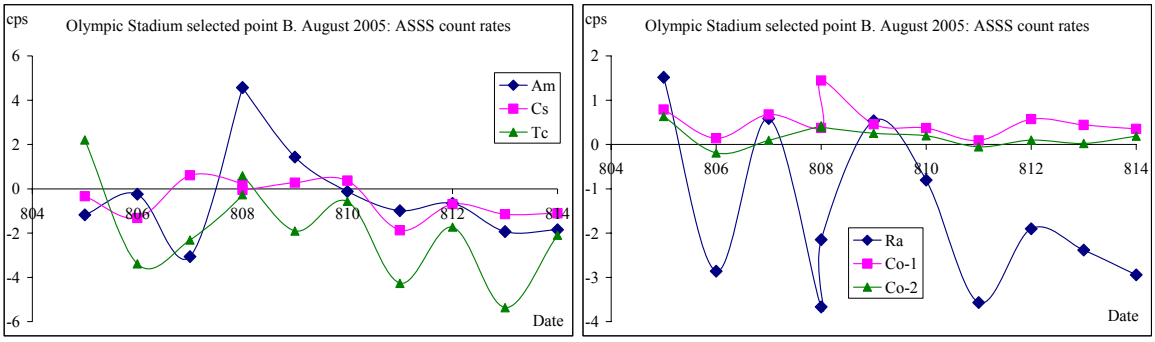

Figure 3.8.12. ASSS count rate for six radionuclide windows at point B.

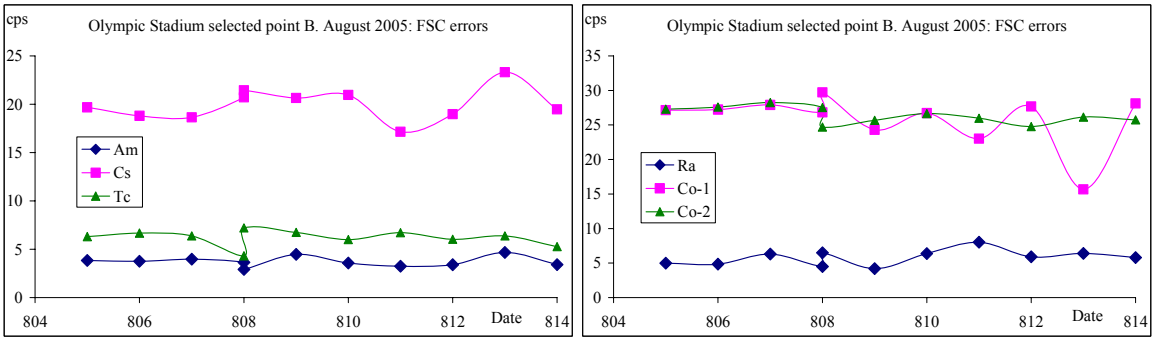

Figure 3.8.13. FSC errors for six radinuclide windows at point B.

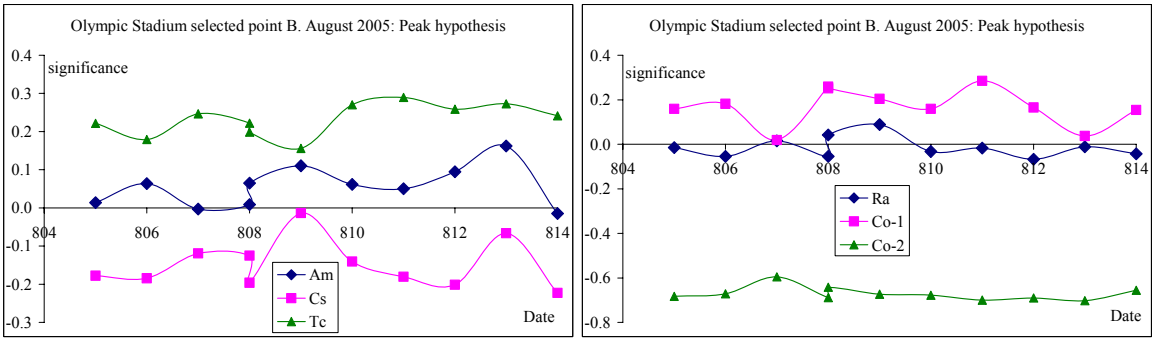

Figure 3.8.14. Peak hypothesis significances for six radinuclide windows at point B.

The peak hypothesis results and the FSC results for point C resemble each other more here than for the points A and B. Again, there is no sign of sources present. The order of

magnitudes of the FSC results depend on the number of channels included with the window. (Please confer the UGS status reports for the mathematical descriptions of the method.) The selected channels are shown in Table 3.2.1.

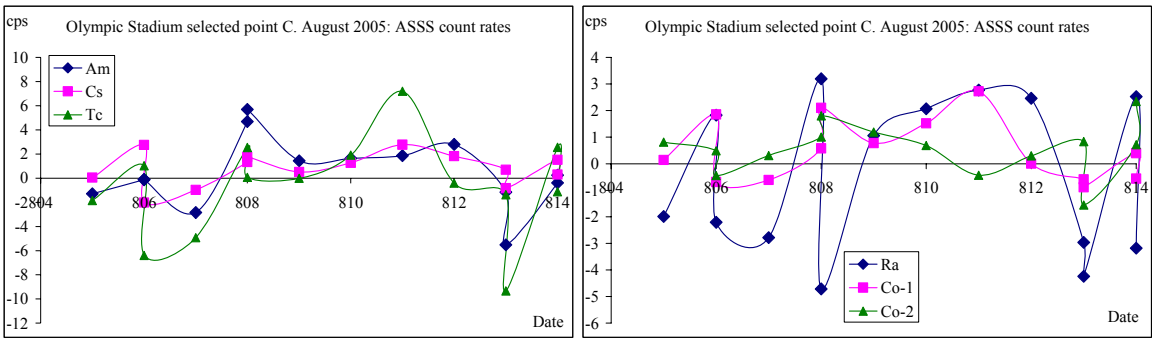

Figure 3.8.15. ASSS count rate for six radionuclide windows at point C.

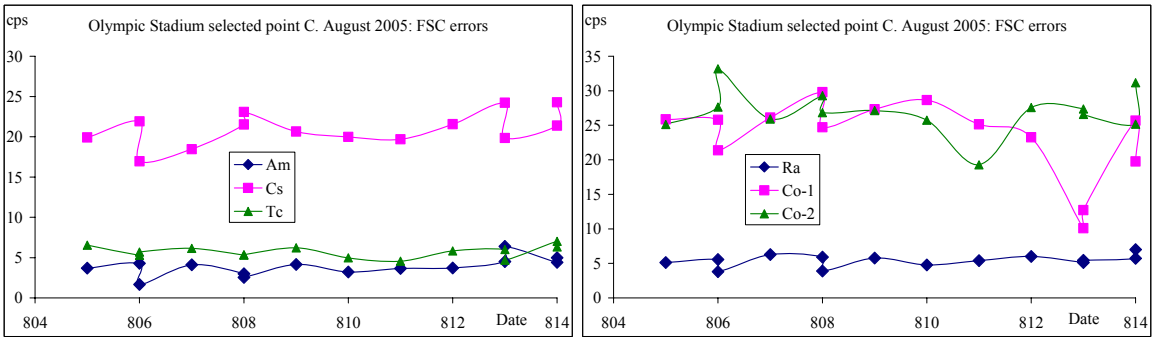

Figure 3.8.16. FSC errors for six radinuclide windows at point C.

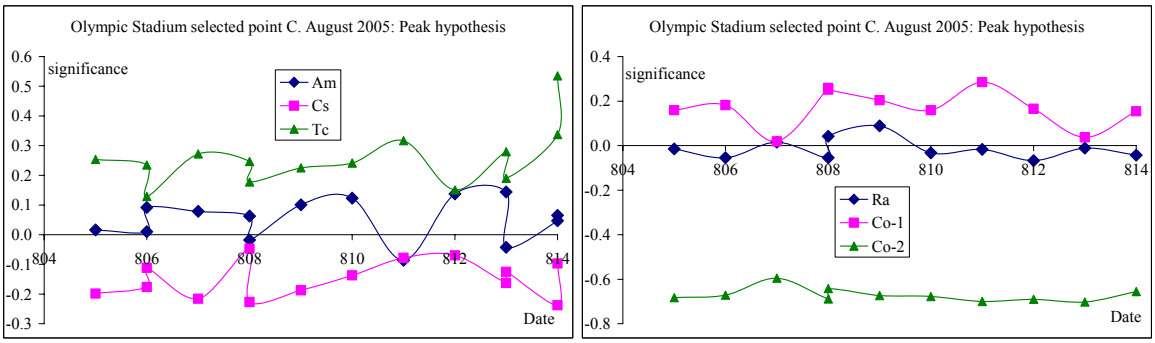

Figure 3.8.17. Peak hypothesis significances for six radinuclide windows at point C.

4 DANISH DATA TREATMENT BY THE FINNISH METHOD

4.1 Importing Measurements from Insitu-xml Format to LINSSI Database

Before running any hypothesis tests to the Danish data, the raw spectral data was put into LINSSI by extracting all needed elements from the xml file resulting from the data conversion from binary .spc files to ASCII files. In the xml file, the same insitu-xml format was used as in transferring the online hypothesis test results from SONNI to STUK (for format description, please see the UGS status report, section 7.3.1).
The Danish station, detector and measurement setup were separately given needed ids for the LINSSI database. An unique id for each of the measurements (measId in LINSSI) were formed by combining the LINSSI keys stationId and detectorId with the measurement start and live times:

measId = stationId_detectorId_measurementStartTime_measurementLiveTime where measurement start time is given in format YYYY/MM/DD_hh:mm:ss.

The original spectrum number in the Danish data set was saved for each spectra in the comments field in the measurements table with <idDKcgs>-tags.

4.2 Applying the Hypothesis Analysis to Danish Data

After the spectra were uploaded to LINSSI, a simple resolution calibration was made with UniSampo. The resolution for peaks with energies at 352 keV and above was made from a sum spectrum of all the spectra measured within a single campaign without any man made sources. Resolution for peaks at energies 100...352 keV were obtained from a separate spectrum with a technetium source in it.
There were some trouble with importing the sum-spectrum and the given energy calibrations as starting from channel 0, which led to making a new energy calibration treating the spectra as they would start from channel 1. For the Danish data files Area051.spc and Area052.spc (see thew UGS status report, section 3.4), the new energy calibration used in the hypothesis test was:

$E=0.00044*(chn)^2+6.07745*(chn)-2.95415$

and the resolution calibration in channels:

$FWHM=2.355*\sqrt{(4.206*10-5*(chn)^2+0.175*(chn)-2.643)}$

4.3 Results for Danish Dataset from Area052 with Added Source Signals

The Danish data for Area052 was delivered as seven separate files each containing the same measured spectra. Six of the files contained eight added signals of one source type and the last file contained only the original measurements. Hence, there were a total of 4826 spectra which were tested 6 times each for the added nuclides with the hypothesis test resulting in total of 28956 tests.

The spectrum shape and the limited resolution of a typical scintillation detector may cause a small bias to the calculated significances. This is called significance offset and is most often caused by a naturally occuring isotope that has a peak nearby the tested peak, e.g. the ^{214}Bi 1120 keV peak protrudes into the ^{60}Co 1173 keV peak calculation area. This means that all given decision limits must be defined with the offset included, i.e. decision limit S>1 becomes S>1+offset. Therefore the significance offsets for each tested nuclide were calculated from the original data prior the hypothesis test and are presented in Table 4.3.1.

Table 4.3.1. Significance offsets for selected nuclides in Danish data and STUK hypothesis testing.

Nuclide	Test peak energy (keV)	Significance offset
^{99m}Tc	140.5	0.1311
^{15}O	511	0.0057
^{137}Cs	662	0.0364
^{60}Co	1173	0.2495

The analysis was run once for each file with kAlpha = 4.753 and type 1 risk level 0.0001 %. This resulted in no findings at significance level 1. In SONNI, breaking the significance level 1 would result in automatic external alarm; i.e. a SDS message to headquarters. The risk level 0.0001% ensures that no more than once in a million tests a false positive occurs. However, the crew gets notification at lower significance level 0.8 (internal alarm level), meaning a 0.0072 % risk for type 1 errors. There were three findings plus one type 1 error at this decision limit in the Danish data.

These two levels are used for automated alarms and tests online. However, in postprocessing, it is possible to query the database with higher risk levels and exclude all the false alerts manually in search of smaller signals. If an orphan source of a known nuclide has to be found, one could set the decision limit for internal alarms significantly lower, say, to 0.6 which would lead to two incidents of type 1 alarms in a thousand measurements.

Table 4.3.2 gives the count of found signals and type 1 errors at six different risk and significance levels. In brief, the most notable results are:

1. ^{99m}Tc was not found regardless of the tested decision limits. In fact, the maximum calculated raw significance for a spectrum with a source is only 0.39. With the 0.13 offset taken into account, the maximum significance stays well below 0.3. Lowering the decision limit further would make the count of type 1 errors too big to handle.
2. Naturally, if the tested peak is fully scattered, as is the case with the CoScat source here (^{60}Co source with no primary peaks, only scattered photons), it is very unlikely to be found with this hypothesis test focusing solely on the primary peak.
3. If there is a definitive peak available, around half of these signals can be spotted with reasonable type 1 frequency 0.22% (see the ^{137}Cs and ^{60}Co peaks with decision limit S=0.6)

In table 4.3.3, the found signals are tabulated by the used source and by the spectrum where the extra counts were added to.

Table 4.3.2. Number of detected signals and type 1 errors depending on the decision limit, S. The total number of tests was 28956 and the total number of real signals 48.

k_α	S	Theoretical risk for type 1 errors (%)	Found signals	Type 1 errors	Experimental risk for type 1 errors (%)
4.753	1.0	0.0001	0	0	0.000
3.803	0.8	0.0072	3	1	0.003
3.326	0.7	0.0440	7	9	0.031
2.848	0.6	0.2200	14	63	0.218
2.326	0.49	1.0000	22	255	0.881
1.645	0.35	5.0000	28	1265	4.370

The calculated significances for the Danish data are plotted in Figures 4.3.1 to 4.3.6. It can be seen that apart from the three cases at level S>0.8 with Bmb60Co (Figure 4.3.2) and CsLab (Figure. 4.3.4) sources the signals do not clearly differentiate from the background noise. The only type 1 error at this level is seen on the left hand side of the ^{99m}Tc plot (Figure 4.3.6).

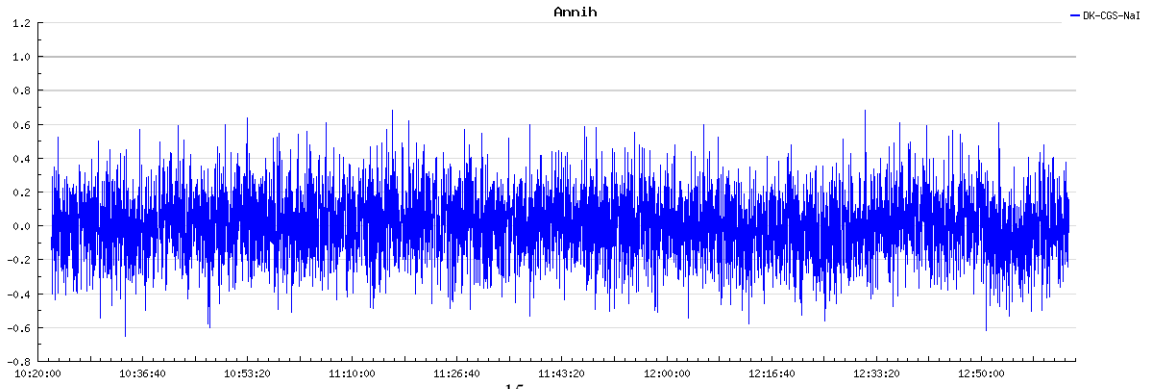

Figure 4.3.1. Raw significance plot for ^{15}O source. The decision limits including any possible bias in the significance (offset) for external and internal limits are plotted with dark and light grey thick lines. Significance for the 511 keV annihilation peak has only negligible positive bias (see Table 4.3.1) and hence these limits are in practise 1 and 0.8.

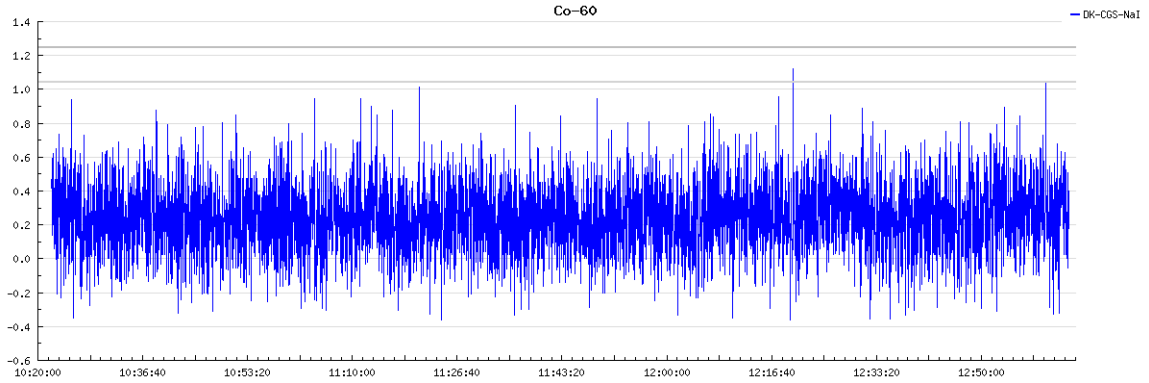

Figure 4.3.2. Raw significance plot for the Bmb60Co source. For explanations, see Figure 4.3.1. Decision limits are due to the offset 1.05 and 1.25.

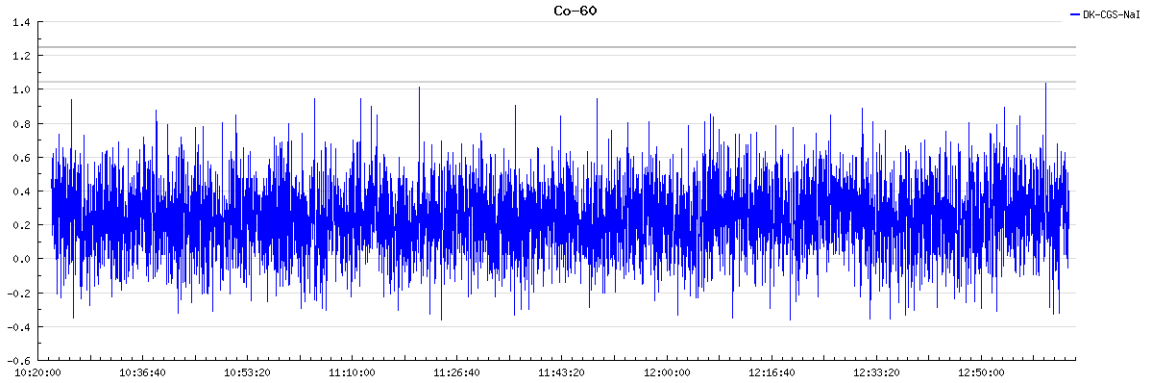

Figure 4.3.3. Raw significance plot for the CoScat source. For explanations, see Figure 4.3.1. Decision limits are due to the offset 1.05 and 1.25.

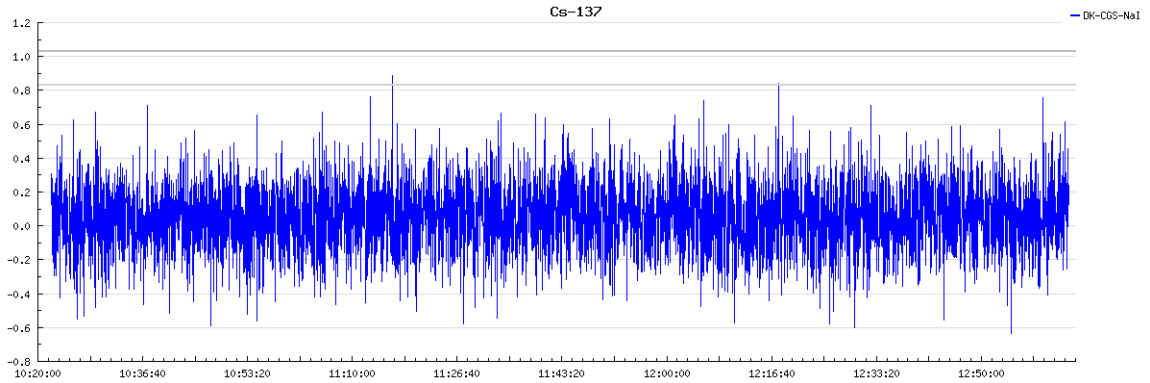

Figure 4.3.4. Raw significance plot for the CsLab source. For explanations, see Figure 4.3.1. Decision limits are due to the offset 0.84 and 1.04

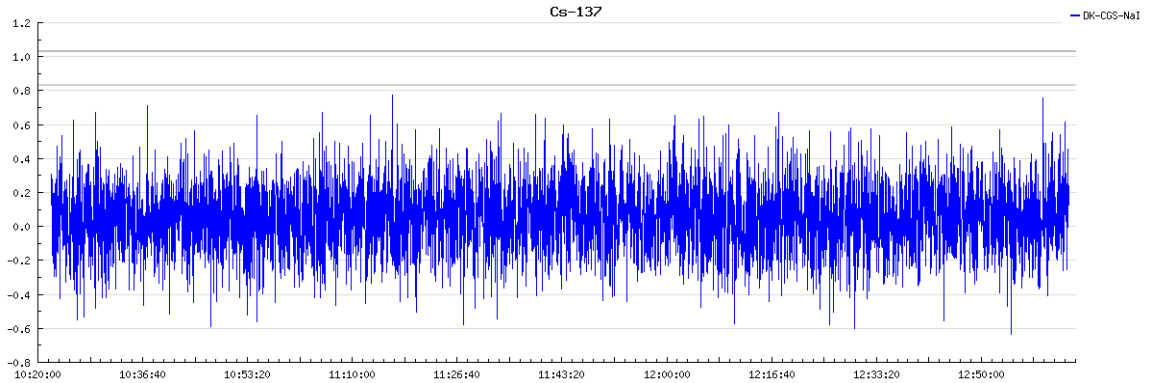

Figure 4.3.5: Raw significance plot for the CsPeak source. For explanations, see Figure 4.3.1. Decision limits are due to the offset 0.84 and 1.04.

On the right hand side of the ^{99m}Tc plot there is a huge signal. From a detail plot in Figure 4.3.7 it can be seen that the signal is visible in more than one measurement. This is most probably a similar case as the findings with SONNI during the Athletics WC2005. It can be stated that, though the hypothesis test is insensitive to the added ^{99m}Tc source signals, it is sensitive enough to spot the nuclide in amounts used in medical treatments. This spectrum is compared to spectrum no 4335 with added ^{99m}Tc source in Figure 4.3.8. It gives some idea about the needed scale of a ^{99m}Tc signal that can be seen with the hypothesis test.

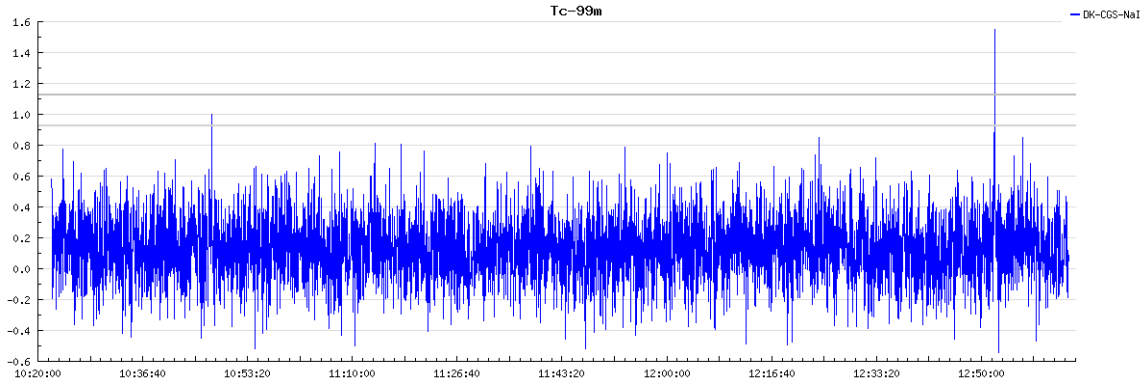

Figure 4.3.6. Raw significance plot for the ^{99m}Tc source. For explanations, see Figure 4.3.1. Decision limits are due to the offset 0.93 and 1.13.

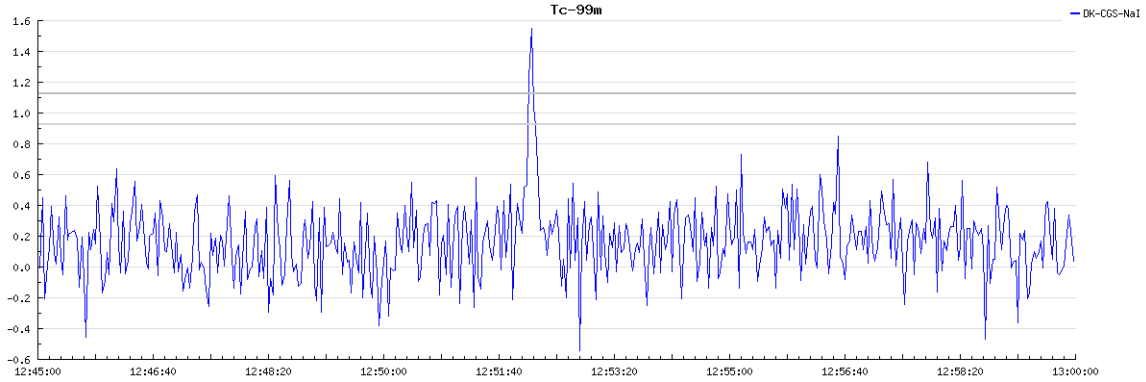

Figure 4.3.7. Detail from the ^{99m}Tc significance plot showing the ^{99m}Tc source. For explanations, see Figure 4.3.1.

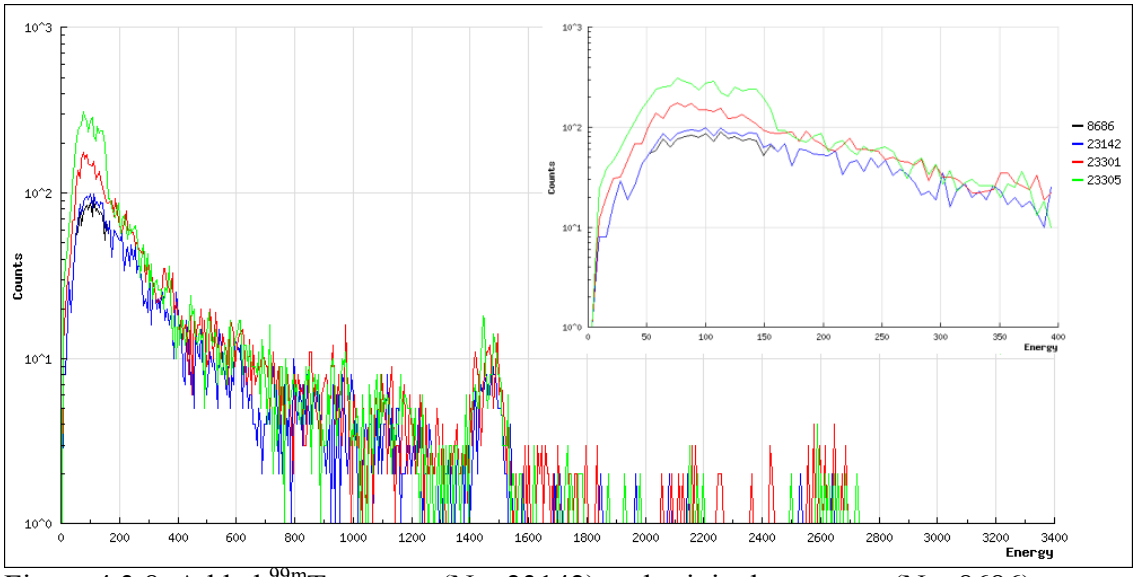

Figure 4.3.8. Added ^{99m}Tc source (No. 23142) and original spectrum (No. 8686) compared with ^{99m}Tc "medical size" source (No. 23305) and nearby background (No. 23301). Spectrum numbers here are the idMeas keys in Linssi database, not the original Danish numbers.

Table 4.3.3. Found signals by source and spectrum, depending on the decision limit, S. For each source, the total number of tests was 4826 and the total number of real signals 8. For source and spectral characteristics, see Status Report,Sections 3.7.1 and 3.6.

O-15

Spectrum No	1522	1625	2282	3109	3466	3537	3907	4335			
Found with type 1 risk (%)									Found signals	Type 1 errors	Experimental risk for type 1 errors (%)
0.0072	0	0	0	0	0	0	0	0	0	0	0.000 %
0.044	0	0	0	0	0	0	0	0	0	0	0.000 %
0.22	0	1	0	0	0	0	0	0	1	6	0.124 %
1	0	1	1	0	0	0	0	1	3	35	0.725 %
5	1	1	1	0	1	0	0	1	5	187	3.875 %

Bmb60Co (Co-60 source with clear primary peaks)

Spectrum No	1522	1625	2282	3109	3466	3537	3907	4335			
Found with type 1 risk (%)									Found signals	Type 1 errors	Experimental risk for type 1 errors (%)
0.0072	0	0	0	0	0	1	0	0	1	0	0.000 %
0.044	0	0	0	0	1	1	0	0	2	2	0.041 %
0.22	0	1	0	0	1	1	0	0	3	13	0.269 %
1	0	1	1	0	1	1	0	1	5	41	0.850 %
5	0	1	1	1	1	1	1	1	7	213	4.414 %

Tc-99m

Spectrum No	1522	1625	2282	3109	3466	3537	3907	4335			
Found with type 1 risk (%)									Found signals	Type 1 errors	Experimental risk for type 1 errors (%)
0.0072	0	0	0	0	0	0	0	0	0	1	0.021 %
0.044	0	0	0	0	0	0	0	0	0	3	0.062 %
0.22	0	0	0	0	0	0	0	0	0	13	0.269 %
1	0	0	0	0	0	0	0	0	0	56	1.160 %
5	0	0	0	0	0	0	0	0	0	238	4.932 %

CsLab (Cs-137 source measured in laboratory with distinctive primary peak and almost no scattered photons)											
Spectrum No	1522	1625	2282	3109	3466	3537	3907	4335			
Found with type 1 risk (%)									Found signals	Type 1 errors	Experimental risk for type 1 errors (%)
0.0072	0	1	0	0	1	0	0	0	2	0	0.000 %
0.044	1	1	0	1	1	0	0	0	4	1	0.021 %
0.22	1	1	0	1	1	1	1	0	6	9	0.186 %
1	1	1	0	1	1	1	1	1	7	41	0.850 %
5	1	1	1	1	1	1	1	1	8	207	4.289 %
CsPeak (Cs-137 source measured in field with lots of scattered photons)											
Spectrum No	1522	1625	2282	3109	3466	3537	3907	4335			
Found with type 1 risk (%)									Found signals	Type 1 errors	Experimental risk for type 1 errors (%)
0.0072	0	0	0	0	0	0	0	0	0	0	0.000 %
0.044	0	1	0	0	0	0	0	0	1	1	0.021 %
0.22	1	1	0	1	1	0	0	0	4	9	0.186 %
1	1	1	0	1	1	1	1	0	6	41	0.850 %
5	1	1	0	1	1	1	1	1	7	207	4.289 %
CoScat (Co-60 source with no primary peaks, just scattered photons)											
Spectrum No	1522	1625	2282	3109	3466	3537	3907	4335			
Found with type 1 risk (%)									Found signals	Type 1 errors	Experimental risk for type 1 errors (%)
0.0072	0	0	0	0	0	0	0	0	0	0	0.000 %
0.044	0	0	0	0	0	0	0	0	0	2	0.041 %
0.22	0	0	0	0	0	0	0	0	0	13	0.269 %
1	0	0	0	0	0	1	0	0	1	41	0.850 %
5	0	0	0	0	0	1	0	0	1	213	4.414 %

4.4 Results of the Finnish Dataset

For this NKS project, the Finnish data was reprocessed for producing the same data on type 1 errors as a function of the decision limit as were done for the Danish data (Table 4.3.2). The results for the Finnish data are presented in Table 4.4.1.

Table 4.4.1. Number of detected signals and type 1 errors depending on the decision limit, S. The total number of tests was 216024 and there were two real signals that are known of.

k_α	S	Theoretical risk for type 1 errors (%)	Found signals	Type 1 errors	Experimental risk for type 1 errors (%)
4.753	[1)]1.0	0.0001	1	0	0.000
3.803	[2)]0.8	0.0072	1	16	0.007
3.326	0.7	0.0440	2	79	0.037
2.848	0.6	0.2200	2	364	0.168
2.326	0.49	1.0000	2	1701	0.787
1.645	0.35	5.0000	2	9570	4.43

[1)]Decision limit for external alarms in SONNI [2)]Decision limit for internal alarms in SONNI

During this postprocessing a previously overlooked signal was identified as a ^{99m}Tc source and thus the dataset contains two sources instead of the one reported previously. The source was observed to lay within 1.5 km from the same hospital as the previous one. Significance plot around this "new" source is presented in Figure 4.4.1. The ^{99m}Tc peak has a positive bias of 0.213 and hence the decision limit for internal alarms and hence the signal falls just little below the internal alarms decision limit of 1.013 (0.8 without offset). In Figure 4.4.2, the signal spectrum is plotted with a background spectrum measured 5 seconds earlier.

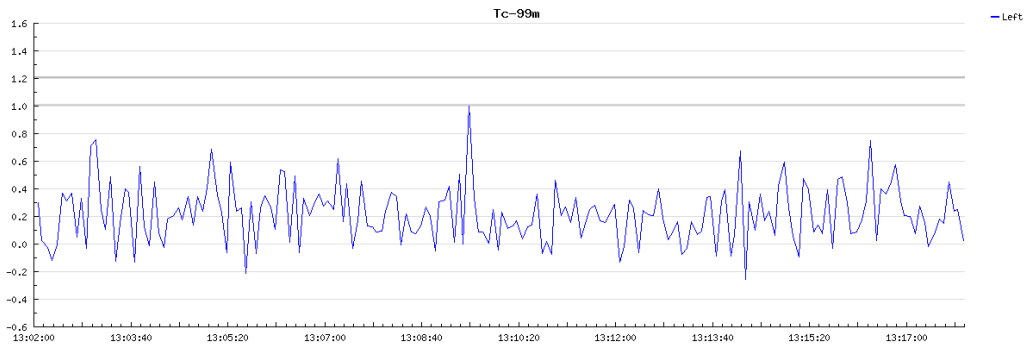

Figure 4.4.1. Significance plot around the second instance of ^{99m}Tc.

When comparing figures 3.6.12 and 4.4.1, describing the same event detected with the same method (peak hypothesis), one notes that the calculated significance is different. This is due to a 0/1 mistake. The peak hypothesis test results which were sent to Denmark were done with an analysis that shifted the 1024 channel spectrum +1 channel forwards in analysis.

Since the hypothesis analysis forgives 1-2 channels fluctuation in the energy calibration, the difference is not fatal (it hasn't affected the results in a sense of source finding capability) but it changes the significance offset and detected signifi-cance values in the 120 keV region where the baseline of the spectrum is farthest away from linear. Significances calculated for higher energy sources, such as Cs-137 are essentially the same.

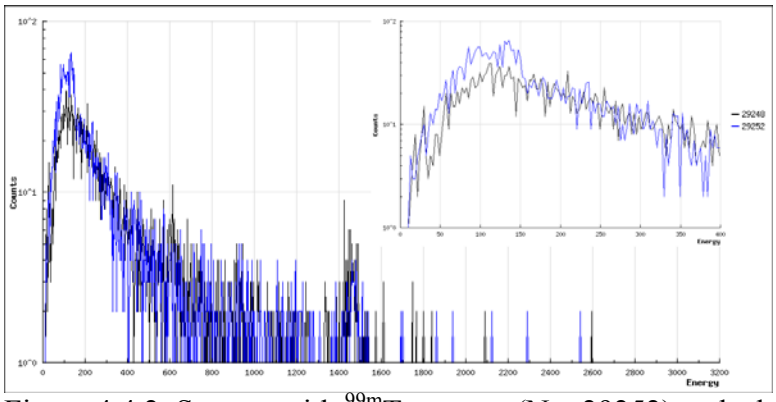
Figure 4.4.2. Spectra with ^{99m}Tc source (No. 29252) and a background spectrum (No. 29248).

4.5 Comparison of the Three Methods with Danish Dataset

The results of the ASSS and FSC methods on the Danish data with added signals are presented in detail in the Status report, Section 6. These results are summarised and compared to the Finnish method in Table 4.4.1 in terms of equalizing the frequency of false alerts in each method. The starting point here is the results from the peak hypothesis test with decision limit of S>0.8, which gave a total of three identified sources of 48 and one type 1 error (see table 4.3.3). This decision limit was chosen because it is the real limit for internal real time alerts used in SONNI.

For comparison with the ASSS and FSC methods, the decision limit for the results of the two methods were set so that all fitting errors clearly above the background fluctuations were marked as found signals. In addition, one observation of an added source at a level equal to natural background was allowed. However, this level was chosen so that a maximum of 1-3 incidents of natural background was allowed to reach the same level.

The FSC method reveals now one ^{15}O source, two cobalt sources with primary peaks, three CsLab sources, two CsPeak sources and all of the scattered cobalt sources. If all false alerts would be excluded, one of the CsLab signals would be excluded (spectrum no 3109).
The ASSS method finds five Cobalt sources with primary peaks and all eight scattered Cobalt souces, two CsPeak sources and two CsLab sources and one ^{15}O source. Alternatively three CsLab sources and no ^{15}O sources would be found depending on which source the false positives would be given.
As stated before, the only sources that the peak hypothesis test finds are two CsLab sources and one cobalt with primary peaks.

The greatest differences between the three different methods working on this dataset are found with the scattered cobalt source, the cobalt source with peaks and with the CsPeak source. Clearly, with totally scattered cobalt source the peak hypothesis test fails completely, whereas the two Danish methods get full points. With the cobalt with primary peaks, the FSC and peak hypothesis test are approximately at the same level but the ASSS method excels. The CsPeak source is only found with the FSC method.

The fact that the ^{99m}Tc source remains hidden for all the three methods regardless of the background, is due to the spectrum shape near the 140 keV line. A lot stronger signal than only 62 additional counts are needed in this part of the spectrum to be detected (see Sections 3.6 and 4.3.)

Table 4.5.1 Comparison on the Danish Dataset results with three different methods. The type 1 errors column indicates observations marked to be found at a level equal to few natural fluctuations.

O-15										
Spectrum No	1522	1625	2282	3109	3466	3537	3907	4335	Found signals	Type 1 errors
FSC	0	1	0	0	0	0	0	0	1	no
ASSS	0	0	1 (0)	0	0	0	0	0	1 (0)	yes (no)
peak hypothesis test	0	0	0	0	0	0	0	0	0	no
Bmb60Co (Co-60 source with clear primary peaks)										
Spectrum No	1522	1625	2282	3109	3466	3537	3907	4335	Found signals	Type 1 errors
FSC	0	1	0	0	1	0	0	0	2	no
ASSS	0	1	1	1	1	0	0	1	5	no
peak hypothesis test	0	0	0	0	0	1	0	0	1	no
Tc-99m										
Spectrum No	1522	1625	2282	3109	3466	3537	3907	4335	Found signals	Type 1 errors
FSC	0	0	0	0	0	0	0	0	0	no
ASSS	0	0	0	0	0	0	0	0	0	no
peak hypothesis test	0	0	0	0	0	0	0	0	0	yes
CsLab (Cs-137 source measured in laboratory with distinctive primary peak and almost no scattered photons)										
Spectrum No	1522	1625	2282	3109	3466	3537	3907	4335	Found signals	Type 1 errors
FSC	0	1	0	1	1	0	0	0	3	yes
ASSS	0	0	1	0 (1)	0	1	0	0	2 (3)	no (yes)
peak hypothesis test	0	1	0	0	1	0	0	0	2	no
CsPeak (Cs-137 source measured in field with lots of scattered photons)										
Spectrum No	1522	1625	2282	3109	3466	3537	3907	4335	Found signals	Type 1 errors
FSC	0	1	0	0	1	0	0	0	2	no
ASSS	0	0	0	0	0	0	0	0	0	no
peak hypothesis test	0	0	0	0	0	0	0	0	0	no
CoScat (Co-60 source with no primary peaks, just scattered photons)										
Spectrum No	1522	1625	2282	3109	3466	3537	3907	4335	Found signals	Type 1 errors
FSC	1	1	1	1	1	1	1	1	8	no
ASSS	1	1	1	1	1	1	1	1	8	no
peak hypothesis test	0	0	0	0	0	0	0	0	0	no

5 DATA FROM SSI: TULLVERKET CGS MEASUREMENTS

The Danish and Finnish data sets represent standard urban spectra for inhabited areas measured along roads with "normal" traffic. However, special urban areas of interest as e.g. measurements from controlled areas, harbours, customs etc. are not represented.

In order to introduce to the UGS project also those types of measurements SSI has kindly supplied a series of data measured with Tullverkets Ford Excursion CGS systems. In addition SSI supplied CGS measurements from a Volvo V70 CGS system. In this report only the measurements made in the Frihamnen container area using three identical CGS systems have been investigated.

5.1 Tullverkets CGS Systems

Tullverkets CGS systems are Exploranium GR-460 systems operating with 512-channels 1-sec measurements. The CGS detectors are one standard 4L NaI(Tl)-crystals, the same type used by the Danish CGS systems, and a NBX neutron detector with 3 He-3 tubes. Here, only the sodium iodide measurements will be commented. In contrast to the Danish CGS systems the Swedish vehicles carry the detectors inside the vehicle, Figure 5.1.1.

Figure 5.1.1. One of Tullverkets CGS systems.

No standard energy calibrations were supplied for the systems. It was found, however, that the measurement response regarding storage of signals in the 512 channels were quite similar for the data sets supplied. An average energy calibration for the three systems was calculated using the position of the full energy peaks from ^{137}Cs (662 keV channel 116), ^{40}K (1460.8 keV channel 248) and ^{208}Tl (2614.6 keV channel 436). The energy calibration starting in channel 0 is shown in Figure 5.1.2 and the standard windows are shown in Figure 5.1.3.

The presented energy calibration was used for the calculation of natural radionuclide windows, other radionuclide windows and "scattered photons"-windows for the ASSS procedure. The calculated windows (channels and energies) are shown in Table 5.1.1. The upper and lower energies were chosen to represent the windows presented in the UGS Status Report for the corresponding Danish systems.

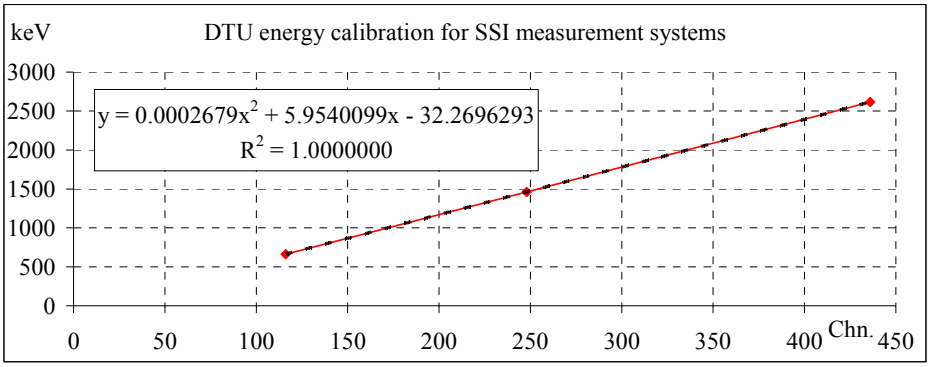

Figure 5.1.2. Energy calibration for Tullverkets's CGS systems, Car 30, Car 32 and Car 34.

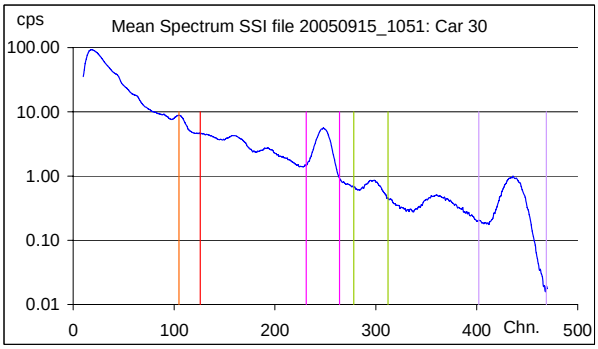

Figure 5.1.3. Standard energy windows for Tullverkets CGS systems (channels).

Table 5.1.1. Standard radionuclide windows (bold) and ASSS windows.

Name	LL (channel)	UL (channel)	LL (keV)	UL (keV)
^{99m}Tc	23	44	105	230
Scatter1	52	69	278	380
Scatter2	54	74	290	410
^{131}I	59	77	320	428
^{137}Cs	105	126	596	722
^{60}Co	188	229	1097	1345
K	**231**	**264**	1357	1558
U	**278**	**312**	1644	1851
Th	**402**	**469**	2405	2819

5.2 Maps of Frihamnen, Stockholm

DTU who have performed the calculations on the Swedish data sets does not have permission to use Swedish electronic maps. Permissions to present in this report aerial photographs from www.eniro.se has been requested but not has not been granted. The reader is therefore urged to look up maps of Frihamnen using the Internet. Comments about the surroundings will be supplied in the text showing calculated maps of the area.

5.3 Background Survey in Frihamnen: No Sources Present

23 September 2005 a survey of Frihamnen, Stockholm was made by Car 30. In this survey no sources were present. This series of measurements will therefore be referred to as "background measurements from Frihamnen". Figure 5.3.1 shows the track lines for this file 20050923_1418.spc. The 5 points represents selected spectra (shown later).

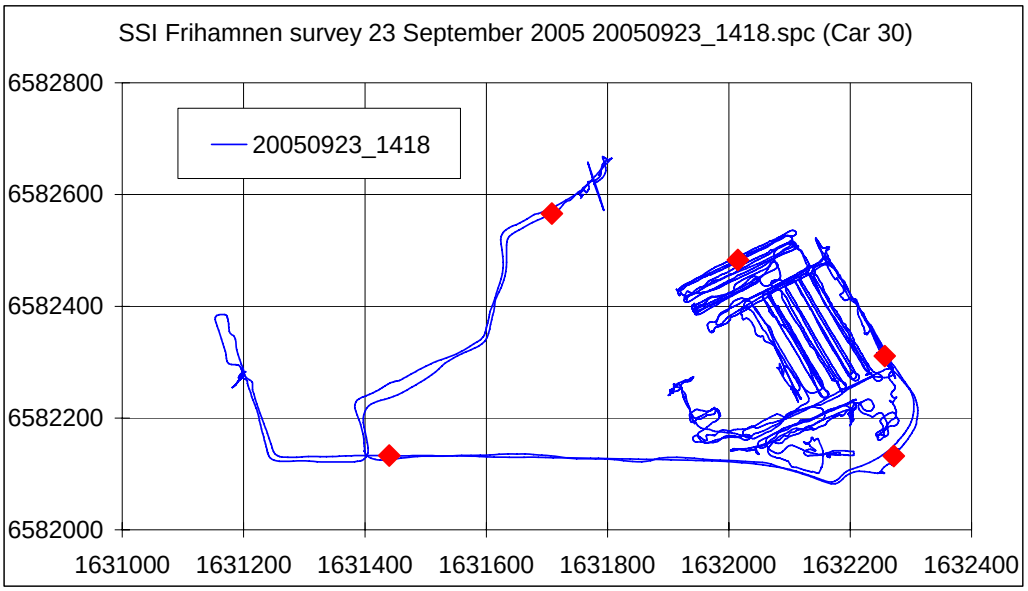

Figure 5.3.1. Track lines for background survey of Frihamnen, Car 30, September 2005.

The data were NASVD processed from channel 15 to channel 475. This interval is slightly larger than a "standard" processing interval from channel 30 to channel 475. The reason for choosing these limits was that the spectral components would be used also for fitting of data sets containing sources, for which no information was supplied. The mean spectrum and the spectral components from S1 to S5 are shown in Figure 5.3.2. Here, also the first three sets of amplitudes are shown. S4 shows the spectrum drift signals and S5 basically shows noise together with some potassium signal.

The amplitude sets b4 and b5 are not very interesting with random fluctuations up and down and are not shown. But b1, b2 and b3 are interesting. The spectral component S1 shows that for some areas a large amount of natural radionuclides should be either added to or subtracted from the mean spectrum. The information of b1 tells that this does not happen "randomly" but is related to special areas at Frihamnen.
S2 shows an almost clean "upside down" potassium spectrum and provides the information that either variations of potassium are of importance of its own independent of thorium and uranium variations – or that uranium, that is not included in the component, varies on its own. This is not a spectral shape usually found in rural data sets and it was not observed with the same importance in the measurements from the Copenhagen area.
S3 shows excess of the natural radionuclides paired with a loss of scattered photons. Fewer scattered photons are to be expected for measurements for which b3 is positive.
The spectral components presented here really do seem to differ in "rank" of importance compared to what has been observed for the other urban data sets.

The relation between the shapes of the spectral components and the positions (Easting, Northing) of the amplitudes called for a further investigation. Since no information of the whereabouts of the various containers in Frihamnen was available as tables with coordinates, the most information is gained from inspection of colour maps showing the amplitude values and a comparison with maps, preferably aerial photographs of the area.
Since it was not possible to obtain a license to print the requested images from Eniro.se it is suggested that the reader visits Eniro's homepage while studying the following comments. A link to Frihamnen, Stockholm is shown here.

http://kartor.eniro.se/query?&what=map&WGS84=18.118015259933568%3B59.342364489440996&zl=7&ms=0&streetname=frihamnen&mapstate=7%3B18.118015259933568%3B59.342364489440996%3B0%3B18.111205642795923%3B59.34545590229032%3B18.12480131739672%3B59.33927633853042&mapcomp=%3B%3B%3BFrihamnen%3B%3B%3B11527%3BSTOCKHOLM%3B%3B%3B%3B%3B1631594.0%3B6582460.0%3B0%3B0%3B0.0000%3B0.0000%3Bmaps_place.42344.21&stq=0&imgmode=2

If the link cannot be followed the reader can go to http://kartor.eniro.se. In the "Address" field write "Frihamnen", next choose "Stockholm", finally choose "Flygfoto or "Hybrid". A good map presentation can be found at the following co-ordinates:

WGS84 Lat/Long: N 59º 20' 32.51" E 18º 7' 4.85" / RT90: X=6582460, Y=1631594.

Figure 5.3.3 shows a map of the b1-amplitudes. The shielded area, Loudden, at the East of Frihamnen shows negative values for b1 meaning that the natural radionuclide content here is low for all three radionuclides (compare with shape of S1). The measurements made on Sandhamnsgaten shows an increase in natural radionuclide contents in the direction from Lindarängsvägan and up Sandhamsgatan with maximum at the inhabited area at the Nothern end of Sandhamsgatan. A number of buildings between Tullvagtsvägan and Lindarängsvägan also contribute positively. The same is seen at the pier (also caused by buildings).

Figure 5.3.4 shows a map of the b2-amplitudes. The positive potassium contribution and excess of scattered photons in general are found along the rails following Lindarängsvägan.

Figure 5.3.5 that shows a map of the b3-amplitudes shows a large "positive contribution" of the negative energy region of spectral component S3". This contribution in not random but is localised to the waterfront. The registered number of scattered photons (possibly the number of scattered photons in general) here is lower.

Even without calculating a background count rate for the natural radionuclides to be subtracted from measurements made with the purpose of search for sources it is evident that the geometry of the harbour area is complicated and the one standard set of background values may not be enough. Especially the large variations in potassium where the "normal" Th/U proportional factor changes could introduce difficulties for sources with energies in the low energy range (the scatter area) and the potassium peak energy range.
(Natural radionuclide count rates are shown in the section of Area Specific Stripping, Figures 5.5.1 to 5.5.3.)

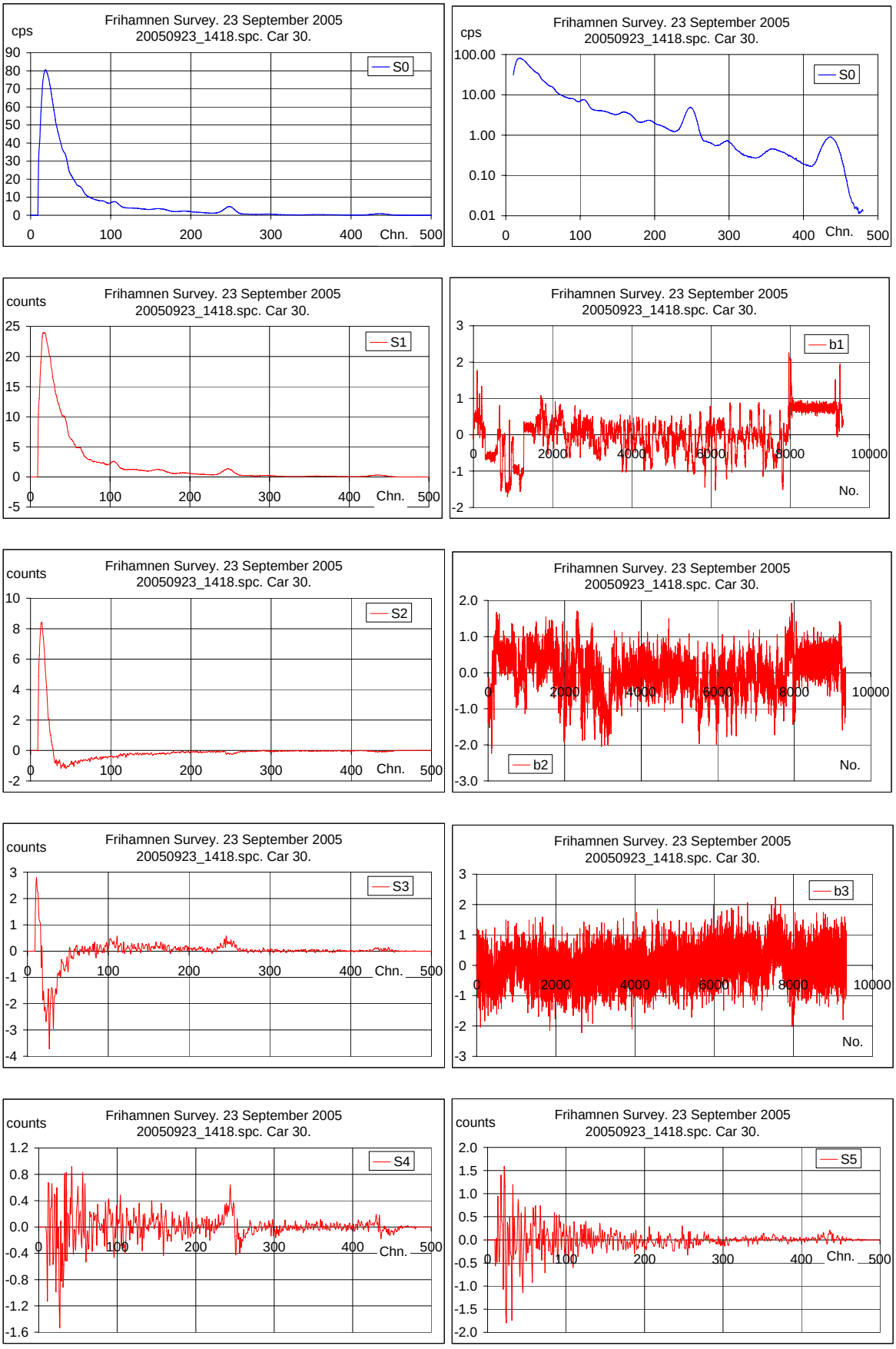

Figure 5.3.2. Spectral components and amplitudes for Car 30 background measurements in Frihamnen, Stockholm.

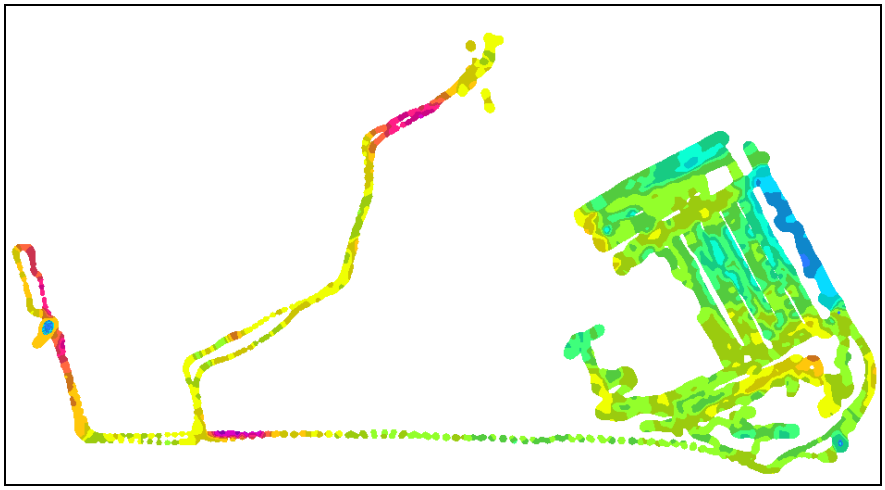

Figure 5.3.3. Map of amplitude b1: Shielded area to the East, low radionuclide contents. Contributions from Th, U and K are subtracted; however K is added again later.

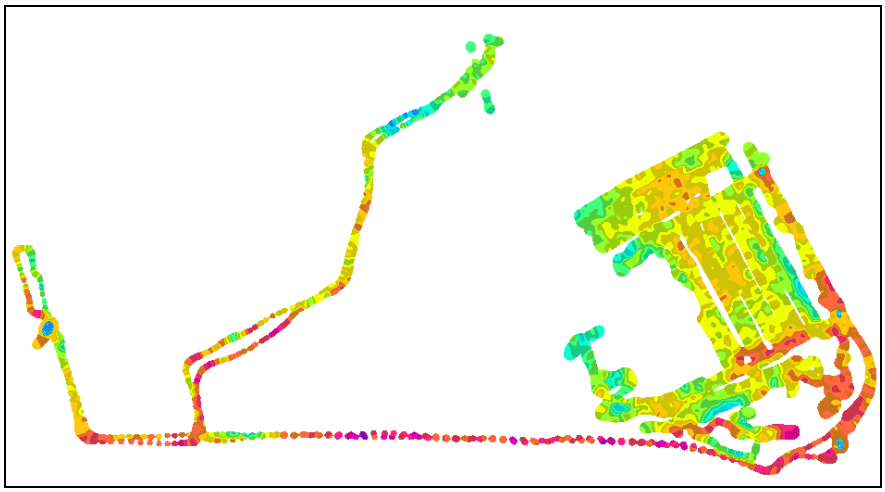

Figure 5.3.4. Map of amplitude b2. Outer concrete walls: potassium in excess.

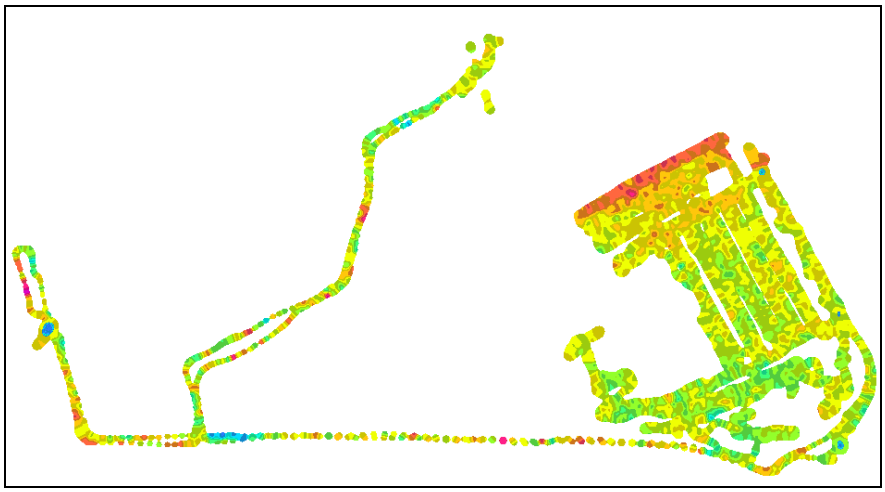

Figure 5.3.5. Map of amplitude b3. Scattered photons are missing at the waterfront.

5.4 Selected Spectra: Radionuclide Variations

Five spectra from Frihamnen were reconstructed using the spectral components from the NASVD processing of the data. The positions (coordinates) for the chosen spectra are shown in Figure 5.3.1.
The number of photons in the low energy region where signals from shielded and partly shielded sources will be found varies more than a factor 2. The high number of low energy photons must be stripped away correctly in order to find a source signal in this region.
The count rates shown in Figure 5.4.1 are gross count rates.

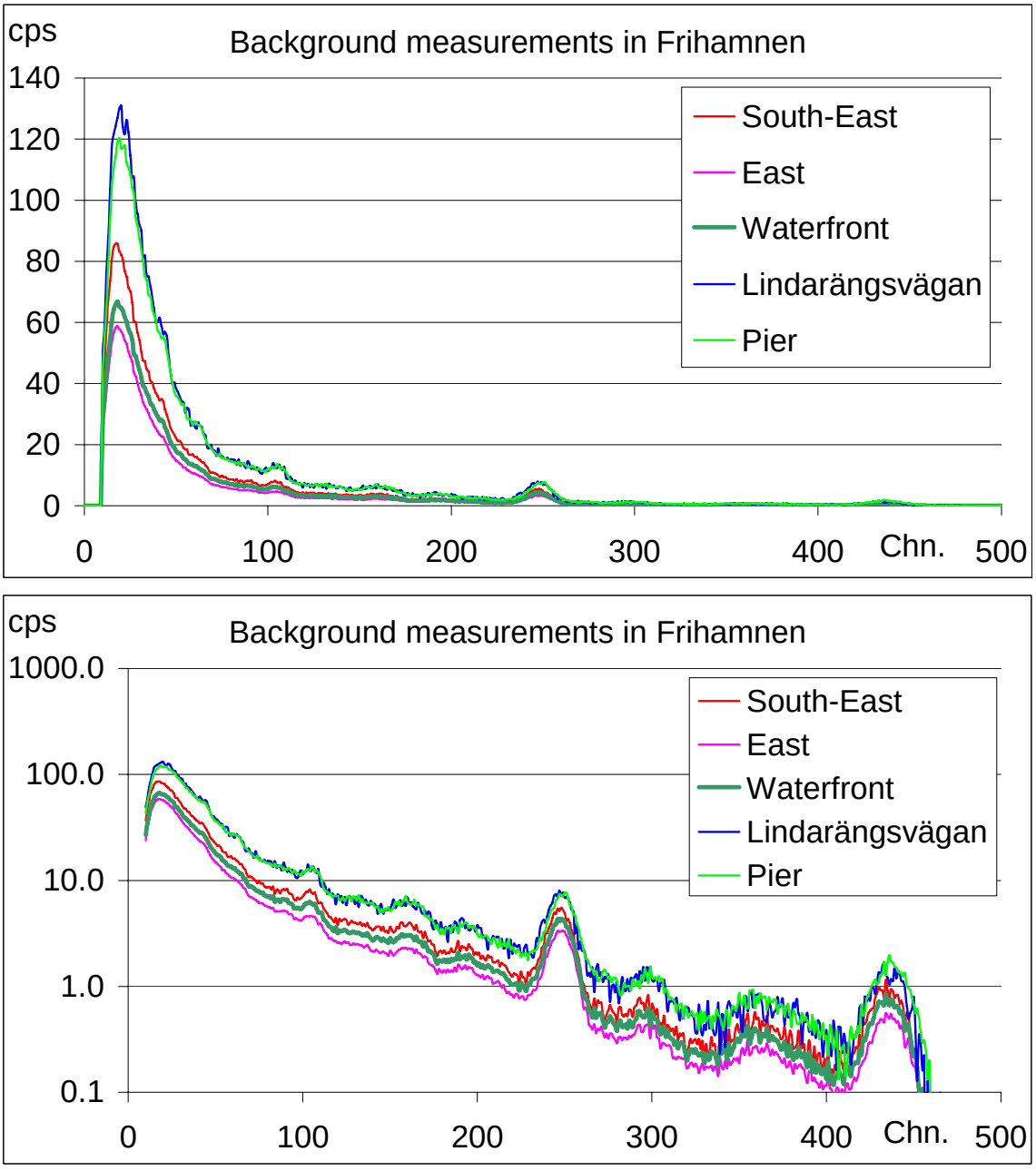

Figure 5.4.1. Gross count rates for five background measurements in Frihamnen.

5.5 Frihamnen Background Measurements: Area Specific Stripping

Based on the energy calibration presented earlier and the gross count rates for the natural radionuclides a set of ASSS factors for Frihamnen was calculated. The stripping factors are shown in Table 5.5.1. For most Danish measurement the ASSS factor C (potassium) has been calculated to approximately half the value of B (uranium). The measurements from Frihamnen differs from this also in the respect that "A" (thorium) is in general the smaller ASSS factor of the three (for Danish measurements only observed for very low energy windows). For the Finnish measurements (Helsinki) C in general was also quite lower than A and B. Again this puts emphasis on the name of the method AREA Specific Stripping and should remind the user that the ASSS method cannot be used without some knowledge of the surveyed area in cases where previously ASSS factors have been calculated and reused.

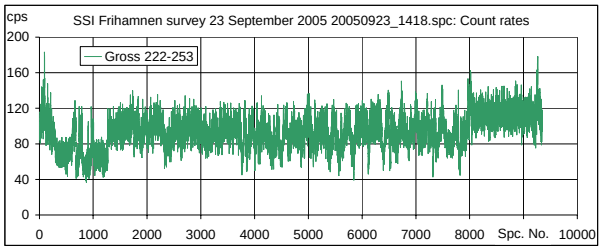

Figure 5.5.1. Potassium gross count rates.

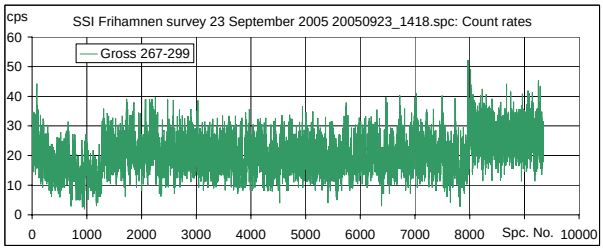

Figure 5.5.2. Uranium gross count rates.

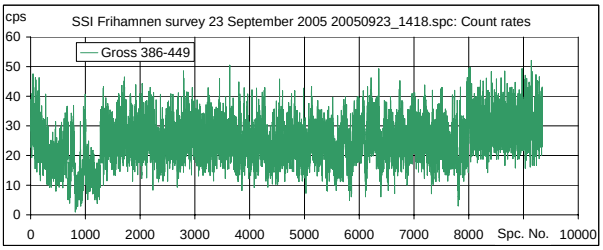

Figure 5.5.3. Thorium gross count rates.

Table 5.5.1. Area Specific Stripping Factors for background measurements in Frihamnen.

Name	A	B	C	LL (chn.)	UL (chn.)	LL (keV)	UL (keV)
^{99m}Tc	6.623	8.132	8.077	23	44	105	230
Scatter1	1.945	2.164	2.066	52	69	278	380
Scatter2	2.032	2.237	2.138	54	74	290	410
^{131}I	1.644	1.769	1.679	59	77	320	428
^{137}Cs	0.844	0.824	0.766	105	126	596	722
^{60}Co	0.443	0.533	0.518	188	229	1097	1345
K				**231**	**264**	1357	1558
U				**278**	**312**	1644	1851
Th				**402**	**469**	2405	2819

The gross count rates and the resulting ASSS count rates are shown in Figure 5.5.4. With reference to the comments above about the lack of proportionality between potassium and the other natural radionuclides it is observed that the stripping of the ^{60}Co-window (188-229) leaves remains of approx. 13 cps on the average for the stripped count rates.

The same is the case for the low energy window (Tc) with 11 cps remaining. The other four windows have non-stripped count rates from 3.23 (Cs) cps to 4.49 (Scatter1) cps.

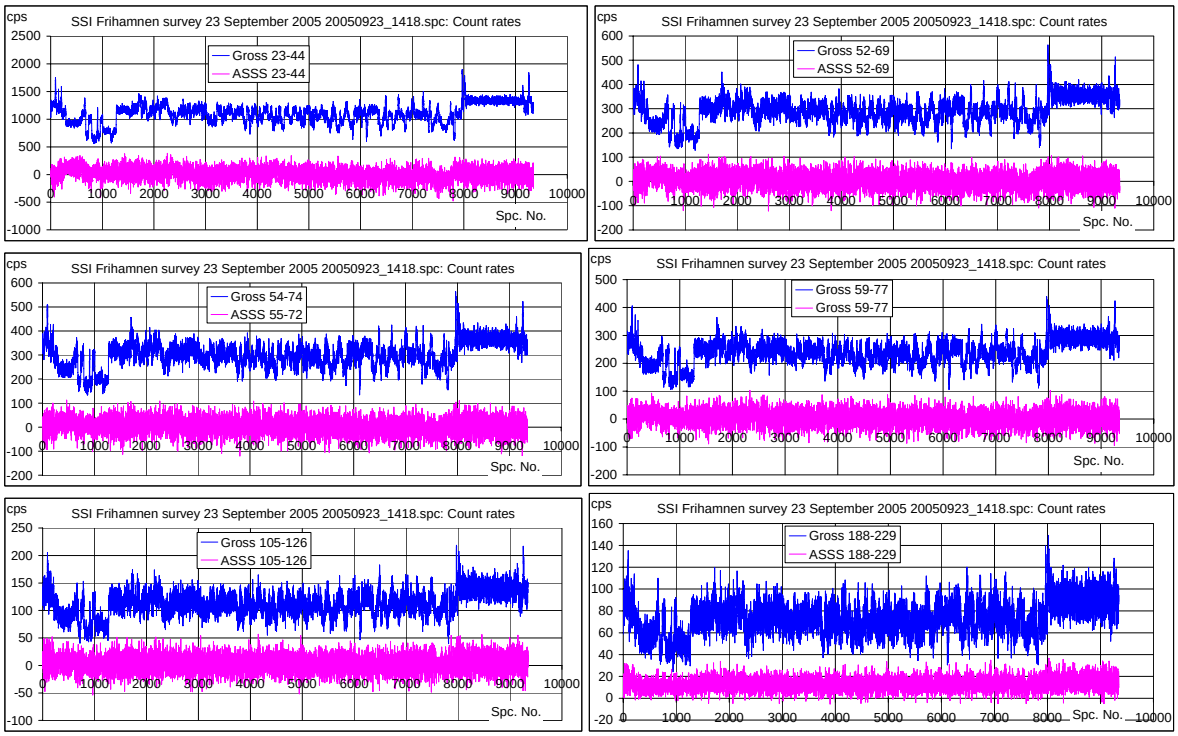

Figure 5.5.4. Gross and ASSS count rates for Car 30 measurements in Frihamnen.

5.6 Frihamnen background measurements: The FSC Method

Fitting errors were calculated using five spectral components and the mean spectrum in the calculations. No significant spikes are observed in any of the six low energy (below potassium) windows. The fluctuations shown represent what is to be expected in this area under normal circumstances for no sources present. A few "could-be-signals" in the caesium window (105-126) would have been possible candidates for spectrum analysis had the survey been a source search.

With the knowledge that the measurements were made in the month of September (autumn) close to the sea side and the knowledge that radon daughters in the air are subject to interfere with calculations of caesium concentrations in general the "spikes" here have not been examined for a possible caesium ground contamination (fallout remains).

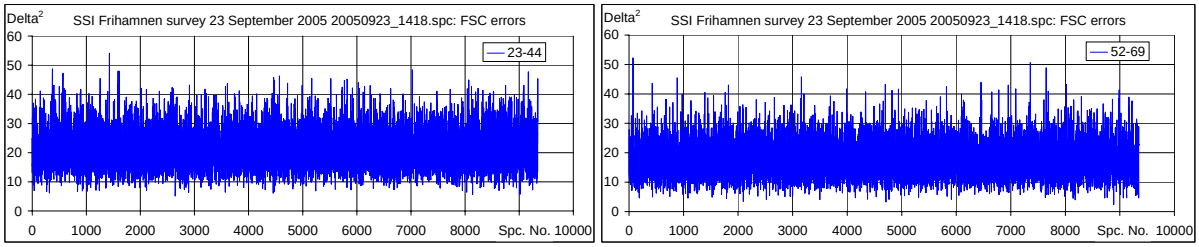

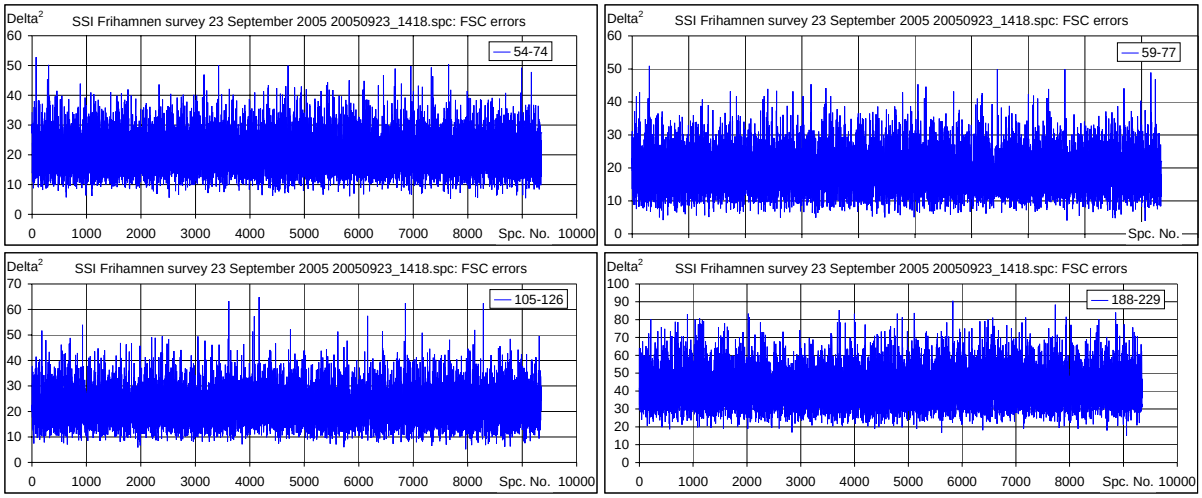

Figure 5.6.1 FSC errors for Car 30 measurements in Frihamnen (no sources present.)

5.7 Tullverkets CGS Measurements in Frihamnen: Source Search by ASSS and FSC

It is characteristic for the data files supplied by SSI that the included source signals are very strong and intended for training purposes. The number of measurements containing source signals is so large, that appropriate ASSS factors cannot be calculated for the Frihamnen area from the measurement files. Therefore, the ASSS factors calculated for the background measurements, i.e. no sources measurements, made with Car 30 in the same area on 23 September 2005 (20050923_1418.spc) were used. The spectral components needed for the FSC method were also the same as used for the background measurements.
Figure 5.7.1 shows the track lines for the three carborne systems.

It is seen that the three CGS systems did not drive on exactly the same path. Every delivered file was found to consist of more than 10000 measurements which is a lot of data to examine. The size of the source signals – the detector response – was found to be of an order of magnitude leaving no doubt whether or not there was a source present.
The vast amount of data delivered, the missing energy calibration and the time spent on debugging the file structure combined with the fact that at least 50% of the measurements from the different cars produced an overlap of data resulted in the decision only to evaluate the measurements from one of the CGS systems assuming a quite similar response for the other systems.

In order to choose the most interesting file of the three files delivered the files were examined for source signals using NucSpec. The measurement numbers containing source signals were noted down and the coordinates for those measurements were extracted and plotted. Since no information about the source positions was available this was the way to localize the sources. Figure 5.7.2 shows the positions of measurements with source signal response. It is seen that Car32 and Car34 each detects a source that the other systems do not register due to the path surveyed.

It was evaluated that the measurements made with Car30 would represent the three CGS systems best and in the following analysis all references made refer to this system.

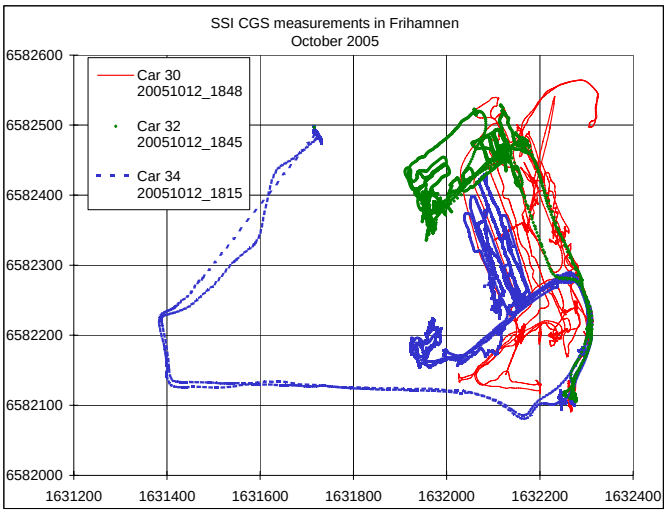

Figure 5.7.1 Track lines for Car 30, Car32 and Car34 in Frihamnen.

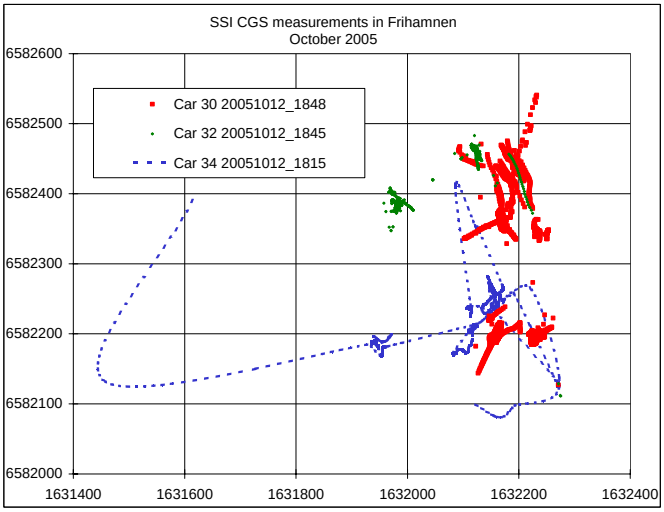

Figure 5.7.2. Source signals by ”eyesight”. Coordinates extracted from NucSpec.

5.7.1 Car30: Area Specific Stripping, ASSS

The mean spectrum for the measurements made with Car 30 is shown in Figure 5.7.1.1. That the sources show very strong signals is obvious from the two ^{60}Co full energy peaks observed. The rest of the spectral components are not shown, but source signals are found all the way through spectral component number S8 with S9 containing the spectrum drift signals. The spectral components are not presented here only the amplitudes of the components for comparison with ASSS and FSC errors. The amplitudes are shown as Figure 5.7.1.2 overleaf.

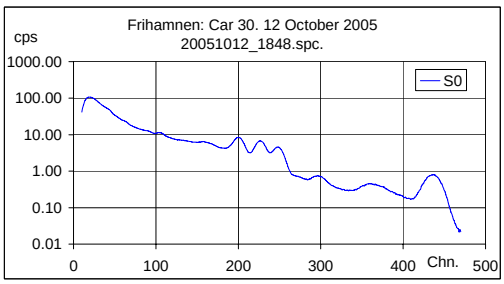

Figure 5.7.1.1. Mean spectrum for Car 30: Source search in Frihamnen.

The sources used were ^{60}Co, ^{137}Cs and uranium stones. The strong cobalt sources at the measurement group from spectrum 2120 to 2430 are seen to have a strong effect on the count rates in the natural radionuclide windows shown in the Figures 5.7.1.3 to 5.7.1.4. Maps of the natural radionuclide gross count rates are shown as the Figures 5.7.1.11, 5.7.1.13 and 5.7.1.15.

The sources used in the exercise have activities high enough to produce pile-up and therefore rendering the ASSS method inappropriate. The energy calibration is also uncertain because of this in that spectrum drift of three channels have been observed when the CGS systems get close to a strong source. Figure 5.7.1.5 and Figure 5.7.1.7 show the ASSS results for the measurement interval from spectrum 8000 to 9000 as an example.

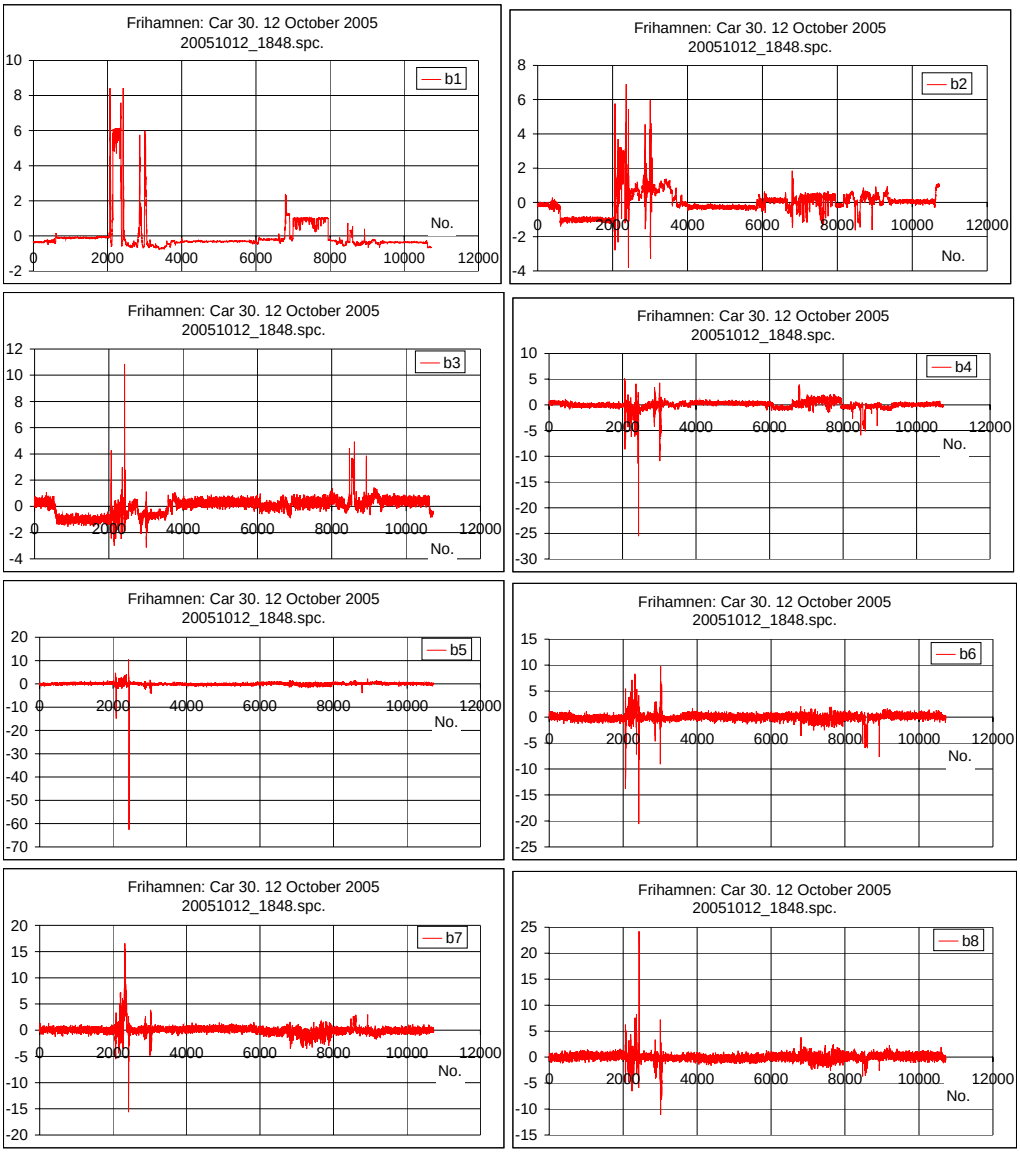

Figure 5.7.1.2. Amplitudes for Car 30 source search measurements in Frihamnen.

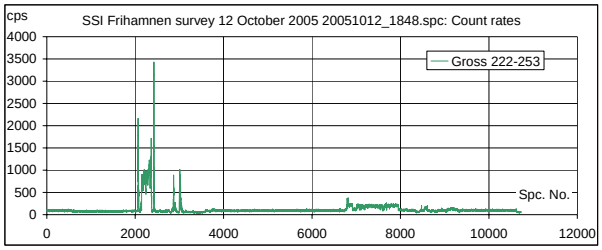

Figure 5.7.1.3. Potassium gross count rates for Car 30 source search in Frihamnen.

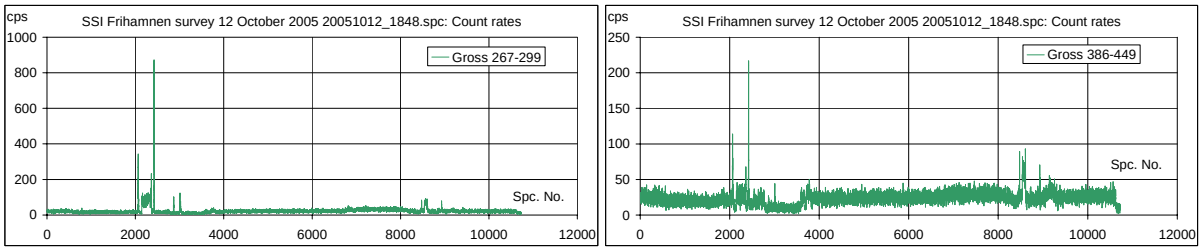

Figure 5.7.1.4. Uranium and thorium gross count rates for Car 30 source search in Frihamnen.

Two signals pointed to by solid arrows are caesium sources for certain. The source type resulting in the measurements pointed to by the dotted arrows are more questionable. Measurement 8478 shown in Figure 5.7.1.6 as raw measurement and NASVD reproduced measurement could be a collimated caesium source, possibly with excess of potassium. Figure 5.7.1.9 shows the NUCspec representation of the spectrum.

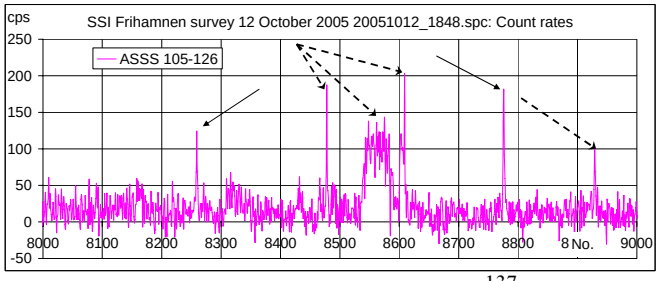

Figure 5.7.1.5: Solid arrows showing ^{137}Cs sources.

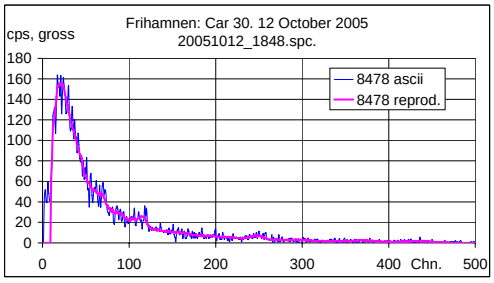

Figure 5.7.1.6. Measurement 8478.

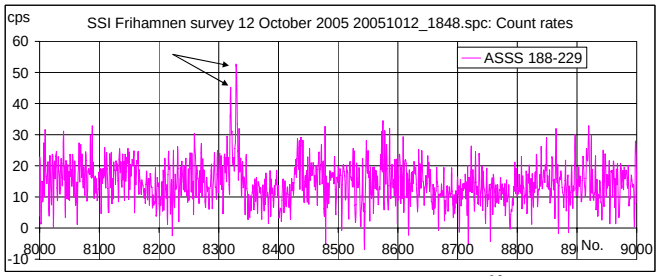

Figure 5.7.1.7. Solid arrows showing ^{60}Co sources.

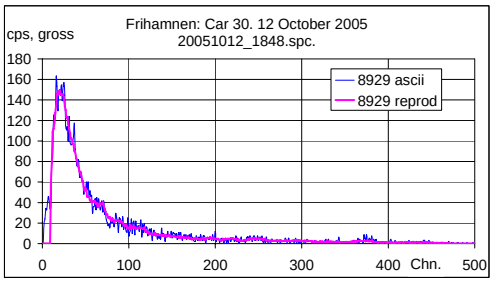

Figure 5.7.1.8. Measurement 8929.

Measurement 8929 seemingly is of the same type as represented in the measurement group from 8540 to 8610 (Figure 5.7.1.9 and Figure 5.7.1.10) but it cannot be said for certain whether there is one source or more – possibly a case of uranium containing stones. Figure 5.7.1.7 presents the two signals from weak cobalt sources (or from sources far away). The signals are reflected in the caesium window, too, as "a broad shape representing a group of scattered photons". (No rainbow plot presented for the cobalt signals of Figure 5.7.1.7.)

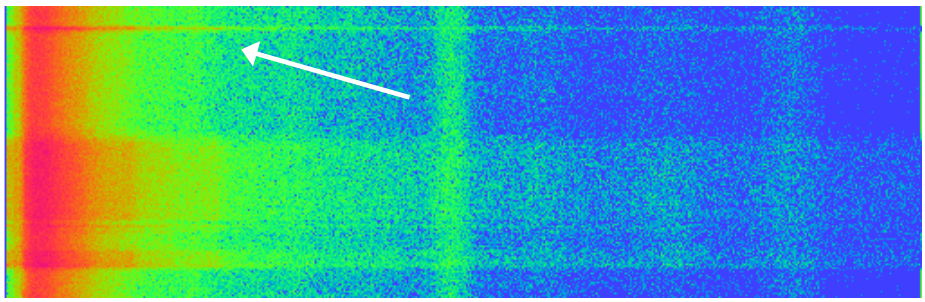

Figure 5.7.1.9. Nuscpec rainbow plot showing spectrum 8478 and spectrum group 8540 to 8610.

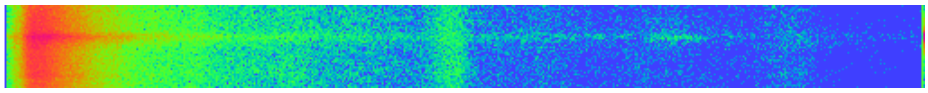

Figure 5.7.1.10. Nuscpec rainbow plot showing spectrum 8929.

Maps of the gross count rates for the natural radionuclides and ASSS count rates for the caesium and cobalt window are shown in the Figures 5.7.1.11 to 5.7.1. The count rate interval for the ASSS count rates is from 0 cps to 100 cps.

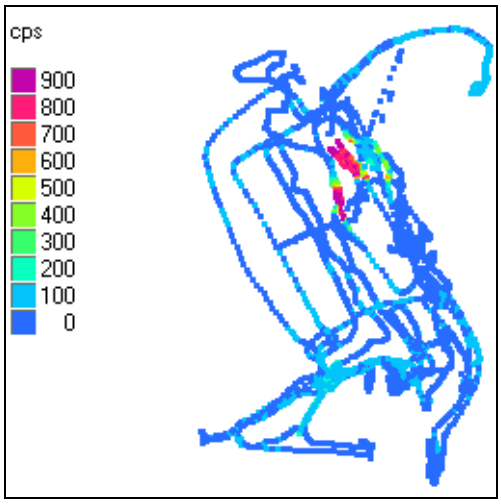

Figure 5.7.1.11. Potassium gross count rates.

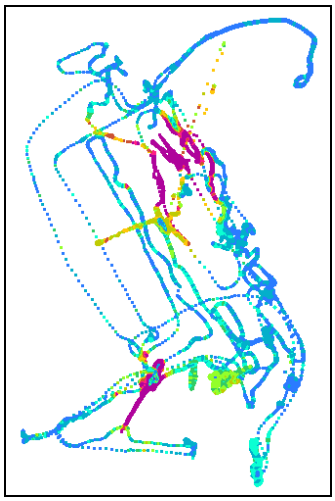

Figure 5.7.1.12. Cs ASSS counts rates 0-100 cps.

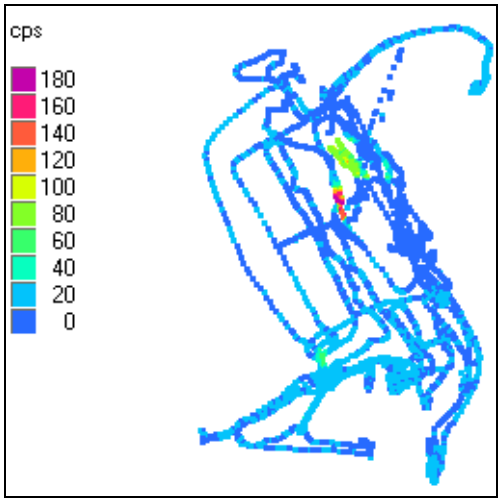

Figure 5.7.1.13. Uranium gross count rates.

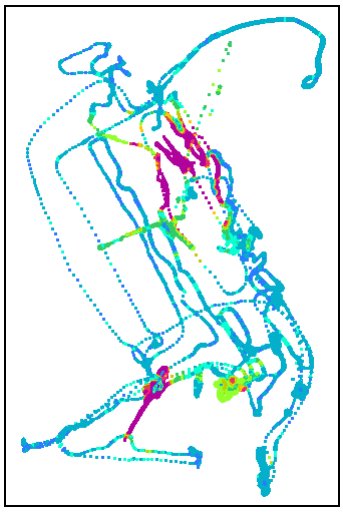
Figure 5.7.1.14. Co ASSS count rates 0-100 cps.

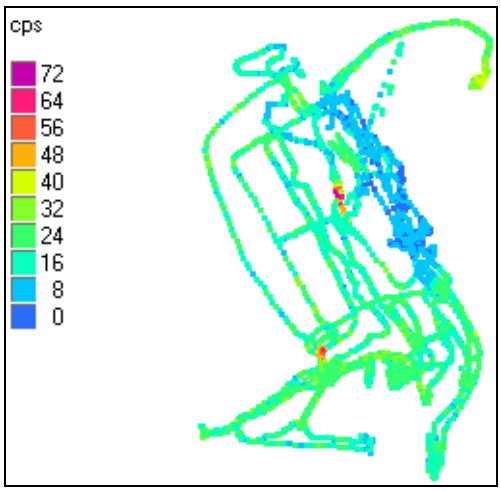

Figure 5.7.1.15. Thorium gross count rates.

5.7.2 Car 30: Fitting with Spectra Components, FSC

The FSC results differ from the ASSS results in interpretation. For the FSC method the signal from the caesium source at measurement 8775 is quite strong compared to the signal for the same ASSS window, Figure 5.7.1.16. Also the ratio between this signal and the caesium signal at measurement 8259 has changed dramatically compared to the ASSS results. Either this is not a true caesium signal or it may represent an environmental caesium signal. In a comparison of the Figures 5.7.1.17 and 5.7.1.18 showing the NUCspec rainbow plots of the mentioned measurements one notices that the first assumed caesium source has a tail downwards. This could indicate an old caesium hot spot with some extent of burial.

The cobalt source(s) found by ASSS shows up with a higher significance for the FSC method where the background fluctuations have been removed, Figure 5.7.1.19. The signal at measurement 8807 is most likely not a source but should have been investigated closer, had the measurements not been an exercise. The measurements presented in the Figures 5.7.1.9 and 5.7.1.10 have almost been fitted away with natural radionuclide shapes indicating that these are not signals from forward scattered photons originating from cobalt.

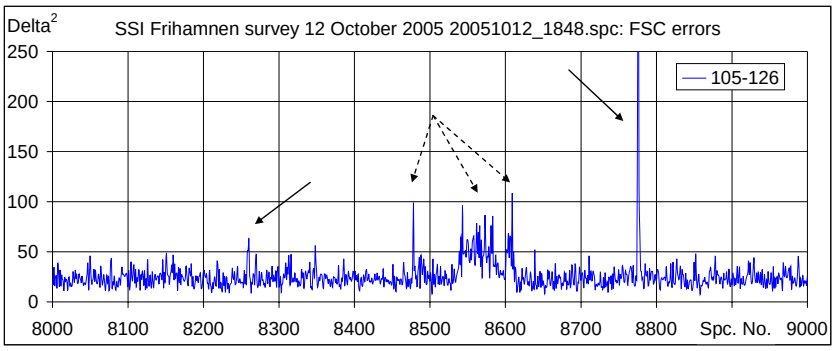

Figure 5.7.1.16. FSC results for Car 30 source search in Frihamnen: caesium window.

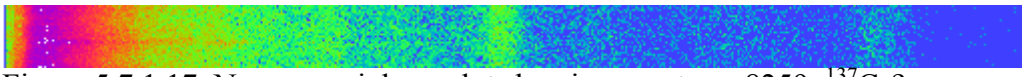
Figure 5.7.1.17. Nuscpec rainbow plot showing spectrum 8259: ^{137}Cs?

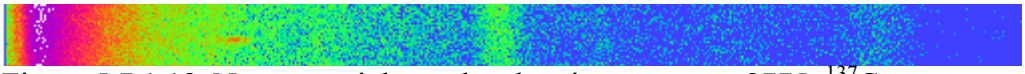
Figure 5.7.1.18. Nuscpec rainbow plot showing spectrum 8775: ^{137}Cs.

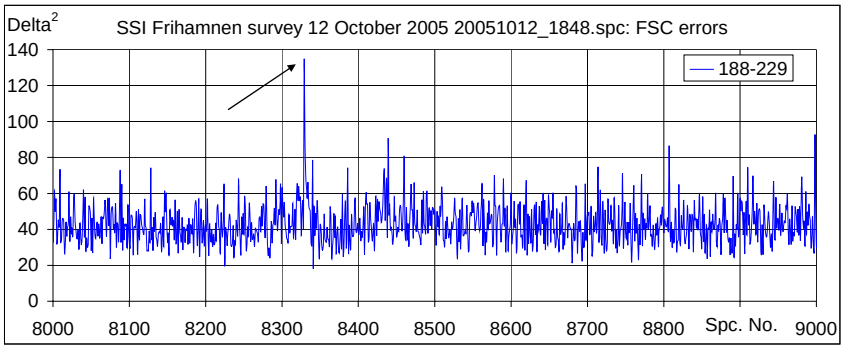

Figure 5.7.1.19. FSC results for Car 30 source search in Frihamnen: cobalt window.

6 DATA CONVERSION

6.1 Data Conversion from Danish Format to Finnish Format and Vice Versa

To exchange data between the analysis software packages used by the participants, data format conversion tools were needed. As described in the Status report Section 3.1, the Danish system uses binary files with little endian number format compatible with programs running under Windows operating system. Finnish system stores the data to a database and data transfer is handled through XML coded text files. Various approaches to the data conversions were studied and distinct methods were chosen for the conversion from Danish data to Finnish data and from Finnish data to Danish data.

Both data formats may contain system specific analysis information, but in this case only the measurement data was converted between the formats. Other required data was generated during the conversion, if the particular piece of information was not available in the original data.

6.1.1 Conversion from Danish data format to Finnish data format

Because the Danish data is in binary files with byte packed data structures, the most obvious choice for the conversion program was a Windows native binary program that can read the data directly from the file and store it internally to correct data structures without any additional processing. The conversion program was created with Microsoft Visual Studio .NET C++ language. The source code is as generic as possible and it can be compiled and run on various operating systems like Linux and Mac OS. However, because the fore mentioned operating systems use the big endian binary number format, the processing of the little endian data files would give incorrect results.
The summary of the converted data is given in the table below:

Table 6.1.1.1. Conversion from Danish data format to Finnish data format.

Target data format (Finnish XML)	**Source data format (Danish binary)**
stationId	Generatred: DK-CGS
idMessage	Genereated: Conversion time in UNIX time stamp format
idMeas	Record_number
acqStart	UTC_time
detectorName	Generated: DK-CGS-NaI
liveTime	Live_time
spatialData time *xCoordinate* *yCoordinate* *altitude* heading	 UTC_time *X, Y, Z (ECEF cartesian coordinates) converted to WGS84 longitude [deg], latitude [deg], altitude [m]* Generated: 0.0 [deg] always
firstChannel	Generated: 0
lastChannel	Generated: 511
firstValidChannel	Generated: 2 *(spectral data seemed to have two*

	channel LLD)
lastValidChannel	Generated: 510 *(one channel HLD)*
spectrum	SPC[512]

The following conversion equations were used to convert the ECEF (Earth Centred Earth Fixed) coordinates (*X, Y, Z*) used in the Danish data to WGS84 longitude, latitude and altitude (λ, ϕ, h):

$$\phi = \arctan\left(\frac{Z + e'^2 b \sin^3\theta}{p - e^2 \arccos^3\theta}\right)$$

$$\lambda = \arctan\left(\frac{Y}{X}\right)$$

$$h = \frac{p}{\cos\phi} - N(\phi)$$

where:

$$p = \sqrt{X^2 + Y^2}$$

$$\theta = \arctan\left(\frac{Za}{pb}\right)$$

$$e'^2 = \frac{a^2 - b^2}{b^2}$$

$$e^2 = \frac{a^2 - b^2}{a^2}$$

$$N(\phi) = \frac{a}{\sqrt{1 - e^2 \sin^2\phi}}$$

The semi-major earth axis (ellipsoid equatorial radius) length a = 6378137.0 m and the semi-minor earth axis (ellipsoid polar radius) length b = 6356752.3142 m were used.

6.1.2 Conversion from Finnish data format to Danish data format

Conversion from Finnish data to Danish data was done with Java (version 1.5), because it has excellent tools for XML processing. NetBeans 5.0 IDE was used to manage the source code and create the jar package. Data structure classes were created to store and combine the different blocks in the XML files and the Danish binary file was written using the combined data. Binary files written with Java use big endian binary number format as default, which guarantees that the files are compatible with all Java implementations in all platforms (Windows, Linux, Mac OS alike). However, Java has built in tools to reverse the byte order of the numbers and conversion to little endian binary file was quite straight forward to implement. Unlike the conversion program that converts the Danish data to Finnish data, this program gives the correct results even if run in Linux or Mac OS.
The summary of the converted data is given in the table overleaf.

Table 6.1.2.1. Conversion from Finnish data format to Danish data format.

Target data format (Danish binary)	**Source data fromat (Finnish XML)**
Record_number	idMeas
Line_number	Generated: -1 always
UTC_time	acqStart
X Y Z	xCoordinate, yCoordinate, alt (WGS84 longitude, latitude, altitude) converted to ECEF cartesian coordinates
Northing Easting	Generated: 0 always Genereted: 0 always
PDOP	Generated: 1 always
DGPS	Generated: 0 always
ralt	alt
Live_time	liveTime
roi[10]	Generated: 0 all ten always
gain	Generated: 0 always
peak	Generated: 0 always
clock_time	Generated: 0 always
spare[8]	Generated: 0 all eight always
SPC[512]	spectralData values with invalid channels (channels outside the firstValidChannel - lastValidChannel region) filled with zeros

Coordinate conversion from WGS84 longitude, latitude and altitude to ECEF Cartesian coordinates was made with jscience 3.1 library, so the exact conversion functions are not known.
The source code and executable programs for the conversion routines can be obtained from the authors on request.

6.2 Conversion from Swedish Data Format to Danish Data Format

The conversion from the Swedish data layout to the Danish data layout turned out not to be a programming task. However, the data layout of the Swedish data files did cause some speculations and required test runs.
Sine the Swedish data files are the results of measurements made with Exploranium CGS systems it was thought that the layouts would probably be very similar. The first thing done was therefore to open a file with Hex Workshop to check the data structure. Unfortunately the information of the data structure was non-existent and turned out also to be a secret for SSI. But the file did give the information -380..1152, Figure 6.2.1.
These numbers are known to DTU who has previously done a lot of work on Exploranium files. A header of size 380 bytes is familiar from older versions of the Exploranium software, Figure 6.2.2 and a data struct size of 1152 bytes is familiar from new Exploranium software, Figure 6.2.3. The contents of the 1152-byte structure therefore could be assumed to be the same as the known struct for the Danish CGS files, but it had to be verified.

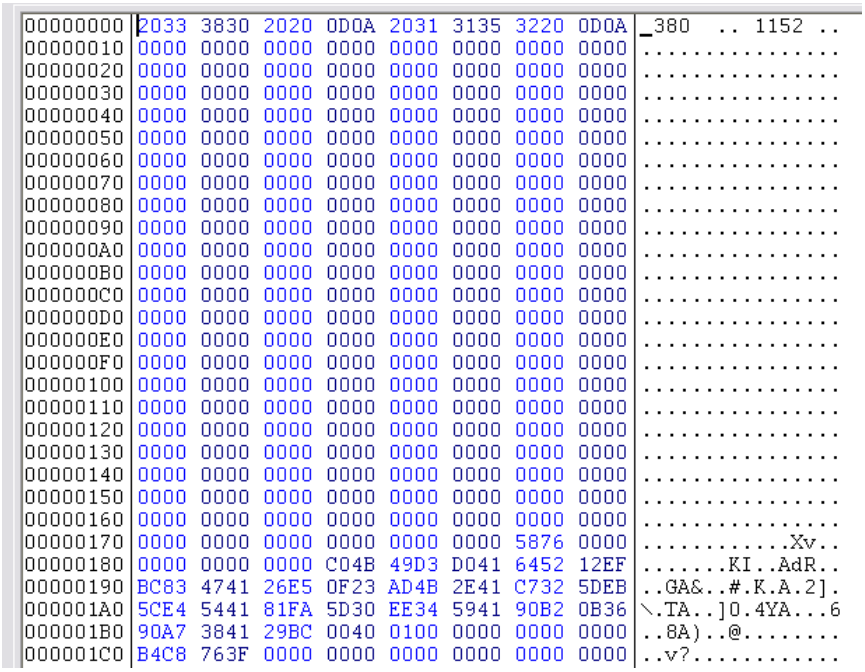

```
00000000 2033 3830 2020 0D0A 2031 3135 3220 0D0A  _380  .. 1152 ..
00000010 0000 0000 0000 0000 0000 0000 0000 0000  ................
00000020 0000 0000 0000 0000 0000 0000 0000 0000  ................
00000030 0000 0000 0000 0000 0000 0000 0000 0000  ................
00000040 0000 0000 0000 0000 0000 0000 0000 0000  ................
00000050 0000 0000 0000 0000 0000 0000 0000 0000  ................
00000060 0000 0000 0000 0000 0000 0000 0000 0000  ................
00000070 0000 0000 0000 0000 0000 0000 0000 0000  ................
00000080 0000 0000 0000 0000 0000 0000 0000 0000  ................
00000090 0000 0000 0000 0000 0000 0000 0000 0000  ................
000000A0 0000 0000 0000 0000 0000 0000 0000 0000  ................
000000B0 0000 0000 0000 0000 0000 0000 0000 0000  ................
000000C0 0000 0000 0000 0000 0000 0000 0000 0000  ................
000000D0 0000 0000 0000 0000 0000 0000 0000 0000  ................
000000E0 0000 0000 0000 0000 0000 0000 0000 0000  ................
000000F0 0000 0000 0000 0000 0000 0000 0000 0000  ................
00000100 0000 0000 0000 0000 0000 0000 0000 0000  ................
00000110 0000 0000 0000 0000 0000 0000 0000 0000  ................
00000120 0000 0000 0000 0000 0000 0000 0000 0000  ................
00000130 0000 0000 0000 0000 0000 0000 0000 0000  ................
00000140 0000 0000 0000 0000 0000 0000 0000 0000  ................
00000150 0000 0000 0000 0000 0000 0000 0000 0000  ................
00000160 0000 0000 0000 0000 0000 0000 0000 0000  ................
00000170 0000 0000 0000 0000 0000 0000 5876 0000  ............Xv..
00000180 0000 0000 0000 C04B 49D3 D041 6452 12EF  .......KI..AdR..
00000190 BC83 4741 26E5 0F23 AD4B 2E41 C732 5DEB  ..GA&..#.K.A.2].
000001A0 5CE4 5441 81FA 5D30 EE34 5941 90B2 0B36  \.TA..]0.4YA...6
000001B0 90A7 3841 29BC 0040 0100 0000 0000 0000  ..8A)..@........
000001C0 B4C8 763F 0000 0000 0000 0000 0000 0000  ..v?............
```

Figure 6.2.1. SSI data file information on file structure.

Figure 6.2.2 and Figure 6.2.3 show screen dumps of the two mentioned Danish data layouts. It is seen that the header actually contains the information of the file structure. If this structure can be "debugged" then the content of the header in itself does not matter.
Because both types of Danish files can be opened with the software NucSpec there was a good probability that the Swedish files also could be opened with NucSpec. This turned out to be correct.

The next question then was if the displayed live times, coordinates and number of counts were correct. In order to find out a data file was NASVD-processed and the resulting spectrum shapes compared to the energy calibration suggested by SSI and request to SSI was made about the length of typical live times.

```
00000000 2033 3830 0D0A 3131 3230 0D0A 2F2F 4752  _380..1120..//GR
00000010 3636 3061 3320 5356 3620 7633 2E30 2073  660a3 SV6 v3.0 s
00000020 6176 6520 2320 3839 340A 2F2F 4D61 7263  ave # 894.//Marc
00000030 6820 3220 3139 3939 0A74 7970 6564 6566  h 2 1999.typedef
00000040 2073 7472 7563 7420 7B0A 756E 7369 676E   struct {.unsign
00000050 6564 206C 6F6E 6734 2072 6563 6F72 645F  ed long4 record_
00000060 6E75 6D62 6572 3B20 0A75 6E73 6967 6E65  number; .unsigne
00000070 6420 6C6F 6E67 3420 6C69 6E65 5F6E 756D  d long4 line_num
00000080 6265 723B 0A66 6C6F 6174 3409 0955 5443  ber;.float4..UTC
00000090 5F74 696D 653B 200A 646F 7562 6C65 3809  _time; .double8.
000000A0 0958 3B0A 646F 7562 6C65 3809 0959 3B0A  .X;.double8..Y;.
000000B0 646F 7562 6C65 3809 095A 3B0A 7368 6F72  double8..Z;.shor
000000C0 7420 696E 7432 0944 4750 533B 0A73 686F  t int2.DGPS;.sho
000000D0 7274 2069 6E74 3220 0950 444F 5F5F 6572  rt int2 .PDOP_er
000000E0 726F 723B 0A66 6C6F 6174 3409 0950 444F  ror;.float4..PDO
000000F0 503B 0A66 6C6F 6174 3409 096C 6976 655F  P;.float4..live_
00000100 7469 6D65 3B0A 666C 6F61 7434 0909 7261  time;.float4..ra
00000110 6C74 3B0A 666C 6F61 7434 0909 6261 6C74  lt;.float4..balt
00000120 3B0A 666C 6F61 7434 0909 726F 695B 3130  ;.float4..roi[10
00000130 5D3B 0A75 6E73 6967 6E65 6420 696E 7432  ];.unsigned int2
00000140 0973 7065 635B 3531 325D 3B0A 7D47 5236  .spec[512];.}GR6
00000150 3630 2020 6461 7461 3B0A 2F2F 7369 7A65  60  data;.//size
00000160 6F66 2047 5236 3630 5F64 6174 6120 3D20  of GR660_data =
00000170 3131 3230 2062 7974 6573 0D0A 0100 0000  1120 bytes......
00000180 FFFF FFFF D060 5948 AAC3 1B37 DCB5 4241  .....`YH...7..BA
```

Figure 6.2.2. DTU data file information on file structure, old data layout structure.

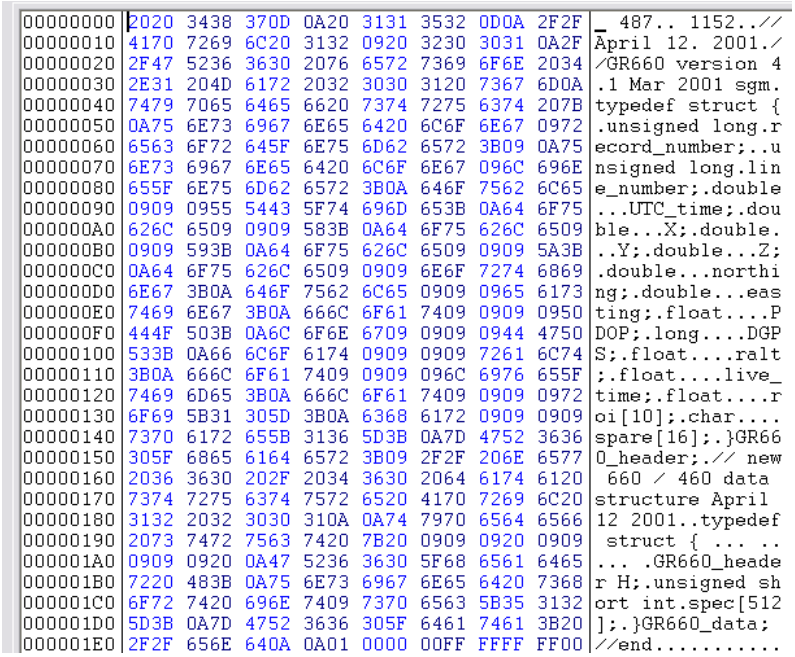

```
00000000 2020 3438 370D 0A20 3131 3532 0D0A 2F2F  _ 487.. 1152..//
00000010 4170 7269 6C20 3132 0920 3230 3031 0A2F April 12. 2001./
00000020 2F47 5236 3630 2076 6572 7369 6F6E 2034 /GR660 version 4
00000030 2E31 204D 6172 2032 3030 3120 7367 6D0A .1 Mar 2001 sgm.
00000040 7479 7065 6465 6620 7374 7275 6374 207B typedef struct {
00000050 0A75 6E73 6967 6E65 6420 6C6F 6E67 0972 .unsigned long.r
00000060 6563 6F72 645F 6E75 6D62 6572 3B09 0A75 ecord_number;..u
00000070 6E73 6967 6E65 6420 6C6F 6E67 096C 696E nsigned long.lin
00000080 655F 6E75 6D62 6572 3B0A 646F 7562 6C65 e_number;.double
00000090 0909 0955 5443 5F74 696D 653B 0A64 6F75 ...UTC_time;.dou
000000A0 626C 6509 0909 583B 0A64 6F75 626C 6509 ble...X;.double.
000000B0 0909 593B 0A64 6F75 626C 6509 0909 5A3B ..Y;.double...Z;
000000C0 0A64 6F75 626C 6509 0909 6E6F 7274 6869 .double...northi
000000D0 6E67 3B0A 646F 7562 6C65 0909 0965 6173 ng;.double...eas
000000E0 7469 6E67 3B0A 666C 6F61 7409 0909 0950 ting;.float....P
000000F0 444F 503B 0A6C 6F6E 6709 0909 0944 4750 DOP;.long....DGP
00000100 533B 0A66 6C6F 6174 0909 0909 7261 6C74 S;.float....ralt
00000110 3B0A 666C 6F61 7409 0909 096C 6976 655F ;.float....live_
00000120 7469 6D65 3B0A 666C 6F61 7409 0909 0972 time;.float....r
00000130 6F69 5B31 305D 3B0A 6368 6172 0909 0909 oi[10];.char....
00000140 7370 6172 655B 3136 5D3B 0A7D 4752 3636 spare[16];.}GR66
00000150 305F 6865 6164 6572 3B09 2F2F 206E 6577 0_header;.// new
00000160 2036 3630 202F 2034 3630 2064 6174 6120  660 / 460 data
00000170 7374 7275 6374 7572 6520 4170 7269 6C20 structure April
00000180 3132 2032 3030 310A 0A74 7970 6564 6566 12 2001..typedef
00000190 2073 7472 7563 7420 7B20 0909 0920 0909  struct { ... ..
000001A0 0909 0920 0A47 5236 3630 5F68 6561 6465 ... .GR660_heade
000001B0 7220 483B 0A75 6E73 6967 6E65 6420 7368 r H;.unsigned sh
000001C0 6F72 7420 696E 7409 7370 6563 5B35 3132 ort int.spec[512
000001D0 5D3B 0A7D 4752 3636 305F 6461 7461 3B20 ];.}GR660_data;
000001E0 2F2F 656E 640A 0A01 0000 00FF FFFF FF00 //end...........
```

Figure 6.2.3. DTU data file information on file structure, new data layout structure.

Coordinate plots showing Easing and Northing were made in RT90 to find out whether the coordinates were still in the same data types as for the Danish files (With time Exploranium has for some variables switched between double and floats and long and shorts.)
In the plotting of the coordinates it was discovered that there actually was an error in the SSI CGS coordinate xml setup files. (However, this has no influence on the file contents.)

It was concluded that the data layout described below was very likely the correct data format and information on this was sent to SSI.

Header 380 bytes (useless for anything)

Struct 1152 bytes):
unsigned long Record_number;
unsigned long Line_number;
double UTC_time;
double X;
double Y;
double Z;
double Northing;
double Easting;
float PDOP;
long DGPS;
float ralt;
float Live_time;
float roi[10];
short gain
short peak
int clock time
char spare[8];
unsigned int SPC[512];

7 PROJECT STATUS

According to the UGS Urban Gamma Spectrometry contract, AFT/B(06)3, all stages have been completed except for a 2-days seminar that will take place on the days 13-14 November at the Technical University of Denmark.

The project group would like to thank SSI, SGU, NRPA and Geislavarnir Ríkisins for having signed up as participants in the seminar. In this respect the project group is thankful for the additional funding granted for the travel arrangements for the participants and for the funding received for the treatment of the SSI custom cars measurements in Frihamnen.

A short seminar report including seminar presentations (slide shows and comments), resumes of discussions and proposals for future work will be delivered to NKS in December 2006.

8 ACRONYMS

AGS	Airborne Gamma Spectrometry
ASSS	Area Specific Spectrum Stripping (previously ASS)
CGS	Carborne Gamma Spectrometry
DEMA	Danish Emergency Management Agency
DTU	Technical University of Denmark
FSC	Fitting with Spectral Components
LINSSI	LInux System for Spectral Information
MDA	Minimum Detectable Activity
NASVD	Noise Adjusted Singular Value Decomposition
NRPA	Norwegian Radiation Protection Agency
SONNI	Sophisticated On Site Nuclide Identification
SSI	Swedish Radiation Protection Authority
STUK	Radiation and Nuclear Safety Authority, Finland
UGS	Urban Gamma Spectrometry
USS	Unisampo-Shaman

9 REFERENCES

1. Karlsson, S., Mellander, H., Lindgren, J., Finck, R., and Lauritzen, B. (eds.). RESUME99 Rapid Environmental Surveying Using Mobile Equipment. NKS-15, ISBN 87-7893-065-0 (2000).
2. Aage, H. K., Korsbech, U.: Search for orphan sources using CGS equipment - a short handbook. (Made for CGS measuring teams in Balticum, Poland, Russia and Denmark, restricted). Ørsted-DTU, Measurement & Instrumentation Systems, Technical University of Denmark, Report IT-NT-59, November 2001.
3. Korsbech, U., Aage, H.K., Byström, S., Wedmark, M., Thorshaug, S. and Bargholz, K. Area specific stripping of lower energy windows for AGS and CGS systems. Nordic AGS and CGS data, NKS-109, ISBN 87-7893-168-1, May 2005.
4. Aage, H. K., Korsbech, U., Bargholz, K., Bystöm, S. Wedmark, M., and Thorshaug, S., 2006. Experience with area specific spectrum stripping of NaI(Tl) gamma spectra. ASSS paper. Radiation Protection Dosimetry, doi:10.1093/rpd/ncl010.
5. Aage, H. K., Korsbech, U. and Bargholz, K. Early detection of radioactive fall-out by gamma-spectrometry. Radiation Protection Dosimetry, 106 (2), 155-164, (2003).
6. Aage, H. K., Korsbech, U.: Fitting of new CGS spectra with base spectral components. Report NT-67, December 2004, Øersted-DTU.
7. Hovgaard, J., 1997a. Airborne Gamma-Ray Spectrometry. Statistical Analysis of Airborne Gamma-Ray Spectra. Ph. D. Thesis, Technical University of Denmark.
8. Aage, H. K., and Korsbech, U. Search for lost or orphan radioactive sources based on NaI gamma spectrometry. Appl. Radiat. Isot., 58 (1), 103-113 (2003).
9. Aage, H. K., Korsbech, U., Bargholz, K., Hovgaard, J.: A new technique for processing airborne gamma ray spectrometry data for mapping low level contaminations. Applied Radiation and Isotopes, Volume 51, pp. 651-662, December 1999.
10. Tsoulfanides, N. Measurement and Detection of Radiation, University of Missouri-Rolla, Hemisphere Publishing Corporation, 1983.
11. Currie L. A. Limits for Qualitative Detection and Quantitative Determination - Application to Radiochemistry.
    Analytical Chemistry 1968, Vol 40, no. 3, pp.586 - 593.
12. Kuukankorpi S., Toivonen H., Moring M. and Smolander P. Mobile Spectrometry System for Source Finding and Prompt Reporting (to be published in 2006).
13. Toivonen H, Kuukankorpi S, Moring M. Smolander P. Radionuclide source finding using a mobile laboratory for supporting counter terrorism actions. Symposium on chemical, biological, nuclear and radiological threats, Tampere 2006 (to be published in 2006).
14. Aage H. K., Toivonen H, Kuukankorpi S, Moring M. Smolander P.
    Urban Gamma Spectrometry, Status Report, NKS, Nordic Nuclear Safety Research.
    Report from the AFT/B(06)3 project group, 01 June 2006.

Title	Urban Gamma Spectrometry: Report 2
Author(s)	[1]Helle Karina Aage, [2]Satu Kuukankorpi, [2]Mikael Moring, [2]Petri Smolander and [2]Harri Toivonen
Affiliation(s)	1) Technical University of Denmark, Kgs. Lyngby, Denmark 2) Radiation and Nuclear Safety Authority, Helsinki, Finland
ISBN	978-87-7893-258-7
Date	June 2009
Project	NKS-B / UGS
No. of pages	62
No. of tables	14
No. of illustrations	122 (21 of which are composites)
No. of references	14

Abstract

Urban gamma spectrometry has been given only minor attention with the focus being on rural gamma spectrometry. However, in recent years the Nordic emergency management authorities have turned focus towards border control and lost or stolen sources. Gamma spectra measured in urban areas are characterized by a wide variety of spectrum shapes and very fast changes in environmental background.

In 2004 a Danish CGS survey took place in Copenhagen. It was found that gamma spectrometry in urban areas is far more complicated to interpret than had previously been thought and a new method "Fitting with Spectral Components", FSC, based on NASVD, was tested with some success. In Finland, a database "LINSSI" has been developed for spectral data management. In CGS search mode a "peak hypothesis test" is applied to the measured spectra. This system was tested during the Helsinki 2005 Athletics World Championship and it provides fast and reliable automated alarms for intermediate and high level signals. In Sweden mobile detector systems are used for border controls and problems are encountered when making measurement in harbour, container areas.

The methods for handling data and for interpretation of urban gamma spectrometry measurements were compared and tested on the same data sets from Copenhagen and Helsinki. Software tools were developed for converting data between the Finnish LINSSI database and the binary file formats used in Denmark and Sweden. The Processing methods used at DTU and STUK have different goals. The ASSS and FSC methods are designed to optimize the overall detection capability of the system, while sacrificing speed, usability and to a certain level robustness. These methods cannot always be used for real time analysis. The Peak Significance method is designed to give robust alarms in real time, while sacrificing some of the detection capability. Thus these methods are not interchangeable, but rather complementary. An ideal system based on these methods would use the Peak Significance method simultaneously with the data collection and the ASSS and FSC methods in post processing to achieve both an optimal detection capability and a fast response. Ideally, the three systems would run simultaneously in a user-friendly environment, such as the LINSSI database.

Key words

Urban Carborne Gamma Spectrometry, Spectrum Stripping, Peak hypothesis, LINSSI, FSC, ASSS, NASVD, Harbour, source search

Available on request from the NKS Secretariat, P.O.Box 49, DK-4000 Roskilde, Denmark.
Phone (+45) 4677 4045, fax (+45) 4677 4046, e-mail nks@nks.org, www.nks.org